THE PROCEEDINGS OF THE PHYSICAL SOCIETY

VOL. 60, PART 3 — 1 March 1948 — No. 339

CONTENTS

PAGE

(Prof.) L. F. BATES and E. G. HARRISON. The adiabatic temperature changes accompanying the magnetization of some ferromagnetic alloys in low and moderate fields . . . 213

(Prof.) L. F. BATES and E. G. HARRISON. The adiabatic temperature changes accompanying magnetization in low and moderate fields: A further study of iron 225

R. STREET. The variation with magnetization of Young's modulus for cobalt . . . 236

K. W. PLESSNER. The electric strength of dielectric films 243

(Prof.) C. A. COULSON. Excited electronic levels in conjugated molecules: I. Long wavelength ultra-violet absorption of naphthalene, anthracene and homologs . . . 257

(Dr.) H. C. LONGUET-HIGGINS. Excited electronic levels in conjugated molecules: II. On the symmetry and multiplicity of molecular states 270

J. B. BIRKS. The measurement of the permeability of low-conductivity ferromagnetic materials at centimetre wavelengths 282

T. SMITH. On perfect optical instruments 293

(Prof.) E. N. da C. ANDRADE. A new device for maintaining constant stress in a rod undergoing plastic extension 304

Letters to the Editor:

(Prof.) L. F. BATES and J. H. DAVIS. The effect of temperature on the heat changes accompanying magnetization of the nickel-silicon alloy W.5 307

Corrigenda 308

Reviews of books 308

Price to non-members 8*s.* 4*d.* net; 8*s.* 10*d.* inclusive of postage
Annual subscription 63*s.* inclusive of postage, payable in advance

Published by
THE PHYSICAL SOCIETY
1 Lowther Gardens, Prince Consort Road, London S.W.7

Printed by
TAYLOR AND FRANCIS, LTD.,
Red Lion Court, Fleet Street, London E.C.4

PROCEEDINGS OF THE PHYSICAL SOCIETY

Beginning in January 1948 (Volume 60), the *Proceedings* is now published monthly under the guidance of an Advisory Board.

ADVISORY BOARD

Chairman: The President of the Physical Society (G. I. FINCH, M.B.E., D.Sc., F.R.S.).

E. N. da C. ANDRADE, Ph.D., D.Sc., F.R.S.
Sir EDWARD APPLETON, G.B.E., K.C.B., D.Sc., F.R.S.
L. F. BATES, Ph.D., D.Sc.
P. M. S. BLACKETT, M.A., F.R.S.
Sir LAWRENCE BRAGG, O.B.E., M.A., Sc.D., D.Sc., F.R.S.
Sir JAMES CHADWICK, D.Sc., Ph.D., F.R.S.
Lord CHERWELL OF OXFORD, M.A., Ph.D., F.R.S.
Sir John COCKCROFT, C.B.E., M.A., Ph.D., F.R.S.
Sir CHARLES DARWIN, K.B.E., M.C., M.A., Sc.D., F.R.S.
N. FEATHER, Ph.D., F.R.S.
D. R. HARTREE, M.A., Ph.D., F.R.S.
N. F. MOTT, M.A., F.R.S.
M. L. OLIPHANT, Ph.D., D.Sc., F.R.S.
F. E. SIMON, C.B.E., M.A., D.Phil., F.R.S.
T. SMITH, M.A., F.R.S.
Sir GEORGE THOMSON, M.A., D.Sc., F.R.S.

Papers for publication in the *Proceedings* should be addressed to the Secretary-Editor, Miss A. C. STICKLAND, Ph.D., at the Office of the Physical Society, 1 Lowther Gardens, Prince Consort Road, London S.W.7. Telephone: KENsington 0048, 0049.

Detailed Instructions to Authors were included in the February issue of the *Proceedings*; separate copies can be obtained from the Secretary-Editor.

CATALOGUES

OF THE

PHYSICAL SOCIETY'S EXHIBITIONS

OF

SCIENTIFIC INSTRUMENTS AND APPARATUS

The three post-war Catalogues are widely acknowledged as very useful records and valuable books of reference.

30th (1946) CATALOGUE (reprinted):
288 + lxxx pages; 176 illustrations.
2*s.*; *by post* 3*s.*

31st (1947) CATALOGUE:
298 + lxxxvi pages; 106 illustrations.
5*s.*; *by post* 6*s.*

32nd (1948) CATALOGUE:
5*s.*; *by post* 6*s.* (Ready 22nd March)

Orders, with remittances, should be sent to
THE PHYSICAL SOCIETY
1 Lowther Gardens, Prince Consort Road, London S.W.7.

THE UNITED IMPERIAL AND AMERICAN PATENT SERVICE
(Patents, Designs, Trade Mark)

M. E. J. Gheury de Bray, A.M.I.E.E., Registered Patent Agent (London), Chartered Electrical Engineer and Fellow of the Physical Society. J. J. Wittal, LL.B., Patent Attorney and Counsellor at Law (New York).

Booklet free on application.
Preliminary interview free by appointment.
102 Bishopsgate, E.C.2.

Telephone : Clerkenwell 1131 — Chancery 8579
London Wall 2121.

Telegraphic Address } IMPERATRIX, CENT, LONDON.

REPORT ON DEFECTIVE COLOUR VISION IN INDUSTRY

by a Committee of The Physical Society Colour Group

52 pp. 3s. 6d., inclusive of postage

Orders, with remittances, should be sent to

THE PHYSICAL SOCIETY
1 Lowther Gardens, Prince Consort Road, London S.W.7

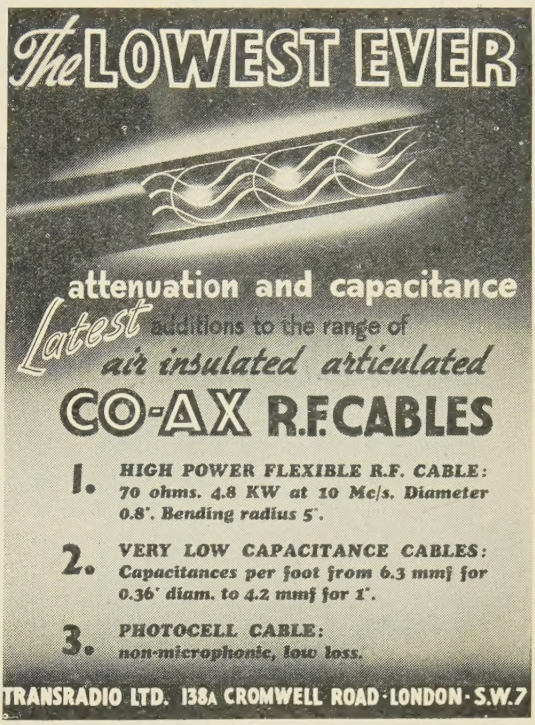
The LOWEST EVER
attenuation and capacitance
Latest additions to the range of
air insulated articulated
CO-AX R.F. CABLES
1. HIGH POWER FLEXIBLE R.F. CABLE: 70 ohms. 4.8 KW at 10 Mc/s. Diameter 0.8". Bending radius 5".
2. VERY LOW CAPACITANCE CABLES: Capacitances per foot from 6.3 mmf for 0.36" diam. to 4.2 mmf for 1".
3. PHOTOCELL CABLE: non-microphonic, low loss.
TRANSRADIO LTD. 138A CROMWELL ROAD · LONDON · S.W.7

REPORT OF AN INTERNATIONAL CONFERENCE
ON
FUNDAMENTAL PARTICLES
AND
LOW TEMPERATURES
HELD AT
The Cavendish Laboratory, Cambridge,
on 22–27 July 1946

Volume I 200 pages
FUNDAMENTAL PARTICLES

Volume II 148 pages
LOW TEMPERATURES

Price of each volume (in paper covers) **15***s., inclusive of postage*

Orders, with remittances, should be sent to

THE PHYSICAL SOCIETY,

1 Lowther Gardens, Prince Consort Road, London S.W.7

DRAYTON

"Hydroflex"

Metal Bellows

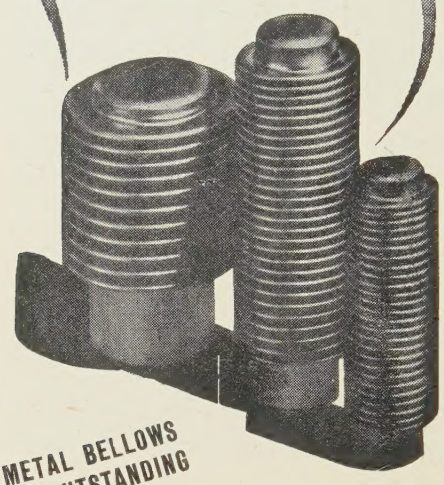

METAL BELLOWS WITH OUTSTANDING ADVANTAGES

(B.2)

These bellows are formed from the initial tube in one gradual continuous operation, resulting in a uniformity of wall-thickness unattainable by any other method The tough resilient product is tested to many times the maximum rated working pressure during formation. Customers' end plates can be fitted prior to forming so that the soldered joint is also pressure tested.

For Gland Seals ; Refrigeration Control ; Thermostatic and Pressure Operated Devices, etc.

- Every Gland uniform in life and performance.
- Pretested during forming.
- Absolutely reliable in operation.
- Provision of closed end eliminates one joint.

Root Diam. 3/8" to 3" Outside Diam. 9/16" to 4½"

Write for the "Hydroflex" Brochure T.

DRAYTON REGULATOR & INSTRUMENT CO. LTD.
WEST DRAYTON *West Drayton* 2611. **MIDDX.**

NEW WAYS

of obtaining

E.H.T.

for cathode ray tube and supplies.

★
★ ★

SEE THE EXHIBIT OF

WESTINGHOUSE
WESTALITE
METAL RECTIFIERS

AT THE FORTHCOMING EXHIBITION

WESTINGHOUSE BRAKE & SIGNAL CO. LTD.
82 York Way, King's Cross, London, N.1

SCIENTIFIC BOOKS

Messrs. H. K. LEWIS can supply from stock or to order any book on the Physical and Chemical Sciences.

CONTINENTAL AND AMERICAN works unobtainable in this country can be secured under Board of Trade licence in the shortest possible time.

SECOND-HAND SCIENTIFIC BOOKS. 140 GOWER STREET.
An extensive stock of books in all branches of Pure and Applied Science may be seen in this department. Large and small collections bought. Back volumes of Scientific Journals.

SCIENTIFIC LENDING LIBRARY

Annual subscription from One Guinea. *Details of terms and prospectus free on request.*

THE LIBRARY CATALOGUE revised to December 1943, containing a classified index of authors and subjects: to subscribers 12s. 6d. net, to non-subscribers 25s. net, postage 9d.
Supplement from 1944 to December 1946. To subscribers 2s. 6d. net; to non-subscribers 5s. net; postage 4d. **Bi-monthly List of Additions, free on application**

Telephone: EUSton 4282

Telegrams: "Publicavit, Westcent, London"

H. K. LEWIS & Co. Ltd.

136 GOWER STREET, LONDON, W.C.1

Established 1844

THE REVIEW OF SCIENTIFIC INSTRUMENTS

GAYLORD P. HARNWELL, *Editor*, University of Pennsylvania, Philadelphia, Pennsylvania

PUBLISHED monthly by the American Institute of Physics, this journal is devoted to scientific instruments, apparatus and techniques.

Subscription price $7.00 *a year*

Other physics journals published by the American Institute of Physics are:

	Yearly Subscription Price
THE PHYSICAL REVIEW	$16.50
REVIEWS OF MODERN PHYSICS	4.40
JOURNAL OF THE OPTICAL SOCIETY OF AMERICA	7.70
THE JOURNAL OF THE ACOUSTICAL SOCIETY OF AMERICA	8.80
AMERICAN JOURNAL OF PHYSICS	5.50
THE JOURNAL OF CHEMICAL PHYSICS	11.00
JOURNAL OF APPLIED PHYSICS	9.00

NOTE: All rates quoted are foreign subscription prices and do not apply to Canada and the U.S.

Send orders with remittances to

American Institute of Physics, 57 East 55 Street, New York 22, New York, U.S.A.

G.E.C.
"Flat End"
CATHODE RAY TUBE

The G.E.C. 9″ diameter cathode ray tube 6501 is intended for high quality television reception, and is magnetically focused and deflected. The screen fluorescence is white.
The tube end is made by a special moulding technique, which produces a screen face nearly flat, and more constant in production than is normally possible with bulbs made by the usual blowing technique.
A picture size of approximately 200x160 mms. is obtainable with slight masking of the edges and corners.
The bulb is made of high insulating glass giving a minimum of screen charging effects.
The electrode gun is designed to give a high picture brightness, with excellent definition for a relatively small voltage drive to the modulator.
Detailed technical data sheet available on request.

Osram PHOTO CELLS · G.E.C. CATHODE RAY TUBES · Osram VALVES

The General Electric Co. Ltd., Magnet House, Kingsway, London, W.C.2.

NGENUITY and GOOD ENGINEERING

Give a 12-foot scale with negligible backlash on a $4\frac{5}{8}$" diameter dial.

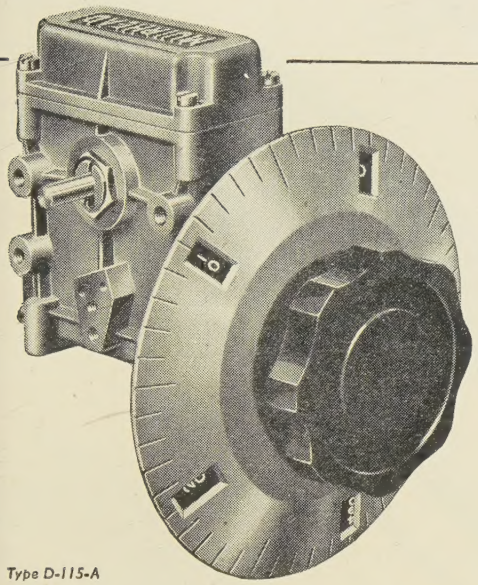

Type D-115-A

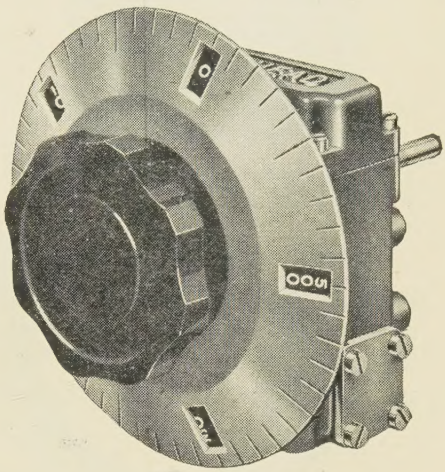

Type D-206-A

DIALS and DRIVES ; TYPES D-115-A and D-206-A

TYPE D-115-A employs a 20 : 1 worm reduction gear providing a right-angle drive for two components.

TYPE D-206-A employs a 20 : 1 spur reduction gear providing a single in-line drive.

OUTSTANDING FEATURES:

High reading and setting accuracy by means of a dial embodying an adding mechanism — effective scale length over 12 feet with 500 divisions • • • Gears spring-loaded to reduce backlash • • • Rugged die-cast construction and substantial bearings for long and continuous service • • • Shafts: $\frac{1}{4}$ in. diameter and $\frac{9}{16}$ in. projection • • • Finish: gunmetal with engraving filled white Weight: $2\frac{1}{4}$ lb • • • • *Dial manufactured under licence from the Sperry Gyroscope Co. Ltd., Pat. No. 419002. Full description in Bulletins B-532-B and B-556-A.*

MUIRHEAD

Muirhead & Co., Limited, Elmers End, Beckenham, Kent. *Telephone : Beckenham 0041-2*

FOR OVER 60 YEARS DESIGNERS AND MAKERS OF PRECISION INSTRUMENTS

C.R.C. 511

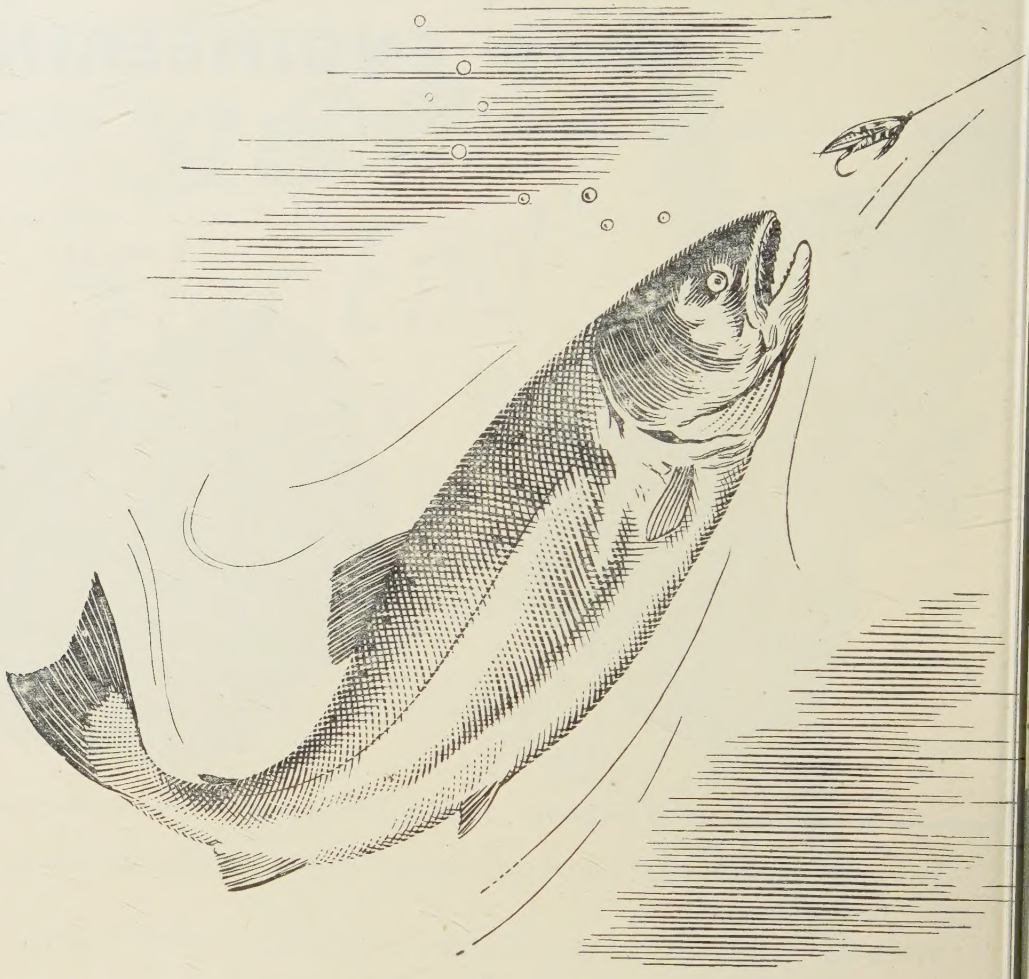

. . . but there's nothing

more attractive than

"TICONAL" PERMANENT

REGD. TRADE MARK

MAGNETS MADE BY Mullard

Mullard

THE MULLARD WIRELESS SERVICE COMPANY LIMITED, MAGN
DIVISION, CENTURY HOUSE, SHAFTESBURY AVENUE, LONDON, W.C

(MT

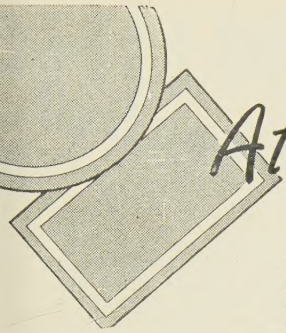

A thousand hours life

One of the stringent tests that each EEL cell must pass before it leaves our laboratories is the continuous short circuit. This is equivalent to something like a thousand hours normal usage, and only after it has passed this rigorous test satisfactorily is it ready to receive its guarantee of performance — the EEL trade mark. This is but one test that has made the EEL selenium photo-cell the best in the world.

EEL

SELENIUM PHOTO-CELLS

VANS ELECTROSELENIUM LIMITED
rlow, Essex

VITREOSIL MERCURY VAPOUR PUMPS

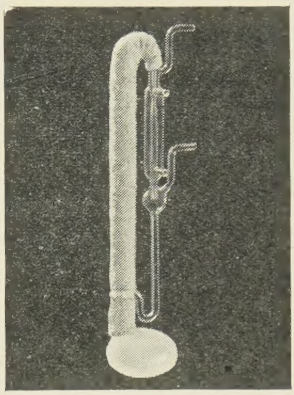

A complete, highly efficient, and inexpensive Vacuum System, including our new M.V. Fore Pump above, will be shown on our Stand at the Physical Society Exhibition, April 6–9.

We will also be exhibiting NEW SPECIAL HIGH TEMPERATURE REFRACTORY PRODUCTS

THE THERMAL SYNDICATE LTD.

Head Office: Wallsend, Northumberland
London Office: 12–14 Old Pye Street, S.W.1

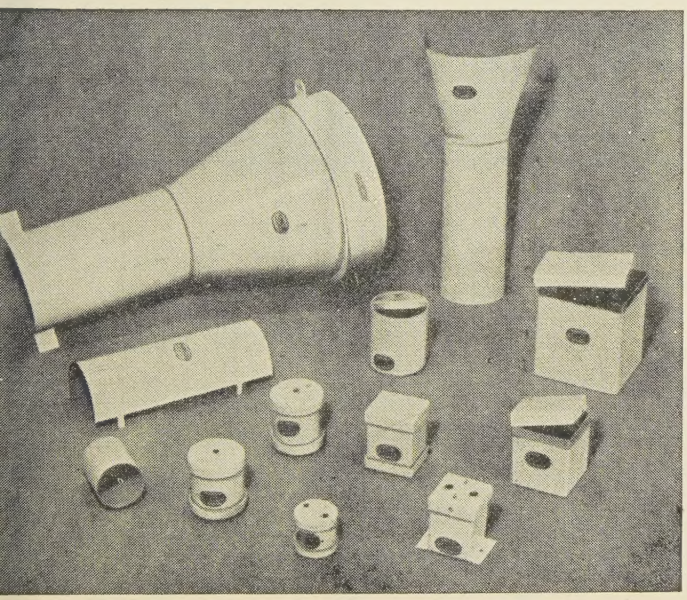

HE TELEGRAPH CONSTRUCTION & MAINTENANCE CO. LTD.
Founded 1864

ead Office: 22 OLD BROAD ST., LONDON, E.C.2. *Tel: LONdon Wall* 3141
nquiries to: TELCON WORKS, GREENWICH, S.E.10. *Tel: GREenwich* 1040

MUMETAL
REGD.

MAGNETIC SCREENS

The high permeability of MUMETAL makes it the outstanding material for the production of all types of magnetic screens. We are in a position to fabricate boxes and shields of practically any shape or size for the screening of delicate instruments and equipment from both uni-directional and alternating magnetic fluxes. A complete range of standard MUMETAL shields is available, examples of which are illustrated. Our technical experts will be pleased to assist in the solution of all screening problems. Your enquiries are invited.

TELCON

TELCON METALS

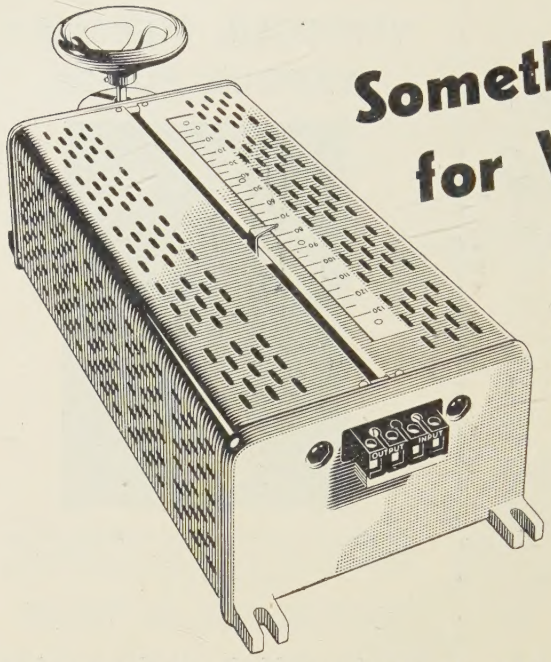

Something NEW for Voltage control

The "Regavolt" is an all-British transformer type regulator of new design and robust construction which make it particularly suitable for heavy industrial use. Special points of performance are: smooth stepless control of voltage, good regulation, high efficiency, and no waveform distortion. Suitable for control of electric furnaces, high voltage testing transformers, speed of electric motors, rectifier equipment, etc.
Write for full details. Booklet 3/3062

BERCO
REGAVOLT
REGULATING TRANSFORMER

THE BRITISH ELECTRIC RESISTANCE CO. LTD., Queensway, Ponders End, Middlesex
Telephone: HOWard 1492 Telegrams: "Vitrohm, Enfield"
BR3062-EHT

P. J. KIPP & ZONEN

We have pleasure in announcing that the well-known firm of P. J. Kipp & Zonen, Delft, Holland, have appointed us their exclusive agents in the United Kingdom. Importation is subject to licence. We shall be glad to receive enquiries. Among their products are:

MOLL RECORDING MICROPHOTOMETERS
INFRA-RED SPECTROMETERS
THERMOELEMENTS
SOLARIMETRIC THERMOPILES
VACUUM THERMOCOUPLES
STAR ACTINOMETERS
PYRHELIOMETERS
DOUBLE MONOCHROMATORS
BOLOMETERS
COLORIMETERS
NEPHELOMETERS
MOLL GALVANOMETERS
MOLL MICRO-GALVANOMETERS
DOUBLE COIL GALVANOMETERS
STRING GALVANOMETERS
GALVANOMETER RECORDERS (FILM)

Please apply for descriptive literature

GRIFFIN and TATLOCK Ltd

Established as Scientific Instrument Makers in 1826

LONDON Kemble St., W.C.2 — MANCHESTER 19, Cheetham Hill Rd., 4 — GLASGOW 45, Renfrew St., C.2 — EDINBURGH 7, Teviot Place, 1

BIRMINGHAM: STANDLEY BELCHER & MASON LTD., Church Street, 3

PHILIPS ELECTRON MICROSCOPE

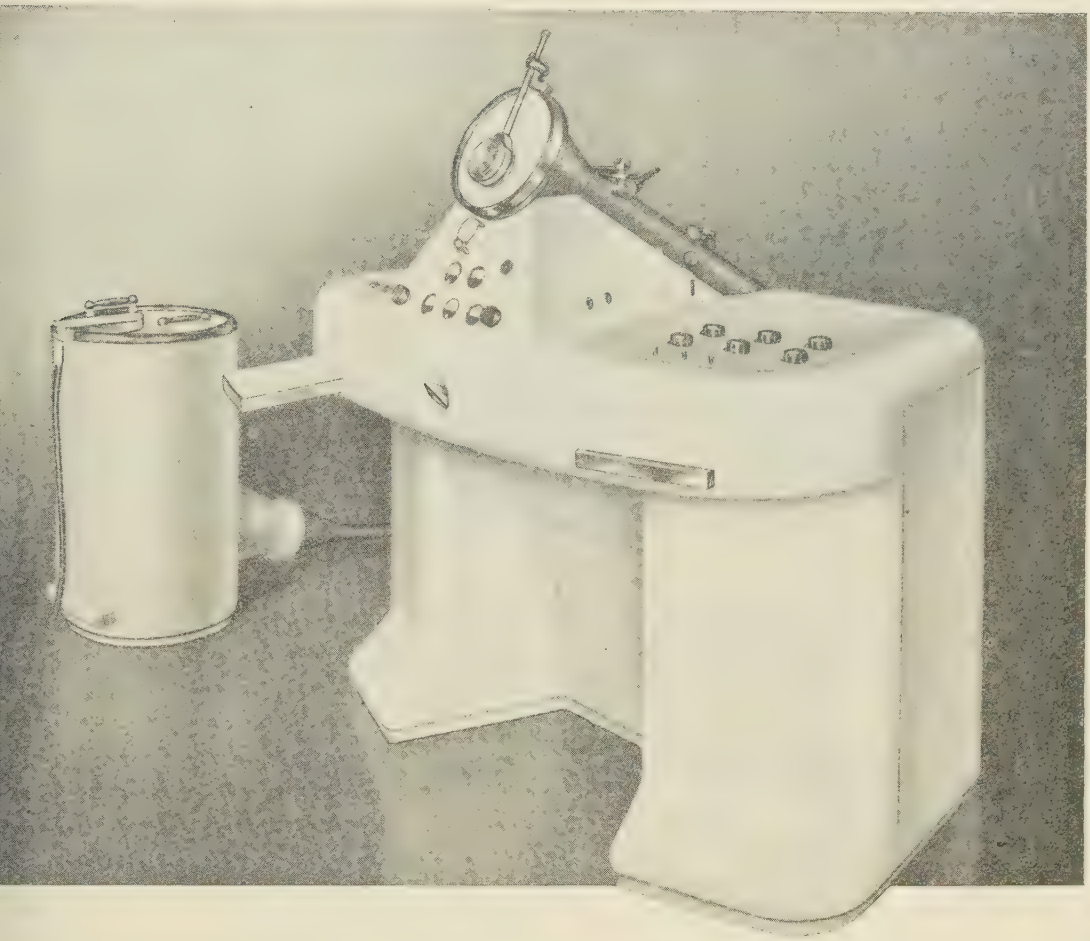

This instrument — entirely new in design — has a performance far in advance of any Electron Microscope of the conventional type. Some of the important features include:

ENTIRELY NEW FOCUSSING DEVICE · HIGH RESOLVING POWER · TWO EXTRA LENSES · CONTINUOUSLY VARIABLE MAGNIFICATION · PRACTICALLY UNINTERRUPTED OPERATION · LARGE SIZE IMAGE OF 20 CM. AT ALL MAGNIFICATIONS · ENTIRELY SHOCKPROOF AND RAYPROOF

PHILIPS ELECTRICAL LIMITED

DUSTRIAL X-RAY DEPT., CENTURY HOUSE, SHAFTESBURY AVENUE, LONDON, W.C.2.
(XB315A)

DAWE UNIVERSAL IMPEDANC BRIDGE

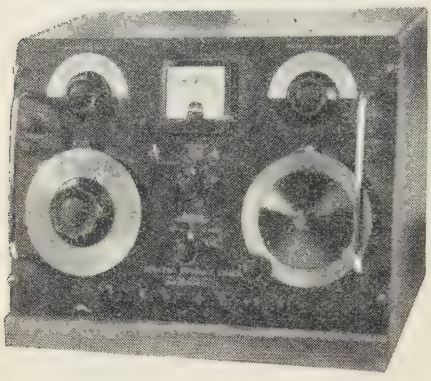

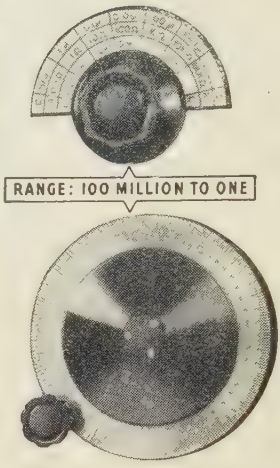

All laboratories using electrical equ ment will find a ready use for t Bridge, which is self-contained, portal direct-reading and sufficiently accur for most routine measurements.

INDUCTANCE:	1 μH—100
CAPACITY:	1 pF—100 m
RESISTANCE:	·001Ω—1 M
POWER FACTOR:	·002—1·0
Q FACTOR:	·02—1,000

The bridge includes built-in standar batteries, a 1,000-cycle tone source a-c measurements, a zero-centre g vanometer null indicator for d-c terminals for head-phones for 1,0 cycle null detection.

DAWE INSTRUMENTS LTD., HARLEQUIN AVENUE, GREAT WEST ROAD, BRENTFORD, MIDDLESEX: EALING 1

From a Research Laboratory Case-Book

S46-763. (Diagrams for School Workshop)

PROBLEM: A teacher wishes to produce a number of diagrams on a material which will stand considerable handling in the school workshop.

ANSWER: The original, drawn in Indian ink, can be copied either in the camera or by means of a 'Kodak' Reflex Plate. The copy can then be reproduced on metal, wood or plastic sheeting by means of 'Kodak' Transfer Sensitising Paper. This reproduction, if lacquered, will stand up to years of rough use.

S46-764. (Radiograph of Mouse)

PROBLEM: A research worker requires a radiograph of the tibia of a mouse. The resolution must be sufficiently high to allow an enlargement of 30 to 40 diameters.

ANSWER: Assuming that a relatively long X-ray exposure is possible, the 'Kodak' Maximum Resolution Plate will give good results. Its resolving power is ample for the purpose, and far exceeds that permitted by the geometric sharpness factors.

S46-765. (Spectrography in Steel Analysis)

PROBLEM: A spectrographer engaged on routine steel analysis requires a plate for use in the ultra-violet portion of the spectrum. Though very suitable in other ways, the 'Kodak' B.10 Plate shows too great a variation in contrast at different wavelengths.

ANSWER: The 'Kodak' Uniform Gamma Plate is expressly made for routine ultra-violet spectrography, and gives a uniform gamma over a wide range of ultra-violet wavelengths.

Based on actual correspondence in files of the Kodak Research Laborator

KODAK Ltd

KINGSWAY · LONDON · W

PIPE COUPLINGS

ELECTRICALLY HEATED PRESSURE HEADS

FILM ASSESSORS AND SCANNING MICROSCOPES

CONTINUOUS FILM RECORDING CAMERAS AND EQUIPMENT FOR CATHODE RAY OSCILLOGRAPHY, ETC.

AVIMO

We undertake the Design, Development and Manufacture of any type of Optical —Mechanical—Electrical Instrument. Including Cameras for special purposes.

Avimo Limited, Taunton, England · Telephone Taunton 3634

11790 D

THE BALDWIN

FARMER

ELECTROMETER

FOR RADIOLOGICAL WORK

A unique electronic instrument for research and routine testing in Hospital Radium and X-ray Therapy Departments.

It has an input resistance of 10^{16} ohms and an input capacity of less than 1 $\mu\mu$F. Developed primarily for use in Radiological work, where small condensers of the Sievert type are used extensively for the measurement of gamma and X-ray intensities.

Fully descriptive leaflet supplied on request.

VOLTAGE RANGES
0 - 50
0 - 100
0 - 250

BALDWIN INSTRUMENT COMPANY LTD.

BROOKLANDS WORKS, PRINCES ROAD, DARTFORD, KENT.

Telephone: DARTFORD 2989

COSSOR

Announce

THE NEW MODEL
1035
DOUBLE BEAM
OSCILLOGRAPH

The Model 1035 is a general purpose Oscillograph, consisting of a Double Beam Tube Unit, Time Base, Y Deflection Amplifiers and internal Power Supplies. The two traces are presented over the full area of a flat screen tube of 90 mm. internal diameter and operating at 2 kv. Signals are normally fed via the Amplifiers, with provision for input voltage calibration. The Time Base is designed for repetitive, triggered, or single stroke operation, and time measurement is provided by a directly calibrated Shift Control.

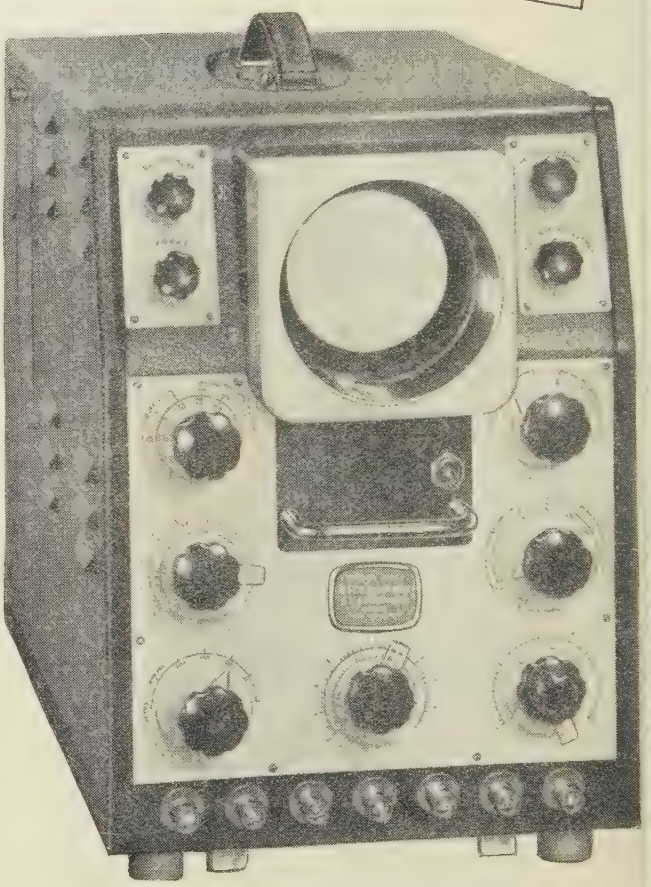

MODEL 1049
Industrial Oscillograph
is designed specifically for industrial use where the main interest is in the observation and measurement of low frequency phenomena. Its presentation is generally similar to that of Model 1035 illustrated and a comprehensive specification includes 4 kv tube operation for transient recording.

For photographic recording, both models have provision for the attachment of a Camera, Model 1428, which may be operated either manually or by motor drive. A similar camera, Model 427, is also available for use with Model 339 Oscillograph.

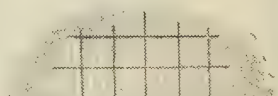

Further details on application to :—

A. C. COSSOR LTD., INSTRUMENT DEPT., HIGHBURY, LONDON, N.5

C1/8

THE PROCEEDINGS OF THE PHYSICAL SOCIETY

VOL. 60, PART 3 1 March 1948 No. 339

The Adiabatic Temperature Changes Accompanying the Magnetization of some Ferromagnetic Alloys in Low and Moderate Fields

BY L. F. BATES AND E. G. HARRISON
University College, Nottingham

MS. received 30 *May* 1947; *read* 8 *November* 1947

ABSTRACT. The method of Bates and Weston for measuring the small heat changes which occur as a ferromagnetic substance is taken through a single hysteresis cycle step by step has been extended to some seven ferromagnetic alloys. In every case a cooling is initially observed as the magnetization of the specimen is reduced from its maximum value. Indications are found that large changes in thermomagnetic properties are caused by small changes in composition, particularly when the latter approximates to that of invar. The results are discussed in terms of the modern domain concepts of ferromagnetic processes.

§1. INTRODUCTION

THE temperature changes which occur when a ferromagnetic substance is taken through an ordinary or so-called 'technical' hysteresis cycle were measured by a new method by Bates and Weston (1941) and described in a paper hereafter termed Paper I. In this paper a fairly comprehensive study was made of the behaviour of pure nickel in the annealed, hard-drawn and externally stressed conditions, and a few measurements on certain nickel-iron alloys such as invar, mu-metal and permalloy were described. Later, Bates and Healey, in Paper II (1942), studied the behaviour of Armco iron, and, more recently, Bates and Edmondson in Paper III (1947) have published results for cobalt.

References to earlier work by other investigators and a full description of the experimental arrangements and technique were given in Paper I and reviewed briefly in Papers II and III, so that only the barest details need be given here. The rod specimen was mounted vertically along the axis of a water-cooled solenoid supplied by a steady current which could be changed in steps. Some twenty separate copper-constantan thermocouples were arranged so that the 'hot' junction of each couple was in intimate contact with the rod, while the corresponding 'cold' junction was close to, but thermally insulated from, the rod. Each couple was joined in series with its own low-resistance primary winding, wound upon a mu-metal spiral core or ring. A low-resistance secondary coil of some 2000 turns was also wound upon the core and connected to a specially designed fluxmeter of high sensitivity. When the temperature of the rod was suddenly changed by ΔT, a current proportional to ΔT flowed for a short interval of time in each of the primary windings, so that the change of flux through the secondary

circuit caused a ballistic deflection of the fluxmeter proportional to ΔT. The instrument could usually be calibrated by producing known changes of temperature by suddenly applying a longitudinal stretching force to the rod.

§2. EXPERIMENTAL PROCEDURE

The magnetic hysteresis cycle was measured by the usual ballistic method, using a search-coil wound over the middle portion of the rod, all measurements being standardized by a calibrated Grassot fluxmeter and by a standard mutual inductance. The sources of error peculiar to the thermal measurements have been discussed in the three earlier papers, and, in the present work, the same steps were taken to avoid errors due to zero drift, lack of thermal insulation, eddy currents set up in the specimen and the effects of stray fields from the solenoid and specimen upon the mu-metal core and upon the thermocouple circuits as were used on the previous occasions.

The fluxmeter, with its electromagnetic field control, was overhauled, and its sensitivity reached that recorded by Bates and Weston, with a steady zero. In addition, we were fortunate in having at our disposal two Tinsley ballistic moving coil galvanometers of low resistance, long period and high sensitivity. One of these, with a coil resistance of 16·5 ohms, was found to be very suitable as a fluxmeter for our work, provided that its permanent magnet was suitably shunted. The makers gave 350 ohms as its critical damping resistance under their standard conditions. It was necessary to reduce this value considerably to be more in line with the resistance of the secondary of the mu-metal core, which was about 30 ohms. By the use of a magnetic shunt the sensitivity for our purposes was increased by some 80% and this figure could have been much increased by the provision of a new secondary with very many more turns.

The Tinsley instrument was very much less 'temperamental' than our own fluxmeter, and it had practically no zero drift. Its lens window was removed and a thin, carefully selected, mica disc was substituted. By very good fortune the mirror, which was of good quality, was slightly convex. This enabled the telescope to be focused on a virtual image considerably nearer to the object glass than would have been the case for the image in a plane glass mirror. The magnified scale divisions were therefore seen with excellent sharpness and clarity, particularly when a narrow rectangular stop was placed before the mirror. The increased magnification allowed the scale to be placed further from the mirror at a distance limited by the dimensions of the research laboratory, namely 9 metres. In these circumstances the sensitivity was about 80% of that of the original fluxmeter as used by Bates and Weston, but the new instrument could, of course, give the same sensitivity if it were used in a longer laboratory. It follows that efforts will be made to provide larger secondaries and longer laboratories for future work. In the present work the new instrument was used in our experiments on 42% nickel-iron and mangonic.

Reference has already been made to the calibration of the temperature measuring system by the Joule loading method. This is excellent, provided that the specimen under examination possesses a reasonably large and accurately known coefficient of linear expansion. If this is not the case, we may assume that Warburg's law holds, and measure the deflection corresponding to the complete

traversing of one cycle which we may then equate to the temperature rise calculated from $\oint HdI$. But, in some alloys, the coefficient of linear expansion is very low, and the value of overall heating so small in comparison with the observed heat changes in certain parts of the cycle, that the overall heating may not be deduced with confidence. It was therefore desirable to have a check on the values obtained by both these methods, and the following was devised.

It was found that the fluxmeter showed no deflection when comparatively large alternating currents, of the order of milliamperes, were sent through the primary windings of the mu-metal core. Hence, while it was impracticable to heat the specimen by direct current, because of 'pickup' effects with the thermocouples, it could be heated by passing an alternating current through it for a known short time, when the fluxmeter showed a deflection corresponding to the rise in temperature. The resistance of the specimen per cm. length was found and the R.M.S. current and the time of flow measured.

For the latter measurement the circuit of figure 1 was used. The alternating current was obtained from a 50 : 1 step-down transformer connected to the mains

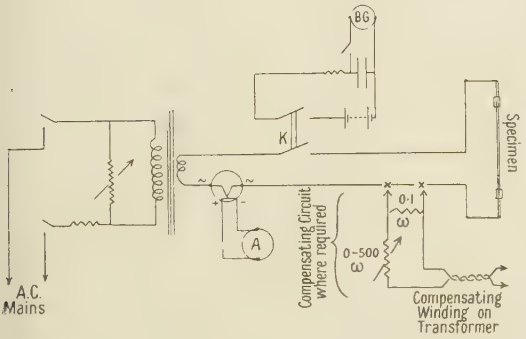

Figure 1. Circuit for A.C. calibration of the temperature-measuring system.

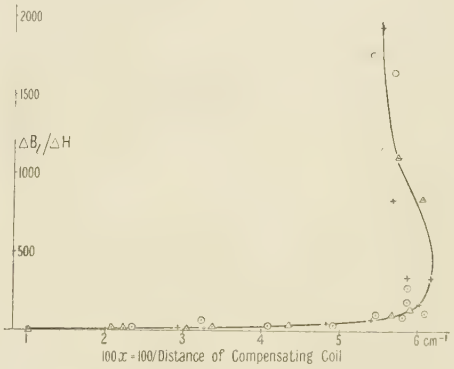

Figure 2. The behaviour of the induction effect for 36Ni—64Fe alloy.

via the resistance network shown. The current was measured by a calibrated thermo-ammeter and entered the specimen through the rigid double mercury key K, carefully arranged so that the heating circuit and the time-measuring circuit were made and broken simultaneously; the heating current was allowed to flow for about 1 second. The time-measuring circuit was of the familiar condenser discharge type. A compensating circuit was found necessary in the case of specimen W.5 to overcome rectification phenomena or pickup by the thermocouples which resulted in a sharp inductive deflection of the fluxmeter; with all other specimens this was not needed.

It is assumed, of course, that the passage of alternating current through the specimen does not produce hysteresis or eddy-current heating. This is the case when the circular magnetization it produces in the specimen is less than the longitudinal magnetization produced in the specimen by an alternating current, supplied to the solenoid, for which the fluxmeter just fails to record a heating of the specimen. In practice, a smaller current than that given by the foregoing

condition was used. Very satisfactory agreement between the three methods of calibration was obtained in all our work. We have, however, recently found that the alternating-current method is unreliable with specimens of pure iron, but it is easy to provide an explanation for the lack of agreement in these cases.

It remains now to mention a few points in which the experimental details differed from those of Papers I to III. The thermocouples were renewed and their individual resistances decreased by shortening the constantan strips; this brought the 'hot' and 'cold' junctions closer together and decreased zero drift. The hot junctions were now lightly bound to the rod with doubled waxed thread, and, since the binding completely covered the tip of each junction, temperature fluctuations and zero drift were thereby reduced. The rate of change of solenoid current with time was cut down by the insertion of a 2-henry choke in the solenoid circuit; this assisted in the reduction of eddy-current heating. The choke was, of course, shorted while the specimen was being demagnetized. Cooling water was not taken direct from the mains, but was siphoned from a reservoir through coils of lead tubing immersed in a second reservoir, so that it reached a constant temperature independent of mains fluctuations.

With some specimens, of large diameter, eddy-current heating was apparent. Its contribution to the total heating observed was estimated for each cycle from the mean thermal deflection, d, observed when the field was changed in a single step from zero to the maximum value. The sum of the deflections, Σd_1, obtained by describing the same change in magnetization in a number of steps, was subtracted from d. We know the square of the change of induction $(\Delta B)^2$, corresponding to d, and the sum of the squares of the changes of induction, $\Sigma(\Delta B_1)^2$, corresponding to Σd_1. Now, $[d - \Sigma d_1]$ must be proportional to $[(\Delta B)^2 - \Sigma(\Delta B_1)^2]$, so we can at once obtain the factor, p, say, which enables us to correct any individual reading, such as d_1, for eddy-current heating. Thus, when we observe the deflection d_1 for a known change in induction ΔB_1, then, in order to correct for eddy-current heating effects, we subtract from d_1 the quantity $p.(\Delta B_1)^2$.

Bates and Weston used a compensating coil, denoted by C in figure 4 of Paper I, to try to equalize the fluxmeter deflections obtained on traversing a given step in magnetization in the two possible directions. It was found that one asymmetry arose from induction between the solenoid and mu-metal core, which could not be lessened by placing the latter in other positions with respect to the solenoid; fortunately, it is rarely serious. Another, and much more troublesome, asymmetry was termed the *induction effect*; it appears to arise from induction between the specimen and the thermocouple materials themselves.

We examined this matter in some detail, and in figure 2 are plotted the values of $\Delta B_l/\Delta H$ against the reciprocal, x, of the distance of the compensating coil from the solenoid when exact compensation was attained, the solenoid field change, ΔH, being kept constant. For, in these circumstances, x is a measure of the asymmetry. Since ΔH varies from step to step in a cycle, we may write $x = f_1(\Delta B_l)/f_2(\Delta H)$, assuming that the change in surface induction is a function of ΔB_l, the change in longitudinal induction. Figure 2 refers to 36% nickel-iron. It appears that the surface induction effect rises to a maximum with $\Delta B_l/\Delta H$ and then falls slightly; the maximum corresponds to the setting of the compensating coil for $H \approx 0$. The circles, triangles and crosses denote measurements made with the

three cycles of magnetization, A, B, and C, with maximum fields of approximately 53, 173, and 350 oersteds, respectively.

§ 3. EXPERIMENTAL RESULTS

The materials used in the present investigation were very kindly supplied, in the hard-drawn state, by Dr. L. B. Pfeil. Their compositions, with the exclusion of that of a nickel-copper-aluminium alloy similar in composition to monel metal, except for the addition of 1·5% of aluminium, are given in the following table. Relevant portions of the largest hysteresis cycles for the several alloys are reproduced in figures 21 and 22.

Table 1

Alloy	Composition per cent						
	Ni	Cu	Fe	C	Si	Mn	S
Monel metal	67·35	30	1·4	0·15	0·1	1·0	0·01
W.5	Bal.	0·1	0·4	0·05	4·0	0·6	0·005
W.6	Bal.	0·1	0·4	0·05	2·5	0·6	0·005
36% nickel-iron	36·0	0·1	Bal.	0·05	0·15	0·5	0·005
42% nickel-iron	42·0	0·1	Bal.	0·05	0·15	0·5	0·005
48% nickel-iron	48·0	0·1	Bal.	0·05	0·15	0·5	0·005
' Mangonic '	Bal.	0·1	0·4	0·05	0·1	3·0	0·005

Monel metal

For this alloy we have the following data:

Cycle	H_m	I_r	H_c	I_m	α	R
B	173	3·6	2·1	9·3	8·0	394
C	365	8·4	2·0	22·5		

In the above list, and in others which follow, H_m is the maximum effective magnetizing field in the solenoid, expressed in oersteds; I_r is the retentivity, or residual magnetization, in gauss; H_c is the coercivity, in oersteds; I_m is the highest intensity of magnetization in a cycle, in gauss; α is the coefficient of linear expansion, in units of 10^{-6} deg^{-1} C.; R is the resistance, in microhms per cm. length of the specimen.

In the case of monel metal, the magnetization is so small that demagnetization effects and eddy current effects are negligible. The Q, I and other curves, for the virgin magnetization and for cycle C, are given in figures 3 and 4, respectively. Following the procedure of Paper I, the sum of the heat changes for the individual steps ΣdQ is denoted by Q; these changes were measured as the effective solenoid field was changed, in the case of closed cycles, from H_m to the same maximum in the opposite sense, and so on. In order to economize in graph space the values, as in figure 4, are plotted for one half-cycle only. In general, the changes in the remaining half-cycle can readily be obtained by rotating the existing Q curve about the axis of ordinates and displacing it vertically until its starting point coincides with the position originally occupied by its end point. In the same figures the values of $\int_{-H_m}^{H} HdI$ and of $\left(\int_{-H_m}^{H} HdI\right) - Q = E_T$ are plotted against I.

Warburg's law is confirmed within the limits of experimental error. The energy changes deduced from $\oint HdI$ are so minute that the Q, I curve is practically the same as the curve of internal energy E_T against I, but reversed in sign. The heat changes are large and there is little change in the general form of the curves for cycle A and for cycle B. Comparing the Q, I curves for virgin magnetization with those for the cycles, it is found that the portions of the curves beyond $I = 0$ in the latter case are practically the same as for the virgin material. It would seem that practically no thermal changes occur in the virgin material until the reversible 90° boundary displacements are succeeded, beyond the knee of the magnetization curve, by vector rotations.

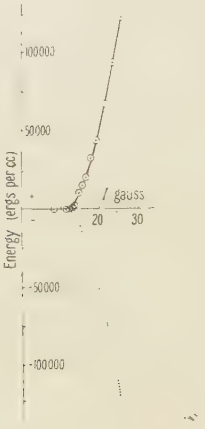

Figure 3. Virgin curve for monel metal. H_m, 365.

—— Q, I;
---- $\int HdI, I$;
. . . . $\int HdI - Q, I$.

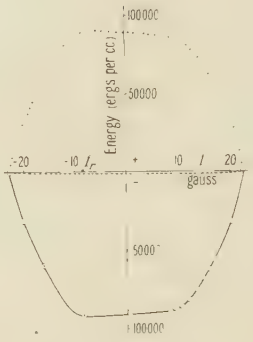

Figure 4. Monel metal. Cycle C. H_m, 365.

—— Q, I;
---- $\int HdI, I$;
. . . . $\int HdI - Q, I$.

Note.—In all the appropriate curves which follow, the Q, I curves are plotted as full lines, the $\int HdI, I$ curves as broken lines and the $\int HdI - Q, I$ curves as dotted lines, as in figures 3 and 4.

Nickel-Copper-Aluminium

The composition of this alloy is similar to that of monel metal, the main difference being the addition of 1·5% of aluminium. For cycle C the following data, expressed in the usual units, were found.

$$H_m\ 350;\quad I_m\ 2{\cdot}7;\quad I_r\ 0{\cdot}15;\quad H_c\ 9{\cdot}5.$$

With the apparatus working under normal conditions the thermal changes were too small to be recorded with certainty; this is in striking contrast with the results for monel metal. There were undoubtedly indications of slight initial cooling and subsequent slight heating effects between I_m and the knee of the hysteresis curve in the cycle measurements. A slight heating in the case of the virgin material was found beyond the knee.

These results suggest that such phenomena may be of some importance in connection with the measurement of heat losses in transformer materials exposed

to alternating-current fields, as a function of frequency. If there is any time lag between the magnetization processes and those responsible for the comparatively huge evolution and absorption of heat found with such materials as monel metal—and such processes may be present to some extent in all ferromagnetic materials—there is bound to arise a new form of heat loss, hitherto little studied, which must be a function of frequency. We must emphasize that so far we have found no proof of the existence of such time lags.

Nickel-Silicon alloys, W.5 and W.6

The magnetic and other data, expressed in the usual units, are given below:

	Cycle	H_m	I_m	H_c	I_r	α	R
W.5	A	58	17·4	3·40	3·02	10·7	355
	B	173	30·8	4·05	4·10		
	C	370	37·3	4·60	4·56		
W.6	A	58	169	18·8	103	10·0	190
	B	173	264	20·6	122		
	C	365	318	20·2	210		

Demagnetization effects were negligible in the case of W.5; for W.6 the demagnetization factor was assumed to be that of an ellipsoid of revolution with the same length-to-diameter ratio. Eddy current effects were absent. The Q, I and cognate curves for W.5 are shown in figures 5 and 6. The thermal changes are

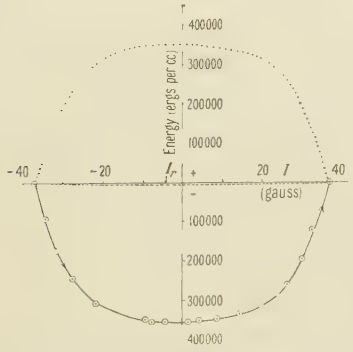

Figure 5. Alloy W.5. Cycle C. Hm, 370.

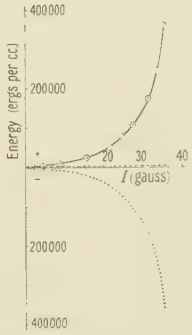

Figure 6. Alloy W.5. Virgin curve. Hm, 370.

enormous; once again the E_T curves are practically mirror images of the Q curves. We have had little opportunity of making measurements at different temperatures, and we do not feel that the present apparatus is well designed for the purpose, but some preliminary measurements were made with W.5 by cutting off the solenoid cooling water to cause rises of temperature from 17° c. to 25° c. and to 42° c. At 25° c. the heating effects of cycle B were halved, and at 42° c. reduced to one fiftieth of their original value; more work on these phenomena is clearly necessary.

The Q, I curves for W.6 vary so much with H_m that the results for the three representative cycles as well as the virgin curve are shown in figures 7, 8, 9 and 10.

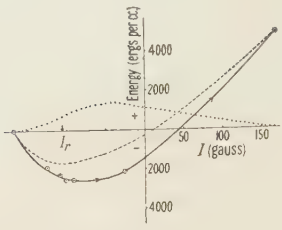

Figure 7. Alloy W.6. Cycle A. H_m. 58.

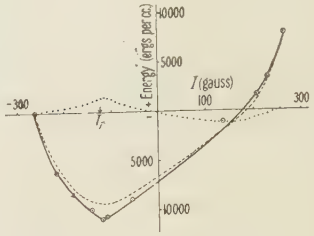

Figure 8. Alloy W.6. Cycle B. H_m, 173.

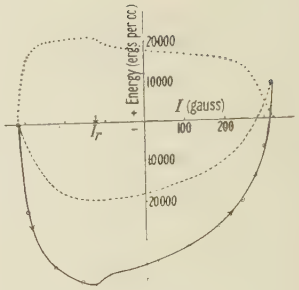

Figure 9. Alloy W.6. Cycle C. H_m, 365.

The Q curve for cycle A is very reminiscent of the corresponding curves for hard-drawn nickel obtained by Bates and Weston, although for W.6 the E_T curve lies above the I axis and its maximum is not at $I = I_r$; but it must be mentioned that the energy scale is so extended that the reliability of the measurements may be over-estimated. The really interesting feature is that as H_m increases, the Q curve becomes more accentuated or "peaked", which is a very unusual phenomenon in our work. Obviously, an abnormal change is taking place at $I = I_r$.

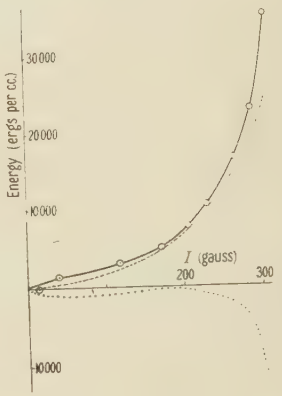

Figure 10. W.6 alloy. Virgin curve. H_m, 365.

Nickel-Iron alloys

The first of these alloys, 36% nickel-iron, approximates in composition to invar, which was examined by Bates and Weston (1940, 1941). The present data, in the usual units, were as follows: the sequence of H_c values with increase in H_m is rather unusual.

Cycle	H_m	I_m	H_c	I_r	α	R
A	52	787	4·86	440	2·3	415
B	167	862	4·43	430		
C	362	910	4·04	440		

Loads as great as 4 kgm. produced no measurable Joule cooling, which would indicate a value of α of the order of $0{\cdot}01 \times 10^{-6}$ per deg. C., whereas between 20° and 120° C. we found α to be $2{\cdot}3 \times 10^{-6}$ by direct experiment. The fluxmeter system could not be calibrated on the basis of Warburg's law, because the values of $\oint HdI$ were so small, and in this instance the alternating-current heating method of calibration was extremely valuable.

Some of the results obtained with 36% nickel-iron are reproduced in figures 11, 12 and 13. The first two figures provide an excellent example of the flattening of the Q, I curves with increase in H_m for measurements between the remanent point and the knee in the reverse quadrant of the I, H curve. The portion of the Cycle C, figure 12, from $I = 0$ to $I = I_m$, is practically identical in form with the virgin Q curve of figure 13. Bates and Weston made measurements

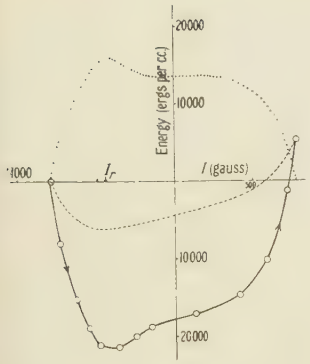

Figure 11. 36Ni, 64Fe alloy. Cycle A. H_m, 52.

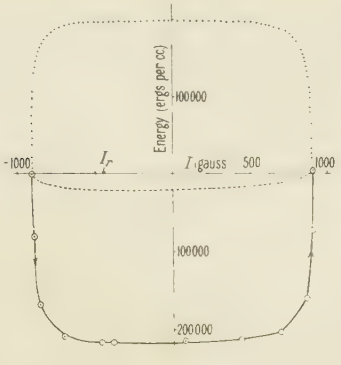

Figure 12. 36 Ni, 64Fe alloy. Cycle C. H_m, 362.

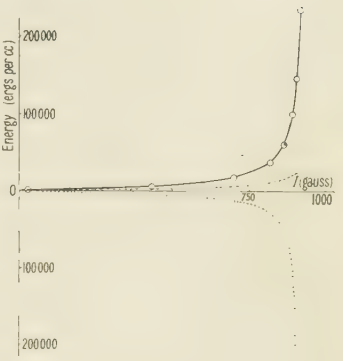

Figure 13. 36Ni, 64Fe alloy. Virgin curve. H_m, 363.

on an alloy of similar composition; they obtained results of the same nature, but the overall range of thermal change in their work was less than one-third of that which would be expected from the present investigation. However, it is well known that slight changes in composition around that of invar have large effects on the coefficient of expansion. The smallness of the latter coefficient for invar has been attributed to the variation with temperature of the spontaneous magnetization giving rise to magnetostriction changes of dimensions which compensate those of ordinary thermal origin during a small temperature change.

The second of these alloys, 42% nickel-iron, gave the following data, in the usual units:

Cycle	H_m	I_m	H_c	I_r	α	R
A	52·3	1017	6·3	697	6·4	482
B	167	1133	6·2	698		
C	363	1157	6·2	690		

Some of the results are shown in figures 14, 15 and 16. An alloy of approximately the same composition was studied by Bates and Weston, but their specimen contained rather more carbon, silicon and manganese than the present one. However, it is satisfactory to note that they obtained the same type and degree of cooling for the intermediate cycle B, the only one which they investigated.

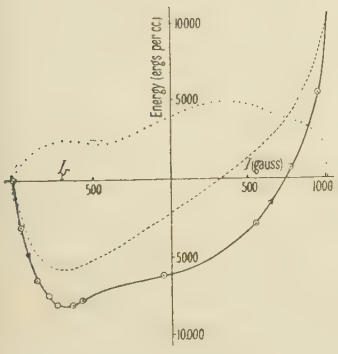

Figure 14. 42Ni, 58Fe alloy. Cycle A. H_m, 52·3.

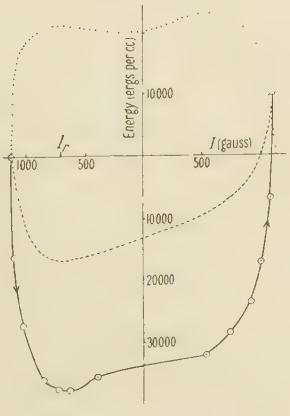

Figure 15. 42Ni, 58Fe alloy. Cycle B. H_m, 167.

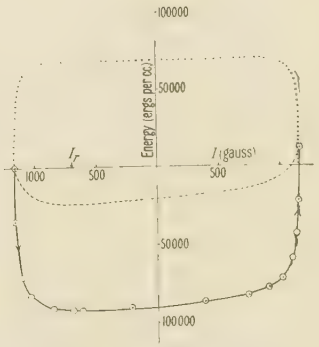

Figure 16. 42Ni, 58Fe alloy. Cycle C. H_m, 363.

The accompanying figures are reproduced here partly to draw attention to the existence of a peak around I_r which is flattened out as H_m is increased. The virgin curve is not reproduced, as it is identical in shape, within the limits of experimental error, with that part of figure 16 between $I = 0$ and $I = I_m$. The peak was not found by Bates and Weston; it may be due to the large magnetostriction effects which the alloy is known to exhibit, and which, no doubt, are sensitive to slight differences in composition.

Mangonic

This alloy, consisting of pure nickel alloyed with 3% manganese, gave the following data, in the usual units:

Cycle	H_m	I_m	H_c	I_r	α
A	56·2	307	19·2	232	11·8
B	171·1	418	20·8	267	
C	362·5	466	20·7	269	

The relevant curves are shown in figures 17, 18, 19 and 20. As in the case of W.6,

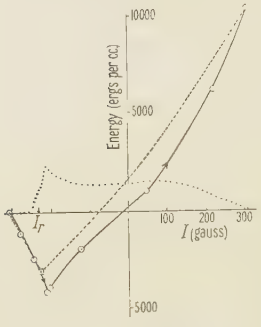

Figure 17. Mangonic. Cycle A. H_m, 56·2.

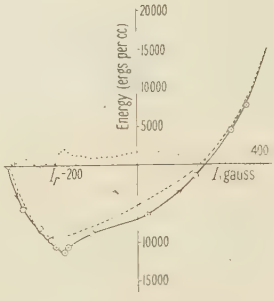

Figure 18. Mangonic. Cycle B. H_m, 171.

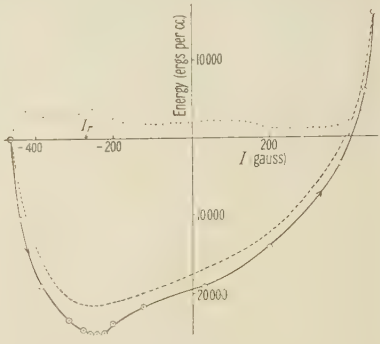

Figure 19. Mangonic. Cycle C. H_m, 362.

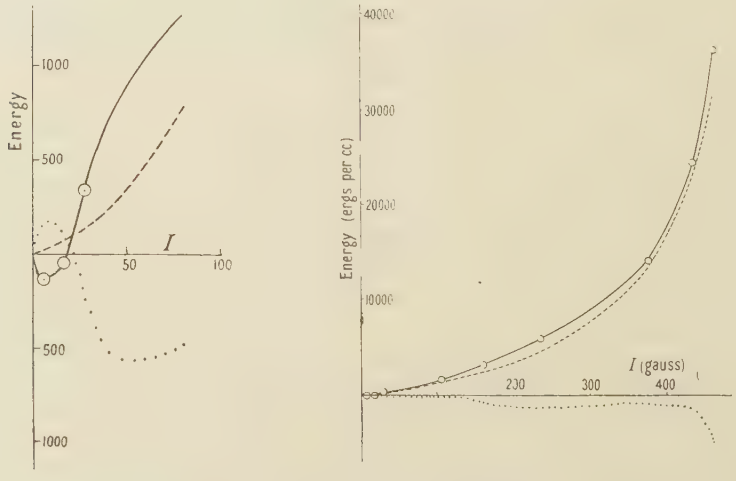

Figure 20. Mangonic. Virgin curve.
(Left-hand curve—portion near origin on enlarged scale.)

a marked peak is found around I_r; the summit of the peak in the E_T, I curve coincides with the knee of the descending quadrant of the hysteresis curve. With increasing values of H_m the protuberance in the Q curve tends to become more rounded, and, no doubt, it would vanish if we could use sufficiently high values of H_m. For the largest cycle there are no less than three definite peaks in the E_T, I curve.

The virgin curve was difficult to obtain, and this is understandable when the initial portion in the immediate neighbourhood of the origin is plotted on an enlarged energy scale. There must, clearly, be much ambiguity in regard to the orientation of the domain vectors in the demagnetized state. In view of the close connection which one supposes to exist between the permeability of the material in the demagnetized state and that in the region $I = I_r$, similar ambiguity must exist in the latter region. It is thought to be essentially a problem in transverse magnetization, to be tackled along the lines of the suggestions made by Von Engel and Wills (1947) and by Takagi (1939). These amount to the postulate that the distribution of domain vectors in a solid angle $d\omega$ oriented in a direction θ with respect to a direction of easy magnetization in a ferromagnetic crystal obeys an exponential expression of the form $dv_\theta = C \exp(-E/E_0) d\omega$, where E_0 is a quantity whose precise physical significance is at present unknown.

§ 4. DISCUSSION

In conformity with the earlier papers we equate the energy HdI supplied to a ferromagnetic substance in any part of a hysteresis cycle to the sum of the change in energy which manifests itself as an increase in temperature, and which is denoted by dQ in this work, and the change in internal energy dE. We may therefore write

$$HdI = (\partial E/\partial I)_T dI + (\partial E/\partial T)_I dT,$$

or

$$\int (\partial E/\partial I)_T dI = \int HdI - Q,$$

so that the $\left(\int HdI - Q\right), I$ curves allow us to follow the variation of $(\partial E/\partial I)_T$ with I. The appropriate curves for the measurements with these alloys are given in the preceding figures.

We find that every virgin Q, I curve with the exception of 'mangonic' lies entirely above the I axis, and that there is a marked cooling on reducing the magnetization from I_m to I_r. In the case of large cycles, i.e., large H_m, there appears to be a flattening out of the Q, I curves between I_r and the value of I at the knee of the magnetization curve in the reverse quadrant. We think that this flattening is illusory in most instances, because the larger the cycle the larger are the initial cooling and the final heating effects, and upon these the much slighter departures from linearity, or peaks, such as the one in figure 14, are superimposed. The necessary changes in scale of the several figures also make it difficult to distinguish these departures, and, in any case, it is difficult to measure with accuracy a small quantity superimposed upon a much larger one.

Every E_T, I curve for a closed cycle lies above the I axis, and some of these curves are almost mirror images of the corresponding Q, I curves. It is perhaps advisable to point out that they lie above the I axis because we take the latter as a

datum line, whereas it would be more correct, if much less convenient, to take the horizontal line through the maximum value of E_T on the virgin E_T, I curve.

In all cases the E_T, I curve has a maximum around $I = I_r$. In several instances it is very sharply defined, and we clearly have evidence of a special phenomenon occurring just before the knee of the demagnetization curve. At first sight one might be inclined to associate the phenomenon with that recently described by Hobson (1947), who finds pronounced peaks superimposed in the hysteresis cycles traced on an oscillograph screen. But Hobson used ferromagnetic wires of unstated nature and composition and he has not yet published his experimental arrangements. Consequently, we cannot rule out the possibility that the peaks he observed were due to eddy currents.

We can, of course, say that the heating phenomenon observed in the experiments described in this paper are due to the change in the type of magnetization from what Néel (1944) terms Type III to Type II. This means that at very high fields the domain vectors lie along the direction of the applied field (Type IV); at less high fields they lie along the particular direction of easy magnetization most nearly parallel to the field (Type III); at lower fields they lie along one of the three directions of easy magnetization (Type II), while at very low fields they lie along all directions provided by the axes of the crystal cube (Type I).

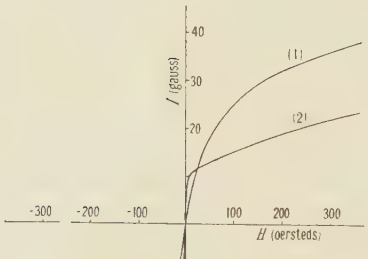

Figure 21. Descending portion of cycle C curve for (1) W.5, (2) Monel metal.

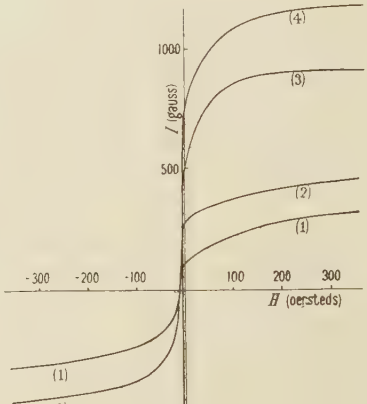

Figure 22. Descending portion of cycle C curve for (1) W.6, (2) Mangonic, (3) 36% Ni-Fe, (4) 42% Ni-Fe.

§ 5. ACKNOWLEDGMENTS

We are deeply indebted to the Government Grant Committee of the Royal Society and to Imperial Chemical Industries Ltd. for the supply to L.F.B. of much of the apparatus used in this investigation. We are similarly indebted to Dr. L. B.

Pfeil of the Development and Research Department of the Mond Nickel Co., Ltd., for the provision of specimens and much helpful advice.

REFERENCES

BATES, L. F., and WESTON, J. C., 1940, *Nature, Lond.*, **145,** 551.
BATES, L. F., and WESTON, J. C., 1941, *Proc. Phys. Soc.*, **53,** 5.
BATES, L. F., and HEALEY, D. R., 1942, *Proc. Phys. Soc.*, **55,** 188.
BATES, L. F., and EDMONDSON, A. S., 1947, *Proc. Phys. Soc.*, **59,** 329.
HOBSON, P. T., 1947, *Nature, Lond.*, **159,** 436.
NÉEL, L., 1944, *Journ. de Phys. et le Radium*, **5,** 241.
TAKAGI, M., 1939, *Sci. Rep. Jôhoku Univ.*, **28,** 20.
VON ENGEL, A., and WILLS, M. S., 1947, *Proc. Roy. Soc.*, A, **188**, 464.

(*Note added in proof.* By a strange accident in transcription the $\int HdI$, I curve of figure 3 is plotted below, instead of above, the I axis.)

The Adiabatic Temperature Changes Accompanying Magnetization in Low and Moderate Fields : A Further Study of Iron

BY L. F. BATES AND E. G. HARRISON
University College, Nottingham

MS. received 15 *August* 1947; *read* 8 *November* 1947

ABSTRACT. It has been found possible to use a commercial instrument in place of a ' home-made ' fluxmeter with the Bates and Weston method of measuring small changes of temperature. The new instrument has been employed to make a further study of the small heat changes which accompany step-by-step changes in the magnetization of iron, using the specimen of annealed Armco iron previously studied by Bates and Healey, and a specimen of H.S. Electrolytic iron (Hilger). In the course of the work the heat changes associated with the virgin magnetization curve have been obtained for the first time.

§ 1. INTRODUCTION

THE heat changes which accompany step-by-step changes in the magnetization of ferromagnetic materials have been studied in some detail by Bates and Weston (1941), Bates and Healey (1943), Bates and Edmondson (1947) and Bates and Harrison (1948). In the present communication we are concerned with measurements on iron, which has proved to be the most difficult metal with which to obtain reliable measurements. Bates and Healey experienced very much trouble from eddy current effects in this material, from strange induction effects and from phenomena which they believed to be associated with a discontinuity in the I, H curve of the kind predicted by Akulov (1931), in addition to the very considerable experimental difficulties inseparable from the measurement of the extremely small changes in temperature, whose order of magnitude may be inferred from a knowledge of the hysteresis cycle. They felt that time-lag effects might also upset their measurements, and they therefore deliberately

sacrificed sensitivity in order to obtain greater stability of zero of the instrument, a special kind of fluxmeter with electromagnetic control, whose deflection recorded the temperature changes.

It occurred to one of us that a Tinsley, Type 4789, moving coil ballistic galvanometer, resistance 17 ohms, might well replace the 'home-made' instrument previously used in all this work. Through the kindness of Imperial Chemical Industries, Limited, two of these galvanometers were obtained on loan, and the more suitable for our purpose was immediately adapted as follows. As the permanent magnet in the galvanometer was much too powerful, it was 'shorted' by the bridging of its gap with safety-razor blades, the number of blades being more or less determined by other factors, such as the impedance of the secondary winding on the mu-metal spiral core, referred to below. The galvanometer mirror was of good quality, and, fortunately, was slightly convex with a radius of curvature of the order of 7 metres. The lens fitted in the galvanometer case was therefore removed and replaced by a mica window, covered by a diaphragm with a suitable horizontal slit. This allowed the lamp and scale to be placed about 9 metres from the galvanometer, and thus a sensitivity was obtained some 70% of the maximum attained with the 'home-made' instrument, and equal to about 12×10^{-6} °c. per mm. scale deflection. However, this is actually a slight improvement on that used by Bates and Healey; and, in addition, there was much greater stability of zero and a sensitivity which was remarkably constant whatever specimen of ferromagnetic material was under examination, so that optimum conditions could always be relied upon. This enhanced stability was in part due to a new method of attaching the thermojunctions by means of binding thread instead of ebonite collars and grub screws. The sensitivity could, of course, be increased by using even greater scale distance, for the quality of the mirror and the sharpness of the divisions in the field of view would easily permit this to be done, but this would involve taking over another laboratory. The scale divisions could be read to 0·1 mm. with ease.

It was therefore decided to repeat certain of the measurements made on Armco iron, 99·89 per cent pure, by Bates and Healey, and to extend the measurements to a specimen of Hilger H.S. Electrolytic iron, 99·96 per cent pure. The latter is reported to contain 0·02 per cent non-metals of no spectroscopic interest, 0·01 silicon and 0·01 per cent metals other than iron. It is supplied as rods approximately 5 mm. in diameter and 17·5 cm. long. Two of these rods were tapped and screwed together to make a rod 34 cm. long, and the magnetic and thermal measurements were carried out on the middle few centimetres of each part of the composite specimen, thus avoiding the small region around the junction of the two rods.

§ 2. EXPERIMENTAL DETAILS

As in the previous measurements, the specimen rod was mounted vertically along the axis of a water-cooled solenoid which gave a field of 121·7 oersteds per ampere when supplied by a steady current which could be varied in discrete steps. Adiabatic temperature changes of the rod were measured by means of twenty copper-constantan thermocouples. The 'hot' junction of each couple was bound in loose contact with the rod, while the 'cold' junction was very close to, yet thermally insulated from, the rod except for conduction along the material of the couple. Each couple was joined in series with its own primary

winding of low-resistance copper wire wound upon a mu-metal spiral core or ring. A low-resistance secondary coil of 2000 turns was wound upon this core and connected to the ballistic galvanometer. The secondary coil used in the present work could, with advantage, have consisted of many more turns of finer copper wire, for the critical resistance of the unmodified galvanometer circuit was 550 ohms, although it was reduced to 100 ohms by our modifications, while the resistance of the secondary was only about 40 ohms; but we were unable to arrange for another core and winding to be supplied within a reasonable time. Twenty identical thermocouples were used, and as each one was in series with its own primary coil on the spiral core, electrical insulation between the 'hot' junctions and the rod was unnecessary. The close proximity of the junctions minimized thermoelectric currents due to temperature fluctuations inside the solenoid, but the galvanometer showed much tendency to drift when large solenoid currents were supplied; this drift was traced to vibrational movements of the specimen within the heated enclosure.

When the temperature of the specimen was suddenly changed by a small increment ΔT, a current strictly proportional to ΔT flowed in each thermocouple circuit and remained constant for a short interval of time. Each primary coil therefore produced its contribution to the total change in flux in the mu-metal core, and there resulted a deflection of the ballistic galvanometer proportional to ΔT. The arrangement was calibrated by producing standard adiabatic changes of temperature, of the order of 0·001° c., by the sudden application of a longitudinal stress of F dynes to the specimen, when a fall of temperature $\Delta T_1 = -\alpha TF/QA$ resulted, where α is the coefficient of linear expansion of the specimen, T its absolute temperature, A its area of cross-section and Q the quantity of heat required to raise the temperature of 1 cm^3 of the specimen by 1° c. (Another method of calibration is possible with certain materials, but was not felt to be reliable in the case of iron; see Bates and Harrison 1948.)

The several sources of error peculiar to the work have been fully discussed in the earlier papers, and only the special arrangements made to neutralize the large induction effects need be mentioned here. The latter were not only large but difficult to interpret; for example, without any reason being apparent, it was necessary at times to change the sense of the compensating coil used to neutralize sharp inductive deflections of the galvanometer which otherwise preceded the more leisurely, true, thermal deflections. A single turn of wire had also to be connected around the magnetizing solenoid to act as part of the compensating coil. The reasons for these large inductive effects have never been elucidated. The authors are inclined to believe that they are due to large variations in magnetization and in the electrical conductivity of the surface from place to place, but they may provide evidence that closure domains (Kittel 1946) or *domains de fermeture* (Néel 1944), which are made manifest by the well-known Bitter figures in the case of single crystals of iron etc., are not effective in polycrystalline materials.

It has been frequently emphasized that, if the effects of induction on thermocouples etc. could be sufficiently reduced, they could be completely eliminated by taking half the sum of the galvanometer deflections obtained when a chosen step in magnetization is traversed in the two possible directions. For example, if one described a hysteresis cycle with a maximum range of field from $+H_m$ to $-H_m$ and thence to $+H_m$ oersteds, one would expect to obtain equal galvano-

meter deflections on changing the field from $+H_m$ to $+H_1$ and from $-H_m$ to $-H_1$ oersteds, under ideal conditions with no induction effects present. It was assumed that, if the latter were in the same sense as the thermal effects in the $+H_m$ to $+H_1$ change, they would be in the opposite sense in the $-H_m$ to $-H_1$ change, so that the mean galvanometer deflection would give the true thermal change. Fortunately the authors did not find the marked asymmetry found by Bates and Healey, possibly because a larger choke coil was used in series with the magnetizing solenoid to reduce the rate of change of the magnetic field.

It must again be reported that in the case of iron there is no satisfactory proof of Warburg's law, viz., the energy dissipated in one complete hysteresis cycle is $\oint HdI$ ergs per cm^3. Eddy current heating played a very large part in these measurements, and there was a large difference between the heat calculated from the magnetic hysteresis cycle data and the nett total heating observed directly when one complete cycle was described. It was assumed that Warburg's law was true and that the above difference was due entirely to eddy current heating. A calculation was therefore made of the sum of the squares of the individual magnetic induction changes of the specimen made during the complete cycle; this was denoted by $\Sigma(\Delta B_1)^2$, and $q.\Sigma(\Delta B_1)^2$ equated to the difference between the thermal change observed directly and that calculated from the magnetic data, q being a constant correcting factor. Thus if a thermal deflection d_1 was observed when a change in induction ΔB_1 was made, the true thermal deflection corrected for eddy current heating was taken to be $d_1 - q.\Delta B_1{}^2$. The several values of q found for the three main hysteresis cycles performed in this work were equal within the limits of experimental error of about 2 per cent, so that the assumption that it was constant was justified.

The magnetic hysteresis cycle was found by the usual ballistic method using a search coil wound on the specimen and connected to a ballistic galvanometer standardized with a Grassot fluxmeter and a standard mutual inductance. The vertical component of the earth's magnetic field was compensated using a separate winding on the solenoid. Correction was made for the demagnetization effects of the free poles at the ends of the specimen by means of a theory of Becker and Döring (1939) which states that the slope of the virgin curve at the origin, i.e. in the region where the Rayleigh law holds, is equal to

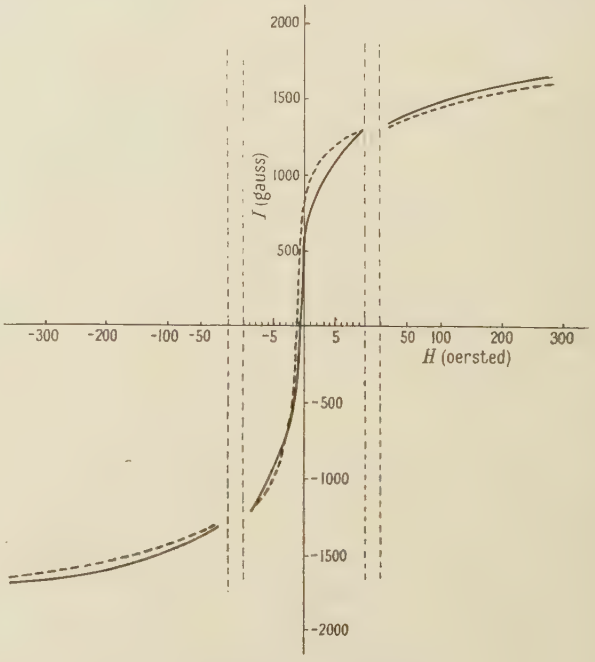

Figure 1. *I, H* curves.
- - - - - Armco iron; ——— Hilger H.S. iron.

1/0·364 times that of the I, H curve at the point $I=I_r$, $H=0$, in the case of annealed iron. If the slope of the former is found to be x, and a line of slope $0{\cdot}364x$ is drawn on the uncorrected I, H graph touching the upper, or descending, portion of the hysteresis curve, then the value of H at the point of contact divided by that of I at the same point is equal to the demagnetization factor, because this point must be transferred to the I axis when correction is made for demagnetization. The values of the demagnetization factor so found for the Armco iron specimen were 0·0033 for all three cycles, while for the Hilger iron specimen they were 0·0081, 0·0083 and 0·0086 for cycles A, B and C respectively. The relevant portions of the I, H curves for the larger cycles are given in figure 1. It will be noted that the values of I_r are small in both cases.

§ 3. EXPERIMENTAL RESULTS

Table 1
Armco iron —Magnetic data for cycle C

H_{oersteds}	$H_{\text{corrected}}$	I_{gauss}
−373·4	−367·9	−1650
−248·3	−243·0	−1584
−116·1	−111·2	−1467
− 60·9	− 56·3	−1388
− 16·75	− 12·50	−1288
− 5·36	− 1·80	−1070
− 3·26	− 0·53	− 823
− 2·07	+ 0·25	− 668
0·00	+ 0·91	− 275
+ 2·25	+ 0·98	+ 385
+ 5·24	+ 2·75	+ 732
+ 9·60	+ 5·90	+1110
+ 16·9	+ 12·8	+1240
+ 62·7	+ 58·1	+1386
+117·3	+112·4	+1460
+250·5	+245·2	+1585
+373·4	+367·9	+1650

Table 2
Hilger iron—Magnetic data for cycle C

H_{oersteds}	$H_{\text{corrected}}$	I_{gauss}
−369·0	−354·4	−1692
−240·3	−227·8	−1449
−111·0	− 99·5	−1333
− 58·5	− 47·7	−1253
− 32·7	− 22·5	−1185
− 15·80	− 6·85	−1039
− 9·01	− 2·11	− 802
− 4·60	+ 0·03	− 539
− 1·42	+ 0·62	− 238
0·00	+ 0·61	− 71
+ 1·34	+ 0·61	+ 85
+ 4·63	+ 1·20	+ 399
+ 8·91	+ 2·76	+ 715
+ 16·00	+ 7·54	+ 985
+ 33·0	+ 23·0	+1164
+ 59·3	+ 48·6	+1242
+112·6	+101·2	+1327
+242·0	+229·5	+1446
+369·0	+354·4	+1692

The more important experimental results are set out in tables 1 and 2 and in the accompanying graphs. The numerical data on which figure 1 is based are given in order that the effect of the demagnetization correction may be fully appreciated. Turning first to the results for annealed Armco iron, which is stated to contain carbon 0·03 %, silicon 0·01 %, manganese 0·03 %, sulphur 0·02 % and phosphorus 0·02 %, it must first be

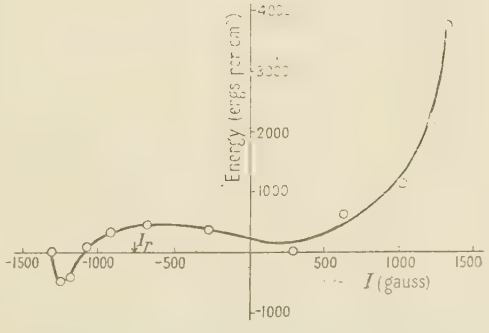

Figure 2. Annealed Armco iron Q, I curve. H_m, 23·9.

emphasized that the present data are much more extensive than those obtained by Bates and Healey, as results have been obtained for much smaller hysteresis cycles and, for the first time, for magnetization from the virgin state. For example, figures 2 and 3 have no counterpart in the earlier paper. The experimental difficulties of obtaining figure 2 were considerable; this is apparent in the distribution of the experimental points about the curve drawn through them. Both the figures show clearly that it is necessary to go to still lower fields to avoid the initial cooling observed in the early stages of decreasing the field from its maximum value. The 'knee' of the virgin part of the I, H curve lies at about 10 oersteds, and the initial cooling on demagnetization is obviously confined to starting fields greater than this value.

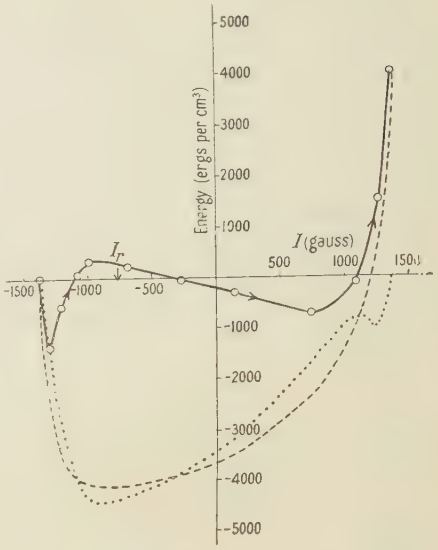

Figure 3. Annealed Armco iron cycle A. H_m, 58.
——— Q, I; - - - - - $\int HdI, I$;
. . . . . $\int HdI - Q, I$.

As is usual in this work, only one half of the experimental points are plotted, in order to economize in graph space. In each graph the heat changes ΣdQ are denoted by Q; these were measured as the effective solenoid field was changed step by step from the stated maximum value

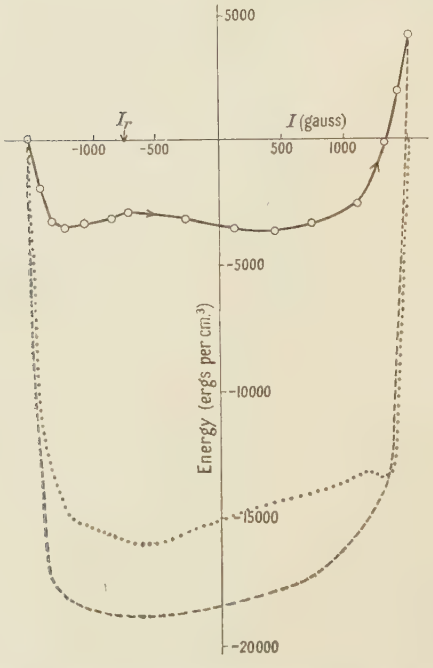

Figure 4. Annealed Armco iron cycle B. H_m, 178.
———Q, I; - - - - - $\int HdI$; . . . . . $\int HdI - Q, I$.

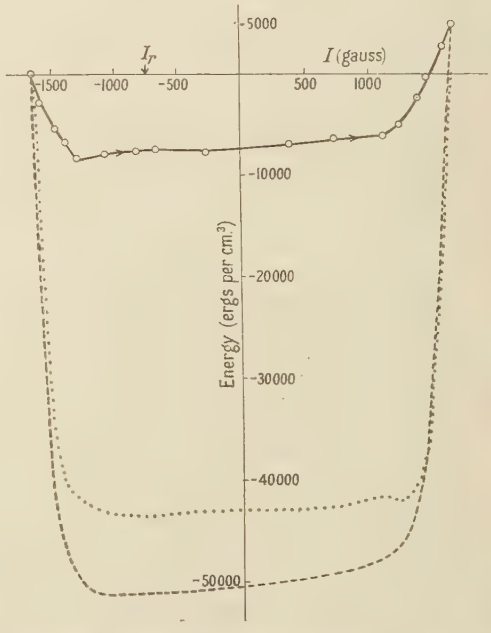

Figure 5. Annealed Armco iron cycle C. H_m, 365.
———Q, I; - - - - - $\int HdI, I$; . . . . . $\int HdI - Q, I$.

$(-)H_m$ to the same maximum $(+)H_m$ in the opposite sense, and Q is plotted as a function of I. In general, each graph should be completed by rotating the printed Q curve about the axis of ordinates and displacing it vertically until its new starting point coincides with its end point. The values of $\int_{-H_m}^{H} HdI$ and of $\int_{-H_m}^{H} HdI - Q$ are also plotted as a function of I.

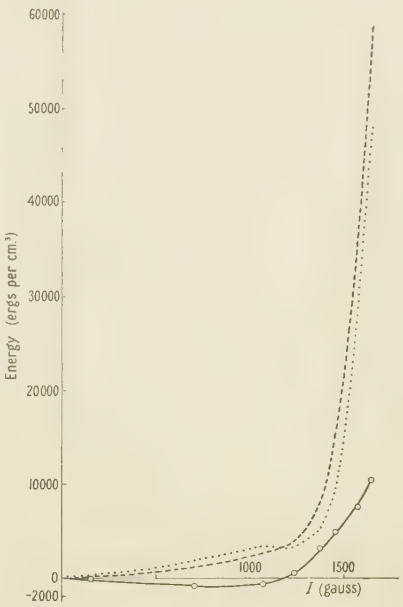

Figure 6. Annealed Armco iron. Virgin curve. H_m, 370.
——Q, I; - - - - -$\int HdI, I$;
. . . . . $\int HdI - Q, I$.

Figures 4 and 5 should be compared with figures 6 and 7 given by Bates and Healey. On the whole, there is good agreement as far as the general course of the phenomena is concerned, although our experiments lead us to conclude that the Q, I curves always slope upwards to the right between the limits of I equal to I_r and to $-I_r$. on the ordinary I, H curve, in agreement with the finding of Hardy and Quimby (1938). There is, however, definite evidence that the pronounced hump of figure 3 persists to some extent in all the curves, although it tends to be suppressed by large changes in the scale of the figures in the larger cycles. The $\left(\int HdI - Q\right), I$ curves, later referred to as E_T, I curves, show a kink on the right side only, whereas Bates and Healey obtained traces of a kink on the left side as well, cf. their figure 6.

The results for magnetization of the virgin material shown in figure 6 are very unusual; this is the only example known to the authors of an annealed material which cools as it is magnetized for the first time, starting from the unmagnetized state. There is, of course, a lack of definiteness about the

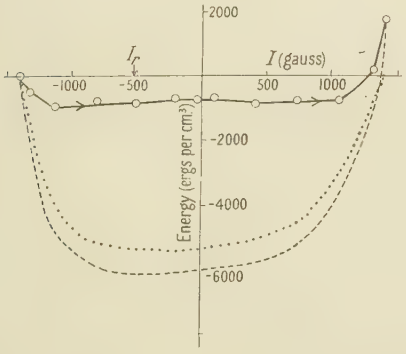

Figure 7. Hilger iron cycle A. H_m, 57.
—Q, I; - - - - -$\int HdI, I$; . . . . .$\int HdI - Q, I$.

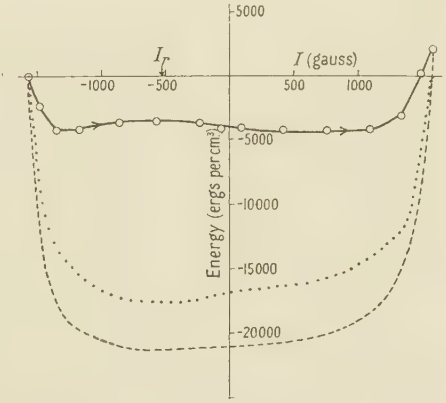

Figure 8. Hilger iron cycle B. H_m, 178.
——Q, I; - - - - -$\int HdI, I$; . . . . .$\int HdI - Q, I$.

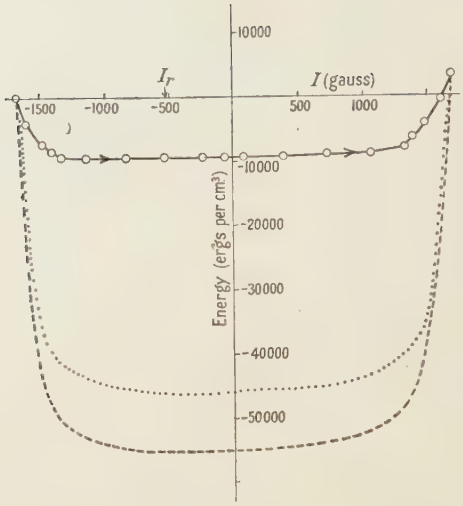

Figure 9. Hilger iron cycle C. H_m, 365.
——Q, I; - - - - -$\int HdI, I$; . . . . .$\int HdI - Q, I$.

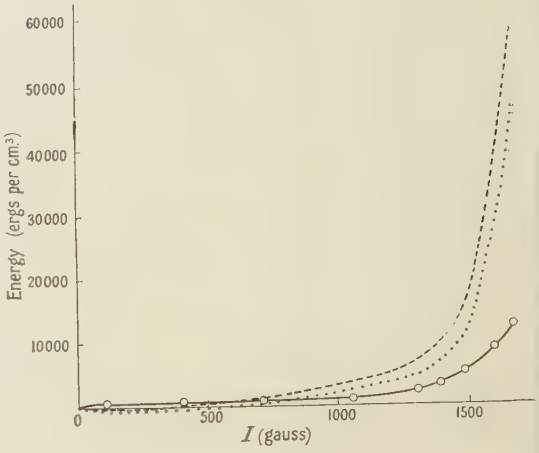

Figure 10. Hilger iron. Virgin curve. H_m, 370.
——Q, I; - - - - -$\int HdI, I$; . . . . .$\int HdI - Q, I$.

unmagnetized state; the specimen was demagnetized by gradually reducing to zero a large alternating current in the solenoid, with the choke coil removed.

The thermal results for Hilger iron are plotted in figures 7, 8, 9, 10 and 10*a*; at once a striking contrast between Armco iron and Hilger iron is evident when figures 3 and 7 are compared: there is only a trace of a hump in the latter curve. The Hilger iron was used exactly as received; it was not subjected to any special annealing process by us. The overall heat losses for a complete cycle may be quickly read from the graphs, and, comparing figure 8 with figure 2*a* given by Bates and Healey for unannealed Armco iron, there is little doubt that the latter iron was magnetically much harder than the Hilger iron. The great difference between the compositions of the two irons clearly lies in the carbon content, and one would naturally seek to explain the hump of figure 3 in terms of the higher carbon content of the Armco iron. Unfortunately, this does not appear to be possible, for we should expect carbon to produce effects similar to those

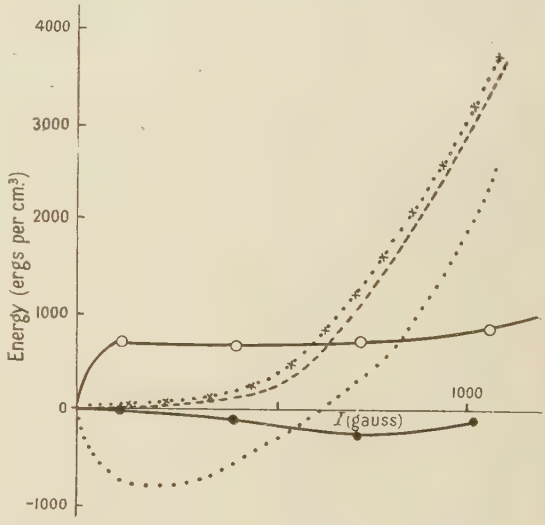

Figure 10*a*. Hilger iron. Virgin curve showing effects of mode of demagnetization.
—⊙— Q, I demagnetized from maximum field of 370 oersted.
—●— Q, I demagnetized from field of 7·4 oersted.
- - - - - $\int HdI, Q$.
. × . . × $\int HdI - Q, I$ for —●— curve.
. . . . . $\int HdI - Q, I$ for —⊙— curve.

reported by Adelsberger (1927) and Constant (1928) in their pioneer work on steels, namely, a more or less continual evolution of heat as the field changes from $+H_m$ to $-H_m$, with a marked evolution of heat as the magnetization changes from $+I_r$ to $-I_r$.

One cannot fail to notice an interesting feature of the hump of figure 3 and of the humps in later figures. If the hump is inverted, it is obvious that the Q, I curve becomes smooth and continuous. It is interesting, too, that if we measure the area enclosed between the hump and a line drawn to touch the lowest portions of the Q, I curves, we find that it is a maximum for cycle A in the case of Armco iron and for cycle B in the case of Hilger iron. It seems fairly safe to presume that for very large values of H_m the hump would completely disappear.

The virgin curve for Hilger iron, shown in figure 10, was obtained after the specimen had been demagnetized by exposing it to a steady field H_m and then to a large alternating field which was gradually reduced to zero, exactly as was done in the case of Armco iron to obtain figure 6. There is no sign of cooling in figure 10, but, again, the unmagnetized state is not uniquely defined, as is seen from figure 10 *a*, where the encircled points of figure 10 are plotted on an enlarged scale for comparison with the points represented by the filled-in circles. The latter points were obtained when the specimen was demagnetized after reaching a field of 7·4 oersteds only, so that the magnetic state was always below the 'knee' of the hysteresis curve. Naturally, the 'filled-in' points were found after one or two preliminary sets of observations had been made and discarded; it is seen that a small cooling effect emerges.

We feel justified in attempting to explain this behaviour on the lines set forth by Néel (1944). He suggests that the I, H curve for a single crystal of iron may be treated in four parts—termed I, II, III and IV, respectively. In part I the crystal is supposed to be magnetically isotropic with the applied field insufficient to overcome the self-demagnetization field, so that within the crystal the field of external origin is neutralized. The domain vectors may then set along six possible directions of easy magnetization, and it may be presumed that the conditions suggested by Von Engel and Wills (1947) also apply. In part II the applied field overcomes the self-demagnetization field, and there is a small resultant field within the crystal acting along a ternary axis, so that the domain vectors can now set along the three directions equally inclined to that axis. In part III the resultant field is large, so that two domain directions only are possible. Finally, when the resultant field becomes very large, we have the state of part IV, in which the vectors are aligned in one direction only. Thus, in part I we are really dealing with a six-phase system as far as the domains are concerned, and it would be truly remarkable if their distributions were the same (*a*) when an ordinary specimen was demagnetized after reaching the state of part IV, and (*b*) after reaching the state of part II at most; indeed, practically any theory of magnetization processes would lead to a similar result.

Néel's treatment leads to the conclusion that, in a bar cut from a single crystal of pure iron parallel to the binary axes and acted on by a field parallel to the axis, the elementary domains are disc-shaped, like fillets perpendicular to the axis. Thus, one may picture a slab cut from a single crystal as made up of transverse slices whose planes are perpendicular to the long axis of the slab, each forming a domain, and magnetized in such a way that there are no free poles inside the material. To avoid the formation of powerful free poles on the lateral surfaces

of the slab, small prism-shaped domains, called closure domains (*domains de fermeture*), abutting upon the edges of the main domains, cause the condition of uniformity of flux to be maintained and close the flux paths of neighbouring discs.

Usually, one tends to think of a single crystal as in no wise unique, and to imagine that a polycrystalline specimen must have magnetic properties resulting very definitely from the superposition of those of a collection of single crystals. But the introduction of the concept of closure domains must cause some modifications of this view, if only because free poles can obviously exist within a polycrystalline specimen. In fact, only in strong fields would one expect to find little or no modification.

§ 4. DISCUSSION

As in the earlier papers, the energy supplied to each cm^3 of specimen in any part of the hysteresis cycle is taken equal to HdI, and assumed responsible for an increase in internal energy dE, according to the equation

$$HdI=(\partial E/\partial I)_T.\,dI+(\partial E/\partial T)_I.\,dT, \quad \text{or} \quad (\partial E/\partial I)_T\,dI=HdI-dQ,$$

which is correct whether the changes are thermodynamically reversible or not. In the preceding figures we have therefore plotted the $\left(\int HdI-Q\right), I$ curves, i.e. $\int (\partial E/\partial I)_T\,dI, I$ curves, whenever possible; such a curve was not included in figure 2, as the magnetic data for such a small cycle were not entirely satisfactory.

The E_T, I curves are much more rounded in the case of the Hilger iron and they do not cross the $\int HdI, I$ curves in the same way as do the corresponding curves for Armco iron. It is thought that this difference can safely be attributed to the greater carbon content of the latter, as evidence of the kind of kink shown in the E_T, I curve of figure 3 was recently found in the case of several alloys (Bates and Harrison 1948). Previous work has led us to expect a minimum in the E_T, I curve in the region of $I=I_r$, referred to the descending portion of the hysteresis curve, and therefore on the left of the I axis in the above figures; this is clearly the case for Hilger iron, but less clearly so for Armco iron, although in neither case is the value of I_r known with high precision.

It is disappointing, to some extent, to have to record that in the present work no confirmatory evidence has been obtained of the strange phenomena observed by Bates and Healey in the range from 350 to 400 oersteds, the region in which Akulov (1931) predicted that a discontinuity ought to exist in the I, H curve for a single crystal of iron magnetized parallel to a [111] direction. Experimental conditions were much more stable than those of Bates and Healey, and the present method of attaching the thermojunctions to the specimen may have been less sensitive to disturbances, or to error, arising from dimensions changes of magnetostrictive origin. For example, with the more rigid fixing system of ebonite collar and lightly adjusted grub screw, alternate expansions and contractions of the cross-section of the specimen might have caused a temporary deterioration in the contact between the 'hot' junction and the specimen which did not occur with the more flexible thread binding.

In conclusion, it appears to the authors that the Q, I behaviour of iron in very low fields depends very much on the purity of the specimen, and that it

would be instructive to repeat the above measurements with different specimens of high purity and known carbon content. They feel that enough is now known of the behaviour of polycrystalline iron and the technique of the method of measuring very small changes of temperature to make the measurement of such changes for a single crystal specimen of iron a possibility. Such an investigation would be extremely interesting because by choosing suitably shaped specimens it should be possible to examine magnetization processes of the type I, III and IV or of the type II only.

ACKNOWLEDGMENTS

Much of the apparatus used in this research was purchased from a grant made to one of us (L. F. B.) by the Government Grant Committee of the Royal Society; the special Tinsley galvanometers were purchased by Imperial Chemical Industries, Limited, for loan to L. F. B.; the specimens of Armco iron were kindly supplied by Professor F. C. Thompson. During a portion of the time spent on this research E. G. H. availed himself of a Government F.E.T. Grant.

REFERENCES

Adelsberger, U., 1927, *Ann. Phys., Lpz.*, **83,** 184.
Akulov, N., 1931, *Z. Phys.*, **69,** 81.
Bates, L.F., and Weston, J. C., 1941, *Proc. Phys. Soc.*, **53,** 5.
Bates, L. F., and Healey, D. R., 1943, *Proc. Phys. Soc.*, **55,** 188.
Bates, L. F., and Edmondson, A. S., 1947, *Proc. Phys. Soc.*, **59,** 329.
Bates, L. F., and Harrison, E. G., 1948, *Proc. Phys. Soc.*, **60,** 213.
Becker, R. and Döring, W., 1939, *Ferromagnetismus*, p. 160. (Springer, Leipzig.)
Constant, F. W., 1928, *Phys. Rev.*, **32,** 486.
Hardy, T. C., and Quimby, L., 1938, *Phys. Rev.*, **54,** 217.
Kittel, C., 1946, *Phys Rev.*, **70,** 967.
Néel, L., 1944, *J. Phys. Radium*, **5,** 241.
Von Engel, A., and Wills, M. S., 1947, *Proc. Roy. Soc.* A, **188,** 464.

DISCUSSION

Professor W. Sucksmith. In addition to the magnetic energy associated with Warburg's law, there will be contributions due to the thermal effect arising from the strain and lattice energies. Have the authors carried out any experiments which would throw light upon the contributions of these effects ?

Mr. A. E. De Barr. With reference to Prof. Bates's remarks about the difficulty of obtaining suitable samples of silicon iron for these measurements, if he will let me know the dimensions I shall be pleased to arrange for specimens to be supplied. These will be rods cut from silicon iron bar before it is rolled into sheets. I should like to ask if the authors have been able to correlate any of their results with measurements of the crystallographic orientation of their specimens. The hard-drawn samples will probably show marked preferred orientation, and this may not remain the same after annealing.

Dr. K. Hoselitz. The great number of experiments described by Professor Bates and Mr. Harrison show that a variety of types of curves of thermal behaviour accompany magnetization in different materials. I would like to ask whether it has been possible to find a correspondence of adiabatic temperature changes with the various elementary processes during magnetization, such as rotations of domain magnetization and reversible and irreversible boundary movements.

Pure nickel, unstressed and under stress, and permalloy under similar conditions can be studied in this connection.

With regard to pure iron, which, as Professor Bates mentioned, is very sensitive to residual impurities, I wonder whether iron-silicon, the material used in transformer lamination, might prove a more suitable material. It should show very similar characteristics to pure iron, but might not be so sensitive to the presence of small amounts of impurities. Furthermore, as it has a much higher specific resistance, eddy currents should not be so serious and there should not be the necessity for applying such large corrections.

AUTHORS' reply. In the early work many experiments with loaded specimens were made in order to elucidate the effects of strain, and we are making at the moment a survey of the magnetostriction properties. We want, of course, to make experiments on single crystals, and we think we now have sufficient experience to make an attempt.

We shall be most happy to give Mr. De Barr details of our needs. With regard to the question of crystallographic orientation, we made experiments on hard-drawn and annealed cobalt in which we obtained very marked differences in thermal behaviour, but, contrary to our expectations, Dr. Lipson found very little difference on X-ray examination.

We have done our best to find the correlation of which Dr. Hoselitz has spoken, and Mr. Harrison pointed out how very similar is the outer portion of the Q, I curve to the outer portion of the virgin Q, I curve; he also drew attention to the 'folding back' phenomenon in the middle of a Q, I curve for a cycle of medium size. We have studied strained and unstrained specimens.

We have not yet tried iron-silicon because we have only obtained this material in the form of thin sheets, and we expect considerable trouble in mounting such specimens; we hope to make an attempt shortly.

The Variation with Magnetization of Young's Modulus for Cobalt

By R. STREET
University College, Nottingham

MS. received 30 *May* 1947; *read* 8 *November* 1947

ABSTRACT. The variation with magnetization of Young's modulus for specimens of annealed and unannealed cobalt has been investigated, for field intensities up to about 700 oersteds, by the method of magnetostrictive oscillation. The decrement of longitudinal oscillation in cobalt rods has also been measured, and found to be of the order of 10^{-3}.

§1. INTRODUCTION

In general the value of Young's modulus of a ferromagnetic material changes when its state of magnetization is varied, and this phenomenon is known as the 'ΔE-effect'. Both static and dynamic methods of measurement have been used to determine Young's modulus for ferromagnetic materials. The static method, in which observations are made on the linear extension of a rod when subjected to an external stress, has been used by Honda and Terada (1907) in their investigation of the ΔE-effect in nickel and other materials. In the dynamic method, resonant longitudinal oscillations are excited in the specimen, which is in the form of a rod, and the value of Young's modulus is determined from observed quantities characteristic of the vibrating system. Various methods have been used for the excitation of the longitudinal oscillations and these are briefly summarized below. Firstly, a combination of cylinders of quartz and the ferromagnetic may be made to oscillate longitudinally by applying an alternating

E.M.F. to suitably disposed electrodes cemented to the quartz. The theory of such composite oscillators has been given by Zacharias (1933), and the method was employed by Siegel and Quimby (1936), Williams, Bozorth and Christensen (1941) and others. Secondly, when a ferromagnetic rod is supported with one end near a small electromagnet, energized by an alternating current, the resultant periodic force excites longitudinal oscillations in the rod. This method was analysed by Akulov (1933) and was used by von Auwers (1933), Wegel and Walther (1935) and Engler (1938). Thirdly, an alternating magnetic field applied to a ferromagnetic rod is generally accompanied by magnetostrictive strains which generate longitudinal oscillations. This method of magnetostrictive oscillation was used in the investigations of the ΔE-effect of Giebe and Blechschmidt (1931) and Yamamoto (1941).

Although the ΔE-effect has been investigated for a number of ferromagnetic materials, detailed measurements of the effect have been made for only two of the three pure ferromagnetic metals, viz. iron and nickel. However, maximum changes in Young's modulus for annealed cobalt subjected to longitudinal magnetic field intensities of 575 and 900 oersteds have been given by Engler (1938) and Yamamoto (1941) as 0·60% and 0·168% respectively. Detailed measurements of the effect in annealed and unannealed cobalt specimens have been made in this laboratory, using the method of magnetostrictive oscillation, and the results are presented here.

§ 2. METHOD AND APPARATUS

If a ferromagnetic rod with zero intensity of magnetization is oscillating longitudinally at its nth harmonic frequency f_0, then $4f_0^2 l_0^2 = v_0 n^2 E_0$ where l_0 = length of the rod and E_0, v_0 are the values of Young's modulus and the specific volume (or density^{-1}). The correction term to account for the lateral motion of the rod is assumed to be negligible. If f, l, E, v likewise characterize the vibrating system when the rod has an intensity of magnetization I, and we write $\Delta f = (f - f_0)$ etc., then by differentiation of the above expression we have

$$\Delta E/E_0 = 2\Delta f/f_0 + 2\Delta l/l_0 - \Delta v/v_0.$$

For cobalt the value of $\Delta f/f_0$ is of the order 10^{-3}. $\Delta l/l_0$ and $\Delta v/v_0$ represent the longitudinal and volume magnetostrictive changes for intensity of magnetization I, and have approximate maximum values of 10^{-5} and 10^{-6}, respectively, in the experiments described below. Therefore, for practical purposes $\Delta E\ E_0 = 2\Delta f\ f_0$, and the relative change in Young's modulus may be measured in terms of the change of resonant frequency of oscillation of the rod.

In this method of measurement the specimen rods of length about 40 cm. and 0·24 cm. in diameter were supported by thin silk threads as close as possible to displacement nodes. Two coils on ebonite formers were placed over, but not touching, the rods at strain antinodes. One coil, referred to below as the exciting coil, was connected to a variable frequency beat frequency oscillator and excited longitudinal oscillations in the rod in the manner already described. The other, detecting, coil was connected to an amplifier and valve voltmeter. Due to the inverse magnetostriction or Villari effect, an E.M.F. was induced in this coil, the magnitude of which indicated the amplitude of oscillations in the rod. Since the final accuracy of the measurements depends on the determination of changes in resonant frequency it is most desirable to have some method of detecting and

eliminating any random changes of the frequency of the current flowing in the exciting coil. A separate cobalt rod with exciting and detecting coils was found to be a convenient form of frequency monitor. This rod was maintained at a constant temperature and its state of magnetization was not altered during an experiment, therefore any apparent changes in its resonant frequency were due to random drifts in the frequency of the beat frequency oscillator. The output of the oscillator may be switched from the rod under test to the monitor when a check of the frequency is required. Alternatively, when the difference of the resonant frequencies of the two rods is large compared with the widths, in frequency, of both resonance curves, the two exciting coils may be joined permanently to the oscillator and both the receiving coils connected in parallel to the amplifier and valve voltmeter. The latter method was usually adopted and a diagram of the apparatus is shown in figure 1. The rods were suspended within an adjustable framework of brass rods. The coils were 2700 turns of 42 s.w.g. enamelled copper wire and their dimensions are given in figure 1. A split disc of copper foil connected to the outer layer of the coil and to earth was cemented to one face of each former and functioned

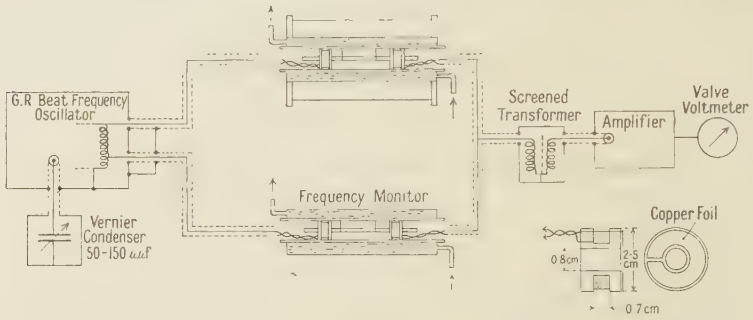

Figure 1. Schematic circuit diagram of apparatus.

as an electrostatic shield. A solenoid, 60 cm. long and wound on a tubular water jacket, surrounded the specimen to be investigated and the frequency monitor rod was permanently magnetized and then placed inside a water jacket. A modified G.R. beat frequency oscillator, Type No. 713, was used in these experiments, the 'cycles increment' condenser being removed and replaced by a Muirhead vernier condenser, Type No. A–429, having a range of 50 to 150 $\mu\mu$F. The total frequency range of the modified oscillator was 0–37 kc/s. and the change in frequency due to the variation of the vernier condenser was about 2 kc/s. An almost linear relation existed between the changes in frequency and the capacity of the vernier condenser, and since the latter was calibrated in units of 10^{-2} $\mu\mu$F., it was possible to read frequency differences to the nearest 0·1 cycles/sec. At various times during the experiments the frequency controls of the oscillator were calibrated against a G.R. primary frequency standard. The detecting coil was connected to a linear resistance capacity coupled amplifier and diode peak valve voltmeter.

Figure 2 shows a typical resonance curve taken for an annealed cobalt specimen with an applied field intensity of 75 oersteds. The experimental results are in very good agreement with the theoretical curve calculated by assuming a simple resonance phenomenon and that the electrical arrangements adopted obeyed linear laws.

The decrement of the oscillating system under various conditions may be determined from the appropriate resonance curves in the usual way, i.e. decrement $\delta = \pi \Delta f/f$ where Δf = width of the resonance peak at points where the amplitude has decreased to $1/\sqrt{2}$ of its value at resonance, and f = resonant frequency. In order to test the operation of the whole apparatus the decrements for the virgin curve of magnetization and the maximum change in Young's modulus were determined for an annealed nickel rod and the values were compared with those already reported by Siegel and Quimby (1936). The change in Young's modulus was found to be 7·0% (Siegel and Quimby, 6·7%) while the decrements were about 5 % greater than those previously published.

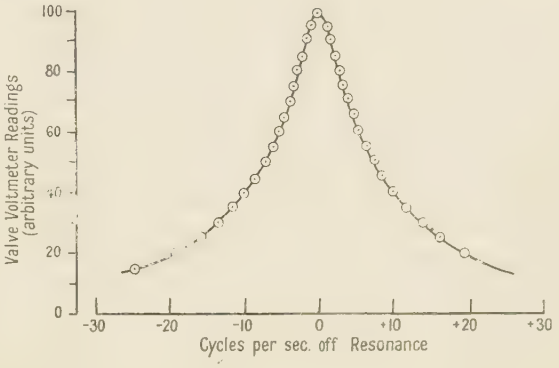

Figure 2. Typical fifth harmonic resonance curve of longitudinal oscillations in an annealed cobalt rod.

§ 3. RESULTS

The measurements were made on specimens of cobalt rod which had previously been used by Bates and Edmondson (1947) in their investigations of the thermal changes accompanying magnetization. The percentage composition was Co 98·40, Ni 0·45, Fe 0·13, CaO 0·23, Mn 0·08, C 0·19, Zn 0·01, Mg 0·11, SiO_2 0·14, S 0·02, loss in hydrogen 0·24. One specimen of length 39·80 cm. was freshly annealed by maintaining it *in vacuo* for two hours at a temperature of 1000° C., and then allowing to cool to room temperature in 8 hours. The other rod of length 38·13 cm. remained unannealed as received from the manufacturers. Measurements were made on both the specimens using the other as the frequency monitor and the majority of the experiments were carried out at the fifth harmonic frequency of about 30 kc/s.

The voltage induced in the detecting coil was a function of the magnetic condition of the specimen rods and a typical curve illustrating the way in which the detector coil output varied with the applied magnetic field in the case of an annealed cobalt specimen is shown in figure 3. The corresponding curve for unannealed cobalt was similar in form but the maximum induced voltage occurred at a field intensity of 260 oersteds

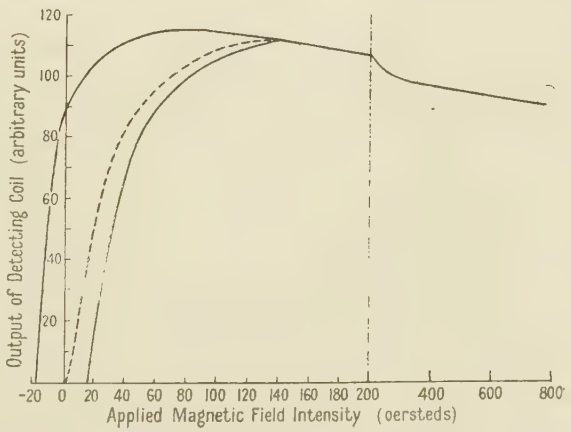

Figure 3. Variation of the output of the detecting coil at resonance with the applied magnetic field intensity.

instead of 70 oersteds. For both specimens the induced voltage was zero when the magnitude of the intensity of magnetization was small, i.e. in the demagnetized state and at the coercive force points on the hysteresis cycle where $I=0$. For this reason it was impossible to investigate the resonance of the rod over the whole range of magnetization available, and this is the main experimental disadvantage of the method. However, in practice the ΔE-effect measurements may be completed by extrapolation without appreciable error. Since the intensity of magnetization along the length of a cylindrical cobalt rod in a uniform externally applied magnetic field is not constant, there will be a corresponding change in Young's modulus for different cross-sections. The resonant frequency of longitudinal oscillation of the rod is determined, to a first approximation, by the elastic modulus of the material near displacement nodes and the inertia of the

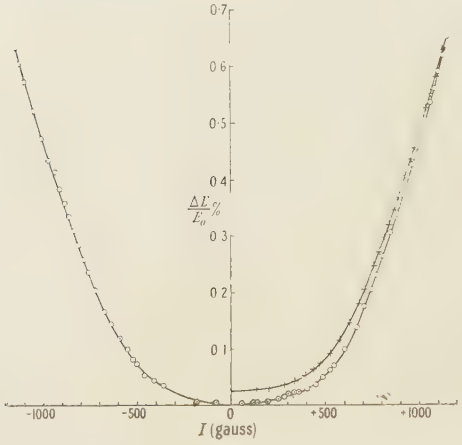

Figure 4. Variation of $\Delta E/E_0$ with I for annealed cobalt.
+ = Virgin curve of magnetization.
⊙ = Hysteresis cycle of magnetization.

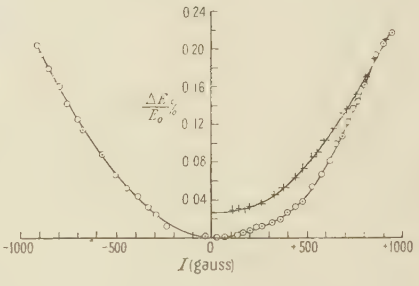

Figure 5. Variation of $\Delta E/E_0$ with I for unannealed cobalt.
+ = Virgin curve of magnetization.
⊙ = Hysteresis cycle of magnetization.

body in the region of displacement antinodes. Thus by comparison of measurements of the ΔE-effect at different harmonic frequencies, i.e. for different wavelengths of sound in the rod, it is possible to estimate approximately the experimental error due to the above variation of Young's modulus. Results for annealed cobalt taken at the third harmonic frequency agree to within 5% with those determined at fifth harmonic operation. This observation indicates that the error in the measured values of $\Delta E/E_0$ due to the non-uniformity of Young's modulus is small.

The curves given in figures 4 and 5 show the relative changes in Young's modulus for the annealed and unannealed specimens respectively. For both rods the smallest values of Young's modulus are observed at the coercive force points of the hysteresis cycle and the changes in the modulus are expressed in terms of this minimum value, E_0. For annealed cobalt the present observations agree well with Engler's result, quoted in § 1 above, which corresponds to a cobalt specimen for which I had a maximum value of about 1100 gauss. (*Note.*—In Engler's work E_0 was taken as the value of Young's modulus for the cobalt in the demagnetized state.) The experimental results for the annealed cobalt taken over the virgin curve of magnetization may be represented to a reasonable degree of accuracy by the

empirical relation $\Delta E/E_0 = 0{\cdot}023 + 0{\cdot}67\, I^3 - 0{\cdot}22\, I^4$, while the corresponding function for the unannealed specimen is $\Delta E/E_0 = 0{\cdot}027 + 0{\cdot}62\, I^3 - 0{\cdot}42\, I^4$. In these expressions the intensity of magnetization, I, is measured in kilogauss. In each case the departures of the measured values from the empirical curves are less than $\pm 5\%$.

By extrapolation the fifth harmonic resonant frequencies of the demagnetized annealed and unannealed rods were found to be 30·83 and 30·72 kc/s. respectively. Thus the experimental results together with the value of the density of cobalt, which was found to be 8·71 gm/cm^3, may be used to determine the absolute values of the moduli of the two specimens. For annealed cobalt $E_0 = 21{\cdot}0 \times 10^{11}$ dynes/cm^2, and this figure is in good agreement with the result obtained by Engler (1938). Since frequency differences may be accurately determined with these

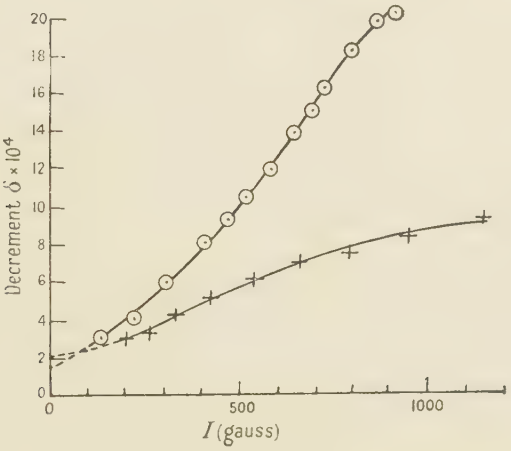

Figure 6. The decrements of longitudinal oscillations in cobalt rods plotted against the intensity of magnetization of the specimens.
+ = annealed cobalt. ⊙ = unannealed cobalt.

experimental arrangements the ratio of the moduli may be accurately calculated from the expression

$$\frac{E_{a0}}{E_{b0}} = \left[\frac{l_a}{l_b}\left(1 + \frac{f_{a0} - f_{b0}}{f_{b0}}\right)\right]^2.$$

In this expression the subscripts a and b refer to the annealed and unannealed rods and the subscript zero indicates extrapolated values representative of the demagnetized state. Hence $E_{a0}/E_{b0} = 1{\cdot}09$.

The variations of the decrements of oscillations in the two rods for the virgin curves of magnetization are shown in figure 6.

§ 4. DISCUSSION

In the domain theory of ferromagnetism it is postulated that the holomagnetization of a material is the summation of the magnetic effects of elementary domains which are spontaneously magnetized to saturation. In a demagnetized material the magnetization vectors of domains lie along directions of easy magnetization which are determined by the crystalline anisotropy. Two domain processes are supposed to occur during magnetization; firstly, domains having magnetization directions close to the field direction increase in size at the expense of those magnetized away from the field direction and, secondly, rotation of the magnetization

vectors towards the field direction may occur. Various attempts have been made to determine the relative sizes of the domains and the orientations of the magnetization vectors within the domains. These analyses are necessarily statistical in nature and are based on the principle of classical mechanics which states that a system is in stable equilibrium when its energy has a minimum value as, for instance, in the work of Brown (1937) and Takagi (1939). The total energy $\mathscr{E}$ of a domain in a material subjected to an external magnetic field is the resultant of three components, (*a*) the energy associated with the orientation of the magnetization with respect to the crystal axes within the domain (the magneto-crystalline or anisotropy energy, $\mathscr{E}_C$), (*b*) the strain energy arising from the internal stresses of the material and from any externally applied stresses ($\mathscr{E}_F$), and (*c*) the magnetic energy of the domain in the field ($\mathscr{E}_H$).

One consequence of the variation of $\mathscr{E}_H$ due to a change in the external magnetic field is the well known magnetostrictive change in the dimensions of the specimen. Thus, in general, a macroscopic change of dimensions takes place when the characteristic sizes and orientations of the magnetization vectors of the domains are altered. Therefore, when an external stress is applied to a ferromagnetic material having either a positive or a negative magnetostriction coefficient, the resultant strain has two arithmetically additive components: one is of purely elastic origin and the other is due to changes in the characteristics of the domains. The value of the latter component depends upon the relative magnitudes of the total energy $\mathscr{E}$ and the change in $\mathscr{E}_F$ produced by the applied stress. This component will be relatively large when the material is demagnetized, i.e. $\mathscr{E}_H = 0$, and smaller when the material is magnetically saturated, for which state $\mathscr{E}_H \rightarrow \mathscr{E}_{H\max.}$ Hence it is to be expected that the value of Young's modulus of a ferromagnetic in the demagnetized state will be smaller than that for the magnetically saturated material, and this conclusion is verified by the experimental results described above.

The qualitative theory also offers some explanation of the observed difference in the magnitudes of the ΔE-effect for annealed and unannealed cobalt by assuming that in the latter material $\mathscr{E}$ is greater than the corresponding value for the annealed specimen. It seems reasonable to suppose that this difference is due to a larger internal strain energy component in the unannealed cobalt. This analysis of the ΔE-effect has been fully described by Becker and Döring (1939).

The experimental curves show that the Young's modulus of annealed cobalt is about 9% greater than that for the unannealed material. A similar observation has been reported by Cooke (1936) who found that for iron $E_{a0}/E_{b0} = 1{\cdot}07$. On the other hand, Giebe and Blechschmidt (1931) have shown that the modulus of nickel decreases on annealing. This has been verified by the present method using two nickel rods of diameter 0·40 cm. one of which was annealed by maintaining it at a temperature of 1000° C. for four hours and then allowing it to cool slowly to room temperature. The value of E_{a0}/E_{b0} was 0·90. Experiments are now being undertaken in this laboratory on the ΔE-effect in materials which are progressively strained and it is hoped that the work will give more information on this anomalous behaviour of the three materials.

ACKNOWLEDGMENTS

The author wishes to record his thanks to Messrs. Ericsson Telephones Ltd. for the loan of a suitable beat frequency oscillator and also for their help in the

frequency calibration of this instrument. He is indebted to Professor L. F. Bates for suggesting this problem and for advice and encouragement throughout the work.

REFERENCES

Akulov, N., 1933, *Z. Phys.*, **85**, 661.
von Auwers, O., 1933, *Ann. Phys., Lpz.*, **17**, 83.
Bates, L. F., and Edmondson, A. S., 1947, *Proc. Phys. Soc.*, **59**, 329.
Becker, R., and Döring, W., 1939, *Ferromagnetismus*, pp. 336–357. (Springer, Berlin.)
Brown, W. F., 1937, *Phys. Rev.*, **52**, 325.
Cooke, W. T., 1936, *Phys. Rev.*, **50**, 1158.
Engler, O., 1938, *Ann. Phys., Lpz.*, **31**, 145.
Giebe, E., and Blechschmidt, E., 1931, *Ann. Phys., Lpz.*, **11**, 905.
Honda, K., and Terada, T., 1907, *Phil. Mag.*, **13**, 36.
Siegel, S., and Quimby, S. L., 1936, *Phys. Rev.*, **49**, 663.
Takagi, M., 1939, *Sci. Rep. Tôhoku Imp. Univ.*, **28**, 20.
Wegel, R. L., and Walther, H., 1935, *Physics*, **6**, 141.
Williams, H. J., Bozorth, R. M., and Christensen, H., 1941, *Phys. Rev.*, **59**, 1005.
Yamamoto, M., 1941, *Phys. Rev.*, **59**, 768.
Zacharias, J., 1933, *Phys. Rev.*, **44**, 116.

DISCUSSION

Professor L. F. Bates. It was hoped that these very interesting experiments by Mr. Street would help in the interpretation of the kind of experimental results which Mr. Harrison and I described earlier today. We are very much puzzled by the failure of a ferromagnetic rod to oscillate even when it possesses marked magnetization. As Mr. Street has pointed out, we have only a tentative suggestion by Snoek to provide any kind of explanation of this failure to oscillate, and, if that explanation fails to satisfy us, we are completely in the dark. I therefore hope that if any Fellows present today have any ideas on this subject they will let us hear them.

Professor W. Sucksmith. Has an x-ray investigation been made of the specimen on which data have been given? Cobalt is a mixture of face-centred and hexagonal lattices, and one would expect the two different structures to make different contributions to the modulus.

Author's reply. An x-ray analysis of the specimens of annealed and unannealed cobalt was very kindly made by Dr. Lipson, and this showed that there was little difference in the crystalline structure of the two materials. A summary of the results of Dr. Lipson's analysis is given in a note added to the paper by Bates and Edmondson cited in the list of references above.

The Electric Strength of Dielectric Films

By K. W. PLESSNER

Electrical Engineering Dept., Imperial College of Science and Technology

Communicated by Willis Jackson ; *MS. received* 17 *June* 1947

ABSTRACT. An attempt is made to verify the rise in electric strength predicted by Fröhlich's theory as the thickness of the dielectric specimen approaches the electronic mean free path. The results obtained on a number of materials both crystalline and amorphous are given and discussed in relation to this theory.

§ 1. INTRODUCTION

THE theory of electric strength which appears capable of the most reliable predictions is that developed by Fröhlich (1937, 1939, 1941). It has shown quantitative agreement with experiment for ionic crystals such as the alkali halides and mica, and qualitative agreement has also been obtained for mixed crystals. Fröhlich's theory is to a large extent based on the calculation of a time of relaxation of the electrons and, associated with this, an electronic mean free path in the dielectric. As the thickness of the dielectric specimen decreases and approaches the dimension of the mean free path, an increase in electric strength is predicted, and this has, in fact, been observed by Austen (Austen and Hackett 1939, Austen and Whitehead 1940) in measurements on thin films of mica. These tests form the only published verification of this particular aspect of Fröhlich's theory, and it is the object of the present work to extend the measurements to other materials having different values of the mean free path.

Calcium fluoride, sodium fluoride and potassium bromide provide a convenient range of mean free paths and were selected for the tests. For comparison, two amorphous materials, silica and polystyrene, for which no dependence of the electric strength on thickness was expected from Fröhlich's theory, were also tested.

§ 2. THEORY OF ELECTRIC STRENGTH

According to Fröhlich, the breakdown field strength is to be calculated from the condition that an electron should gain more energy from the field than it gives up to the crystal lattice in the form of heat. Both these energy components involve τ, the average time between collisions (time of relaxation), and in the final expression for the electric strength $1/\tau$ enters as a factor, showing that the strength increases as the time of relaxation decreases, i.e. the shorter the mean free path, l. Thus, the less ordered the structure the higher the electric strength, since the mean free path is shorter. The increased strength of mixed crystals over that of the pure components observed by von Hippel (1937) is an example of this effect of disorder, and when other things are equal, as, for example, with quartz and fused silica, the electric strength of the amorphous phase is higher than that of the crystalline phase. From similar reasoning it is predicted that in a crystalline chain compound, such as a hydrocarbon, the electric strength in a direction across the chains should be higher than along the chains.

Fröhlich gives the following formula for the mean free path, applicable to diatomic ionic crystals:

$$l = \frac{16E^2a^2}{2^{2/3}\pi^2(\epsilon-\epsilon_0)\boldsymbol{e}^2\boldsymbol{h}\nu} \Big/ \left(1+\frac{2}{e^{\boldsymbol{h}\nu/\boldsymbol{k}T}-1}\right),$$

where

E = energy of the electron, to be equated to J, the internal excitation energy of the lattice,

ν = reststrahlen frequency in the infra-red,

a = half-lattice spacing,

ϵ, ϵ_0 = dielectric constants for static and visible frequency fields, respectively.

$\boldsymbol{e}$, $\boldsymbol{h}$ and $\boldsymbol{k}$ have their usual meanings.

A slightly modified expression is used for more complex crystals.

The values of l given in table 1 for a number of substances have been calculated from this formula using infra-red data given by von Hippel (1937) and values of the internal excitation energy provided by Hilsch and Pohl (1930).

Table 1

Substance	Mica	Crystal quartz	CaF_2	NaF	KBr
Mean free path in 10^{-6} cm. ..	0·5	1·2	1·5	1·1	2·5

If the behaviour of the halides is analogous to that of mica, then, according to the work already quoted (Austen *et al.* 1939, 1940), a rise in electric strength should be noticeable at thicknesses between 10^{-4} and 10^{-5} cm. The mean free path in amorphous materials cannot at present be calculated, but it should be appreciably shorter than for crystalline ones. Thus, no dependence of the electric strength on thickness would be expected for amorphous silica for thicknesses of this order.

In von Hippel's view of the mechanism of breakdown no mean free path is defined, his criterion for the limiting field being that the electrons should gain about twice the ' reststrahlen ' quantum of energy ($h\nu$) in traversing the distance between neighbouring ions, i.e. a distance of only about 3×10^{-8} cm. However, both von Hippel's and Fröhlich's points of view require that the electrons be accelerated from thermal energies to the internal excitation energy J of the lattice. This implies that the voltage necessary for breakdown cannot be less than J expressed in electron volts. A minimum is therefore set to the electric strength equal to J/t v/cm., J being of the order of 10 v.; this minimum becomes larger than the normal electric strength at thicknesses t between 10^{-5} and 10^{-6} cm.

§ 3. EXPERIMENTAL METHOD

The first problem in the work undertaken was the production of films suitable for breakdown tests, of thickness appropriate for showing the effects predicted and of a texture which would not adversely influence the processes postulated in the theory. Thus, single crystal sheets of thickness between 0·1 and 10×10^{-5} cm. would be ideal, but in practice could hardly be prepared to be sufficiently uniform.

The method adopted was therefore that of evaporation under high vacuum, the vapour condensing on a suitable surface to form a uniform thin film. The process is used extensively by the optical industry in the ' blooming ' of lenses to produce non-reflecting surfaces, and is particularly suitable for giving uniform films of any required thickness up to about 10^{-4} cm.

Here, the films were condensed on a layer of silver on a glass slide, the silver having been newly deposited by the same process of evaporation. This acted as the basic electrode for the electrical tests, and also enabled an approximate determination of the refractive index of the film to be made. A further layer of silver was deposited over part of the dielectric film to allow the film thickness to be measured by interferometry.

(i) *The preparation of films*

For the preparation of vapour-deposited films an evaporation plant of the usual design has been employed, consisting of bell jar and base-plate mounted on an oil-diffusion pump, so that a vacuum of about 10^{-5} mm. Hg could be attained.

Heavy electrodes were brought through the base-plate to supply the evaporation heaters, and a brass cone fitting into the top of the bell jar allowed a ' clean-up ' discharge to be passed through the vessel. This cone could be rotated to move a revolving carrier inside the vacuum, so bringing the glass slide used as substrate over the various shields and filaments. Figure 1 shows the arrangement inside the bell jar, with a clean glass slide in position to be silvered. Two filaments of molybdenum strip were employed, one to evaporate silver, the other for evaporating the crystalline powders of CaF_2, NaF or KBr. Materials of the purest grade commercially available were used, and weighed amounts were evaporated completely at temperatures ranging from 730° c. to 1360° c. In the preparation of silica films, the filaments were of tungsten wire (m.p. 3400° c.), since, although molybdenum does not melt below 2600° c., it was feared that a small amount might vaporize at the high temperature (>1700° c.) required to evaporate silica.

Since the mean free path in air at 10^{-5} mm. Hg is of the order of 8 metres, the evaporated molecules travel essentially in straight lines and behave to some extent like rays of light. Thus, sharp shadows can be thrown by placing shields close to the receiving surface, and the intensity of the beam varies inversely as the square of the distance from the source. From the latter law, the thickness of the film could be predetermined approximately, and it could also be estimated that the film thickness should be uniform to within 3% over a two-inch diameter circle of the specimen slide.

Evaporation was normally carried out at a pressure of 10^{-5} mm. Hg as measured by an ionization gauge, and proceeded as follows:—

(*a*) The whole of the specimen slide was silvered to opaqueness.

(*b*) The carrier was rotated to bring the slide over the second filament, and in this position a narrow strip of the slide was screened off by a piece of brass close to it, as shown in figure 2. The dielectric powder was then evaporated during a period of about 1 minute.

(*c*) The slide was moved over a different shield and a small region, including part of the strip left free from dielectric, was resilvered to allow thickness measurement by the method described below.

In the preliminary measurements the specimen was then taken out and tested, but later the breakdown measurements were made with the specimen remaining in the bell jar, using a magnetically operated electrode.

In addition to the vapour-deposited films, some films of polystyrene, an organic polymer, were produced by the evaporation of a dilute solution. Silvered glass slides were immersed in the solution and withdrawn at a constant rate, during which process the solvent evaporated, leaving behind a uniform film of the polymer. By varying the concentration of the solution and the speed of withdrawal, a thickness range from 0·3 to 3×10^{-5} cm. was covered.

(ii) *Electric strength tests*

Electric strength tests were carried out by pressing a highly polished steel sphere 1/16″ diameter lightly on to the dielectric surface and applying a uniformly increasing voltage between this electrode and the basic silver film until breakdown occurred. As time effects were observed with some materials, a pulse generator was built, the circuit of which is given in figure 3 to the left of

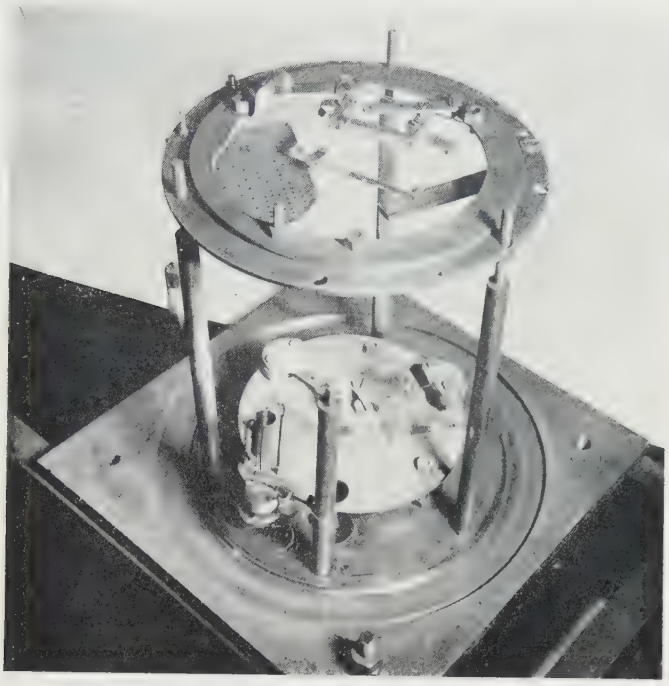

Figure 1.

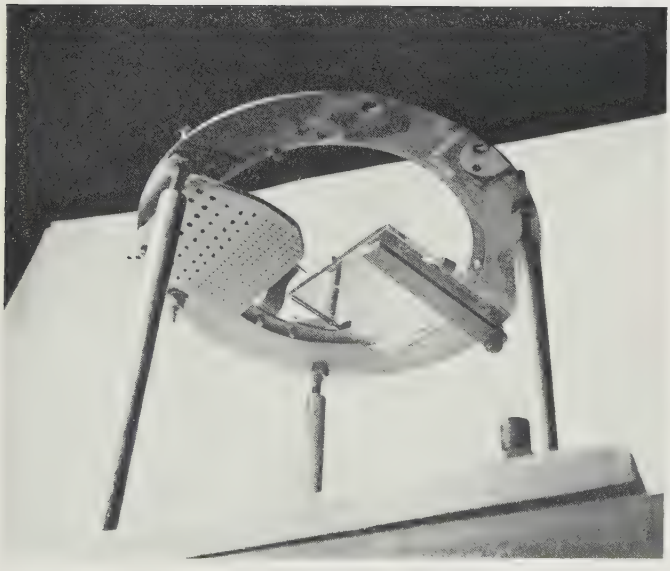

Figure 2.

To face page 246

the dotted line. A single pulse, of the triangular shape shown in figure 3 (*a*), is produced when button A is pressed. The action of the circuit is based on two condensers charging up through two resistances. The first condenser, C_1, is normally shorted by a triode V_2, but by pressing button A, the grid of V_2 is connected to a negative potential through condenser C_2 and so C_1 is allowed to charge up through R_1 to give the front of the pulse. At the same time C_2 charges up through R_2, and when the grid of V_2 returns to zero potential, the valve again becomes conducting and C_1 is short-circuited abruptly, so terminating the pulse. The voltage across C_1 is taken through the cathode follower V_3 and the output is obtained at P from the potentiometer R_3. Potentiometer R_4 provides a bias

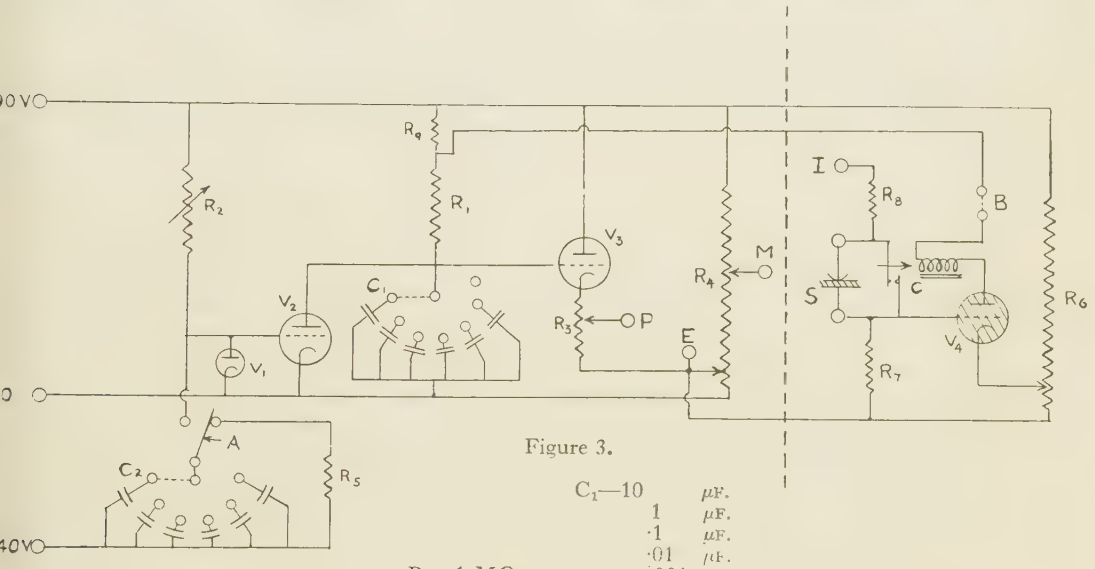

Figure 3.

R_1—1 $M\Omega$	C_1—10	μF.
R_2—1·1 $M\Omega$	1	μF.
R_3—0·1 $M\Omega$	·1	μF.
R_4—0·1 $M\Omega$	·01	μF.
R_5—3 000 Ω	·001	μF.
R_6—50 000 Ω	·0001	μF.
R_7—25 000 Ω	Strays	
R_8—15 000 Ω	C_2—20	μF.
R_9—15 000 Ω	2	μF.
	·2	μF.
	·02	μF.
	·002	μF.
	·0002	μF.

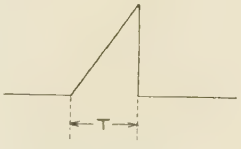

Figure 3 (*a*).

for V_3 and, at the terminal M, allows manual voltage control, should a very slow rate of rise be required. The pulse duration T could be varied between 10 seconds and 40 μsec. by controlling C_1, C_2 and R_2. The pulse amplitude is variable from 0 to 430 volts.

A number of pulses with gradually increasing amplitude had to be applied until breakdown took place, but once the necessary value was known approximately only a few pulses, starting with an amplitude about 10% below the expected value, were required. The amplitude of the pulses was measured to an accuracy of about 3% on a cathode-ray tube.*

The occurrence of breakdown was indicated by the relay circuit shown to the right of the dotted line in figure 3. The test voltage is connected at I, and is

* It should be mentioned that Turner and Lewis (1947) have used a pulse method for measuring the dependence on field strength of the conductivity of thin glass films.

applied to the specimen S through the safety resistance R_8 and the triggering resistance R_7. V_4 is a gas-filled triode whose cathode bias is just below the critical value, so that the voltage drop across R_7, which occurs when the specimen breaks down, causes the valve to strike. The resulting current operates a relay C which short-circuits the specimen to avoid pitting of the electrode, and gives an audible click as an indication of breakdown.

The state of cleanliness and polish of the sphere electrode proved important. When an abnormally high value of the electric strength had been observed, a dust particle or a chip of the film was nearly always found on the electrode. In the early tests, when the specimens were withdrawn from the evaporating chamber and tested in the open, frequent repolishing of the electrode was necessary, until no appreciable marks were visible under a microscope ($\times 120$). In the later tests under vacuum only occasional repolishing was called for.

In the tests carried out in the open, a stream of dry air was blown over the surface of the specimen. This was found insufficient, however, to eliminate

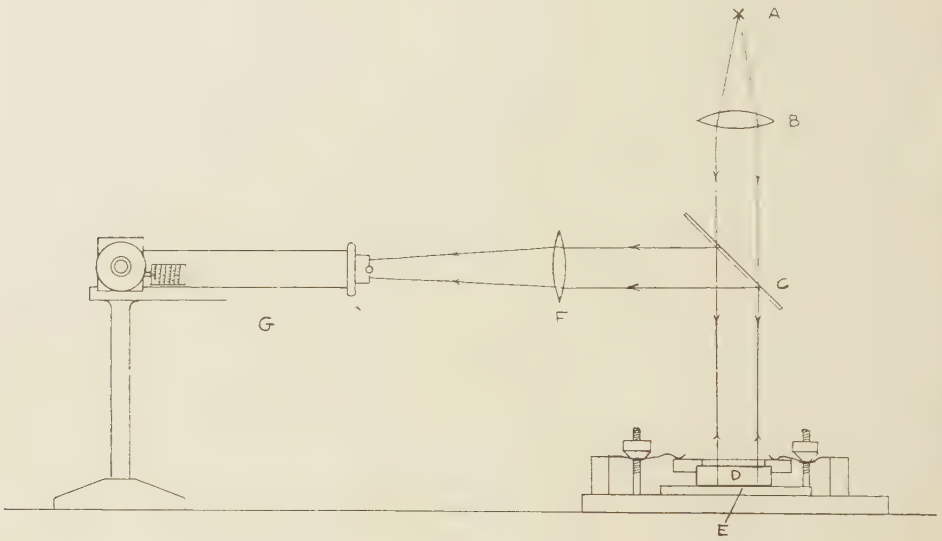

Figure 4.

the effects of moisture, and as stated above, the later measurements were made in the evaporation chamber without exposing the specimen to atmospheric conditions. The effect of moisture was very pronounced, an increase by a factor of 2·5 in electric strength being obtained by testing NaF under vacuum or in thoroughly dry air rather than in the atmosphere.

(iii) *Thickness measurement*

The thickness of the films was determined by the technique of multiple beam interferometry (Tolansky 1945).

Interference took place between the silvered surface of the specimen slide and the half-silvered surface of an optical flat which was brought into close contact with it. The experimental arrangement is shown diagrammatically in figure 4. White light from the source A is collimated by the lens B and illuminates the interference surfaces consisting of the specimen slide E and the optical flat D pressed together by three adjustable springs. The reflected light from D–E

is then reflected in the half-silvered mirror C, and is focused on to the slit of the spectrometer G by the lens F. In the spectrum sharp dark fringes are visible, corresponding to wavelengths λ, which satisfy the equation $n\lambda = 2t_0$, where n is an integer and t_0 is the optical distance between the silver surfaces.

If t_0 changes by an amount δt_0 owing to a step on one of the surfaces, such as that produced by the shielding of a strip during deposition of the dielectric film, then the fringe system is displaced, as sketched in figure 5. A shift of one fringe separation corresponds to $\delta t_0 = \lambda/2$, while a relative shift s/d (figure 5) means $\delta t_0 = (s/d)(\lambda/2)$.

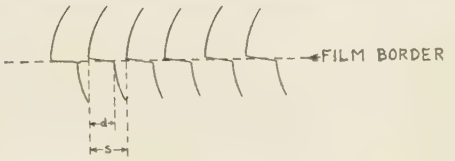

Figure 5.

The accuracy with which the fringe displacement, and hence the value of δt_0 can be determined, depends on the sharpness of the fringes and on irregularities in the surface of the specimen slide, which impose small ripples on the fringes. Taking into account these factors, and the smoothing effect due to using the mean of a number of readings, it was estimated that the error in δt_0 should not be larger than ± 25 A.

The step δt_0 is equal to the film thickness t in the region of the specimen slide which was resilvered after depositing the dielectric; whereas in the part with only the first layer of silver, the change in optical thickness is from a film of refractive index μ to air, i.e. $\delta t_0 = (\mu - 1)t$. Thus, both the thickness and the refractive index of the films can be determined by this method.

Although no inaccuracies other than the reading errors mentioned above affect the measurement of film thickness, disturbances due to the imperfect reflectivity of the silver, and to the inadequacy of the equation $n\lambda = 2t_0 + 2\mu t$ to describe interference in a composite gap, influence the determination of the refractive index (Plessner 1946). An approximate correction is possible for thick films, but for films thinner than about 3×10^{-5} cm. the results are not trustworthy.

§ 4. EXPERIMENTAL RESULTS

(i) *Vacuum evaporated films*

The results of measurements on silica, CaF_2, NaF and KBr, carried out under vacuum soon after deposition of the films, are given in this section.

The value of electric strength at each value of the pulse duration is the mean of about six readings whose scatter amounted to approximately $\pm 6\%$ for the crystalline films. For silica, where the electric strength was nearly independent of pulse duration, rather more scatter was encountered, and more readings were taken.

Allowing for the scatter, the error in voltage measurement, and the error in thickness measurement, the standard error in the means has been estimated as $\pm 4{\cdot}5\%$ for film thicknesses greater than 10^{-5} cm. For thinner films the inaccuracies represent a higher percentage, approximately $\pm 10\%$ at 5×10^{-6} cm. and $\pm 20\%$ at 10^{-6} cm.

The values of electric strength found for films of silica are shown in figure 6 plotted against thickness. A slight dependence of the strength on pulse duration was found, but, as its order of magnitude was the same as, or smaller than, that of the scatter, the two have been combined to give the rather extended vertical

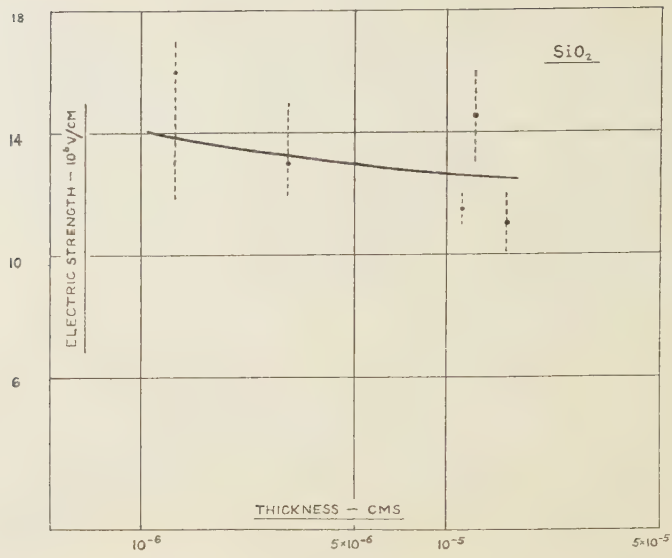

Figure 6.

lines in figure 6. It is seen that there is no significant variation of electric strength with thickness; the slightly higher value found for the thinnest films is not reliable in view of the large error at that thickness.

The three halides CaF_2, NaF and KBr each show a variation of electric strength with both pulse duration and thickness, as shown in figures 7, 8 and 9, where electric strength is plotted against pulse duration, for a number of constant thicknesses. It will be seen that at a constant pulse duration the strength increases in general with decreasing thickness, as predicted by Fröhlich's theory.

(ii) *Polystyrene films*

The electric strength of polystyrene films was found to be independent of pulse duration, and no significant variation with film thickness between 0·37 and 3×10^{-5} cm. was encountered (table 2).

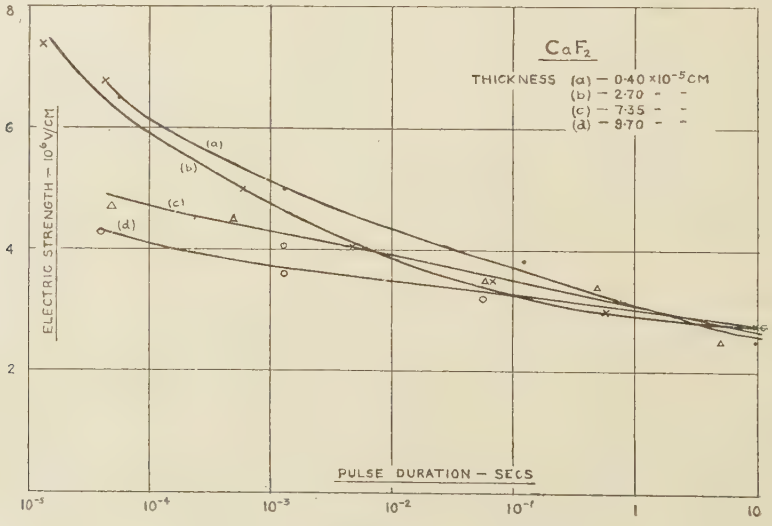

Figure 7.

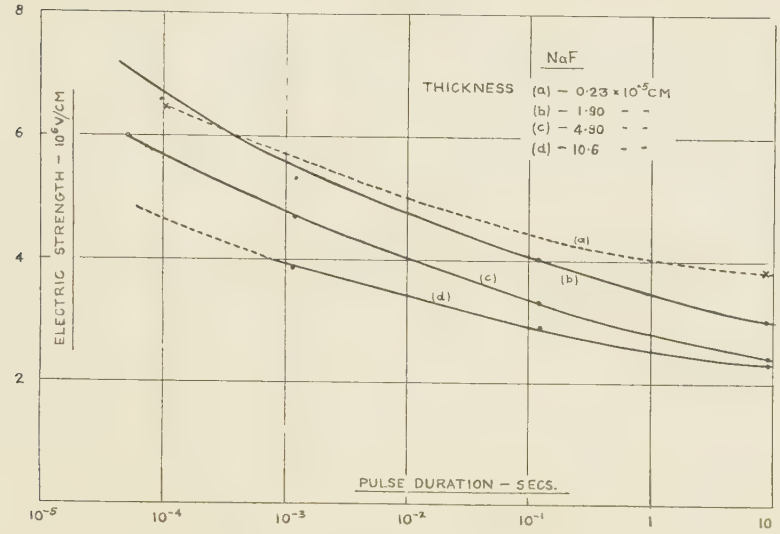

Figure 8.

Table 2

Thickness (10^{-5} cm.)	0·37	0·47	0·84	1·72	3·1
Electric strength (10^6 v/cm.)	4·9	6·0	5·5	5·5	5·6

The figures given are each the mean of about 20 readings, the scatter among which amounted to about $\pm 15\%$.

The overall mean value is $5{\cdot}5 \times 10^6$ v/cm.

§ 5. DISCUSSION

(i) *Ambient medium discharges*

In all measurements of electric strength it is necessary to ensure that no discharges take place in the ambient medium of the electrode system, since such discharges generally lead to premature breakdown.

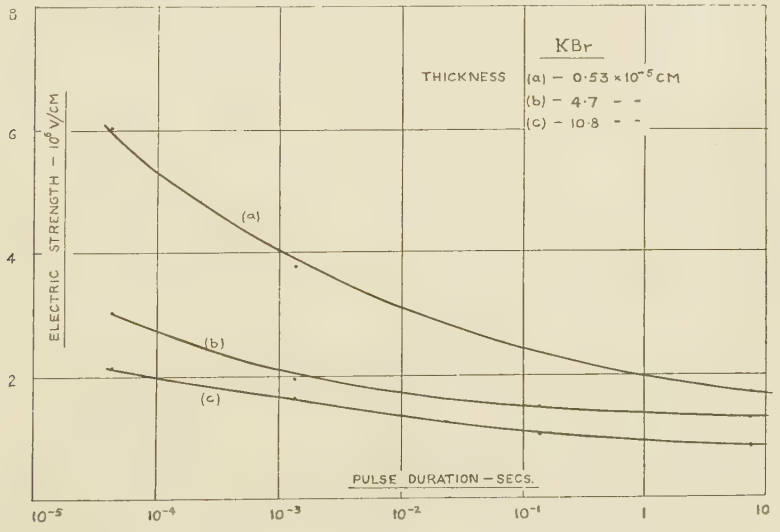

Figure 9.

For thick specimens air is unsuitable as an ambient medium, but Austen and Whitehead (1940) suggest that for thicknesses below about 6×10^{-5} cm. no adverse effects occur. The present measurements were carried out in air at a low pressure, but it was ascertained that the same results could be obtained in dry air at atmospheric pressure. The conditions of test were therefore similar to those of Austen and Whitehead, and their view is supported by a number of circumstances.

Thus, the electric strength values observed for nearly all the films are higher than those of the bulk material, measured under conditions which are claimed to preclude ambient discharges. Further, the effect of discharges would be expected to vary with film thickness and with pulse duration, whereas silica and polystyrene films show electric strengths independent of these two variables. Finally, the occurrence of discharges is generally accompanied by a large scatter in the readings of breakdown voltage, whereas a comparatively small scatter was observed with the crystalline films. From the theoretical point of view the absence of discharges in the case of thin films at atmospheric pressure is not obvious. In fact, on comparing the voltage V_A in the air gap between dielectric and electrode with the Paschen curve of spark-over voltage in air, V_S, for corresponding gap lengths, it is found that $V_A > V_S$ over an appreciable range of the gap, whenever the total voltage applied to the specimen is greater than the minimum value of 325 v. in the Paschen curve. Thus, discharges would be expected in such cases, in contradiction to the experimental evidence. The explanation of this disagreement may be sought in several effects:

(*a*) The Paschen curve applies to spark-over in an irradiated gap between two metal electrodes. The gap in question being between a steel electrode and the dielectric may affect the spark-over potential and may raise the minimum.

(*b*) The absence of irradiation may increase the apparent breakdown potential by introducing a time lag.

(*c*) The nature of the discharge may be different for the very small gaps involved; for example, the pointed sparks, which are thought to be responsible for premature breakdown in the case of thick specimens, may give way to a relatively harmless glow discharge.

In the absence of data on discharges in small composite gaps, no conclusions can be drawn.

(ii) *The structure of films deposited by the vacuum evaporation process*

Limited information is available in the literature regarding the structure of deposited dielectric films, but the very considerable literature on metallic films affords a general picture which is useful as a basis for consideration of the probable structure in the dielectric case.

As a general rule, the films consist of an agglomerate of small crystals, whose lattice structure is the same as that of the bulk material. The extent to which the films are broken up depends on the size of the crystallites, and this is determined very largely by the nature and the temperature of the substrate on which the films are condensed, as well as by the particular metal of which the film is composed. The lower the substrate temperature, the smaller the crystal size, and vice versa.

Appleyard and Lovell (1937) by measuring the conductivity of very thin caesium films find evidence that at 64° K. the crystallization is inhibited altogether, but at higher temperatures crystallization takes place and the films break up into agglomerates.

The effect of both temperature and nature of the substrate is demonstrated by the behaviour of zinc films (Picard and Duffendack 1943), which are found to be reflecting when deposited on glass at liquid oxygen temperature, but of a dark bluish appearance when deposited at room temperature. Reflecting films can be obtained at room temperature by evaporating on copper or aluminium instead of glass or collodion. The interpretation of this effect is based on electron microscope studies of the films deposited on collodion. It appears that the reflecting films consist of crystals which are smaller than the wavelength of light and so form a relatively uniform surface, whereas the blue films consist of larger crystals which scatter the light instead of reflecting it.

The crystal size of some dielectric films has been estimated by Germer (1939) from the line width of electron diffraction patterns. Films of CaF_2, NaF, CsI and CuCl were produced under conditions similar to those applying in the present work, but thin ' Formvar ' films were used as substrate to allow electron diffraction in transmission. Because of the use of this substrate, which in addition may have been warmed up appreciably by the evaporating filament, it is thought that the films tested here may consist of crystals somewhat smaller than those investigated by Germer. For CaF_2 and NaF of average thickness 30–550 A. Germer gives the crystal size as 100–150 A., with a lower limit of 70 A. CsI and CuCl have similar values, and presumably the crystal size of KBr will not be very different.

Taking the crystal size of the present films as 70 A. approximately, it may be said that the thinnest CaF_2 and KBr films tested ($t = 500$ A.) should present a reasonably uniform surface, while the thinnest NaF film ($t = 230$ A.) may be seriously broken up into agglomerates.

Evaluation of the refractive index of the various films from the interferometric data referred to in § 3 (iii) gives values somewhat lower than for the corresponding single crystals and indicates that the films consist of aggregates of tiny crystals with voids between them. Thus, for CaF_2, 1·29–1·35 was found instead of 1·41, NaF gave 1·29–1·31 instead of 1·32, and only KBr gave values close to the true refractive index of 1·56.

The effect of this film structure on the mechanism of breakdown may be two-fold. If the electrons suffer additional collisions at crystal boundaries, then the mean free path, which is rather larger than the crystal size, will be reduced, and the electric strength should be increased. No such effect will take place if the bridges between crystallites are so perfect that no additional scattering occurs.

From a more macroscopic point of view, the porosity may give rise to local field concentrations and so cause premature breakdown.

The structure of silica films is not known, but, if the rule that evaporated films have the same lattice structure as the bulk material may be generalized, then the silica films should be amorphous.

(iii) *The structure of polystyrene films*

Polystyrene is a non-polar hydrocarbon polymer, the chain molecules of which are about 1000 carbon atoms long; it is in this respect rather similar to

polythene, for which some work on the structure of thin films has been published. Charlesby (1945) produced thin films of polythene (approximately 1000 A. thick) by placing a drop of a dilute solution on water at 90° C. and allowing the solvent to evaporate. From the electron diffraction pattern obtained in transmission, and from consideration of the shape of the polythene molecule it was deduced that the molecules were oriented so as to make an angle of 56° with the plane of the film, and were tightly packed forming small crystals. When preparing the film by placing a drop of solution on a metal surface, less orientation resulted.

Orientation in polystyrene may be further inhibited in view of the bulky side chains on the molecules compared with polythene, and so the films may be mainly amorphous. The effect of any orientation of the chains into the direction of the field would, according to Fröhlich, be to lower the electric strength.

(iv) *The experimental results in relation to theory*

The experimental results fall into two groups, those on crystalline films, where a variation of electric strength both with pulse time and thickness was found, and those on silica and polystyrene films for which no such variation was observed.

Considering the latter group first, the absence of a variation of electric strength over the thickness range tested is in agreement with Fröhlich's theory, if the films are assumed amorphous in structure. This is probably the case. The average value of $5{\cdot}5 \times 10^6$ v/cm. found for polystyrene compares well with the electric strength of $6{\cdot}1 \times 10^6$ v/cm., determined by W. G. Oakes* for recessed specimens of thickness about 0·04 mm. The lowering by 10% is barely significant, but may be due to orientation of the molecules. The average electric strength found for silica films, $12{\cdot}5 \times 10^6$ v/cm., is appreciably higher than the values found by von Hippel and Maurer (1941) for a number of thick specimens, their highest figure being 8×10^6 v/cm. for a thickness of 6×10^{-4} cm.

Several explanations are possible:—

(*a*) Silica has been observed to give varying results depending on the particular specimen and its history (von Hippel and Maurer 1941), and the difference between the figures quoted may be due to this cause.

(*b*) In spite of the precautions taken, some tungsten from the filament may have evaporated simultaneously with the silica and introduced metallic centres into the film. According to Fröhlich (1937, 1939, 1941), this should reduce the mean free path and raise the electric strength.

(*c*) The scatter accompanying the results does not allow a definite line to be drawn, and the figure of 8×10^6 v/cm. at 6×10^{-4} cm. thickness may, in fact, lie on the continuation of a curve which is inclined rather more than that drawn in figure 6.

The case of the crystalline materials CaF_2, NaF and KBr is complicated by the time dependence of the electric strength, which is not predicted by Fröhlich's theory. At a given value of the pulse duration, however, the electric strength rises with decreasing thickness, as shown in figures 7, 8 and 9, and in columns (2) and (3) of table 3. The electric strengths of the thickest films at the longest

* Data kindly communicated to the author prior to publication.

pulse durations agree well with the values found by von Hippel (1937) for thick specimens. No exact calculation of the rise in electric strength to be expected for thin films has been carried out by Fröhlich and therefore no direct correlation with theory is possible. On the other hand, a numerical comparison based on the calculated mean free paths appears desirable and the final column of table 3 headed ' Estimated value ' has been drawn up, assuming Austen's result on mica to apply, viz. a 60% increase in strength at a thickness of 40 mean free paths. Thus, this column gives the observed limiting electric strengths at large thickness and long pulse durations increased by 60%, which may then be compared with the corresponding experimental figures at a thickness of 40 mean free paths shown in the two preceding columns for two different pulse durations. It is seen that the estimated values lie between the experimental figures for the two pulse durations.

Table 3

	Thickness	Electric strength values in 10^6 v./cm.			
		(1) von Hippel's value	(2) Experimental value, Pulse duration 10 sec.	(3) Experimental value, Pulse duration 10^{-4} sec.	(4) Estimated value
CaF_2	6×10^{-5} cm. (40l)	—	2·8	4·6	4·5
	10^{-5} cm.		2·8	6·4	—
NaF	$4{\cdot}4\times10^{-5}$ cm. (40l)	2·4	2·6	5·7	3·9
	10^{-5} cm.		3·2	7·1	—
KBr	10^{-4} cm. (40l)	0·75	0·75	2·1	1·2
	10^{-5} cm.		1·6	4·8	—

l=mean free path.

(v) *Possible explanations of the time effect*

There are two major possibilities :—

(*a*) the effect is inherent in the properties of thin crystalline layers,

(*b*) the effect is due to some undesired influence.

Although not brought out explicitly, figures 7, 8 and 9 show that there is a tendency for the time effect to disappear as the film thickness increases. The reality of the effect is therefore possible, since it would not be noticed with thick specimens. At the same time, an explanation on the basis of electronic breakdown is difficult to find, since one would expect electronic movements to be completed in times of the order of 10^{-8} sec. or less. Possibly a connection could be sought with the shortness of the path available for the acceleration of the electrons

and the consequent necessity for a number of relatively improbable collisions to occur before instability sets in.

Any possibility that the time dependence might be associated with some characteristic of the testing circuit, a crushing effect on the test specimen arising from electrostatic attraction between the electrodes, electrolytic decomposition of the film and ambient medium discharge has been ruled out either by test or by rough calculation. There remain the possibilities of impurities in the films causing increased conductivity and heating, or some interfacial polarization effects due to the polycrystalline structure of the films. An attempt was made to probe into the question of impurities by evaporating a different sample of CaF_2 from a tungsten instead of a molybdenum heater. Although the results agreed with the previous ones within experimental error, this does not constitute proof of the absence of impurities. Conductivity measurements and tests with shorter pulses, when at some stage the heating effect should become negligible, would be better tools to employ.

§ 6. CONCLUSIONS

It may be said that the results obtained agree qualitatively with Fröhlich's theory, which predicts a rise in electric strength as the specimen thickness approaches the electronic mean free path.

In view of the uncertainty whether evaporated films with their polycrystalline structure are truly representative of the ideal lattice postulated in theory, and because of the time effect, the cause of which is not yet known, it is not possible to draw any definite conclusions.

ACKNOWLEDGMENTS

The author wishes to express his gratitude to Professor Willis Jackson for constant guidance and encouragement and to Dr. W. K. Donaldson for help with the optical work. Thanks are due to the Department of Scientific and Industrial Research for financial assistance in the form of a special research grant.

REFERENCES

Appleyard, E. T. S., and Lovell, A. C. B., 1937, *Proc. Roy. Soc.* A, **158,** 718.
Austen, A. E. W., and Hackett, W., 1939, *Nature, Lond.*, **143,** 637.
Austen, A. E. W., and Whitehead, S., 1940, *Proc. Roy. Soc.* A, **176,** 33.
Charlesby, A., 1945, *Proc. Phys. Soc.*, **57,** 496.
Fröhlich, H., 1937, *Proc. Roy. Soc.* A, **160,** 230; 1939, *Ibid.*, **172,** 94; 1941, *Ibid.*, **178,** 493.
Germer, L. H., 1939, *Phys. Rev.*, **56,** 58.
Hilsch, R., and Pohl, R. W., 1930, *Z. Phys.*, **59,** 812.
von Hippel, A., 1937, *J. Appl. Phys.*, **8,** 815.
von Hippel, A., and Maurer, R. J., 1941, *Phys. Rev.*, **59,** 820.
Picard, R. G., and Duffendack, O. S., 1943, *J. Appl. Phys.*, **14,** 291.
Plessner, K. W., 1946, *Nature, Lond.*, **158,** 909.
Tolansky, S., 1945, *J. Sci. Instrum.*, **22,** 161.
Turner, C. H. M., and Lewis, W. E.,1947, *Nature, Lond.*, **159,** 334.

Excited Electronic Levels in Conjugated Molecules: I. Long Wavelength Ultra-Violet Absorption of Naphthalene, Anthracene and Homologs

By C. A. COULSON
Physical Chemistry Laboratory, Oxford*
* Now at King's College, London

MS. received 28 *June* 1947

ABSTRACT. The method of molecular orbitals has been applied to study the long wave ultra-violet absorption of the polyacene series, naphthalene, anthracene, ... The longest wavelength in an allowed excitation probably arises from a transition between mobile electron levels of symmetry $A_{1g} \rightarrow B_{2u}$, and polarized across the width of the molecule. In the first four or five members of the series, the second wavelength is due to a transition $A_{1g} \rightarrow B_{1u}$, polarized along the length of the molecule. Discrepancies between this theory and both the valence-bond resonance treatment and the Lewis-Calvin theory of colour are elucidated. This assignment of transitions is in agreement with (1) calculation of absolute energies as a function of chain length, (2) calculation of relative energies of the B_{2u} and B_{1u} transitions, (3) limiting condition for a large number of rings, (4) calculations of intensities, and (5) some experimental work on fluorescence.

§ 1. INTRODUCTION

THE series of molecules shown in figure 1 may be called the polyacene series, individual members being defined in terms of the number n of rings. This means that the molecule n has a formula $C_{4n+2}H_{2n+4}$. Their long wavelength u.v. absorption spectra have been measured from benzene with one

benzene naphthalene anthracene naphthacene pentacene

Figure 1.

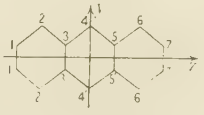

Figure 2.
Notation in anthracene.

ring ($n = 1$) up to pentacene with five rings ($n = 5$). The close similarity of these spectra (see e.g. Bowen, 1946, p. 127, where they are reproduced on the same diagram) shows that a similar process is responsible for them all. There is, indeed, a characteristic shift to longer wavelength with increasing size of molecule. Thus each additional ring gives rise to a red shift of about 1000 A. from naphthalene (2750 A.) to pentacene (5800 A.). This shift proves that the process must be the excitation of a conjugation, or mobile, electron, so that the absorption is of the kind called $N \rightarrow V$ by Mulliken (Mulliken and Rieke 1941, subsequently referred to simply as M.R.). Our object in this paper is to show that the magnitude of the red shift can be calculated by the theory of molecular orbitals; and we shall be led to quite definite conclusions regarding the direction of the transition moment.

This, is of course, simply the direction of the electric vector in the absorbed, or fluorescent, light. Since the transition is $N \rightarrow V$, the electric vector must lie in the plane of the molecule. This conclusion has been explicitly verified for the related molecule chrysene (Krishnan and Seshan 1939), for anthracene (Krishnan and Seshan 1936) and for naphthacene (Scheibe 1938, Scheibe and Kandler 1938). We shall have occasion to refer to some of this work later. Now the fact that the transition moment lies in the plane of the molecule does not complete our knowledge. For if, as in figure 2, we take the x-direction perpendicular to the plane,* the transition moment may lie along the z or y directions. In this it differs from a straight polyene chain, or a linear dye molecule, where the moment must lie along the chain length. The classical analogy is to electrons oscillating in the y- or z-directions. It has hitherto been customary (e.g. Förster 1938) to suppose, by analogy with the conjugated polyenes, that the moment is along the greater axis of the molecule, which we have called z; and, indeed, the valence-bond treatment of Förster, in so far as it is valid, supports this view, as also, for the special case of naphthalene, do some recent improved calculations of Mr. D. Craig, now in course of publication. But we shall show that the molecular orbital treatment leads to a transition moment in the y-direction. Here then is an interesting case where the two main methods disagree in a specific prediction. For that reason we have set out all the arguments that we can find, so that all possible evidence may be used to form a final judgment. It does not seem possible to decide unequivocally one way or the other, though we shall show that the molecular orbital (m.o.) calculations are supported by no less than five distinct lines of argument. It would seem, therefore, that they have a considerable plausibility. These arguments are (i) calculation of absorption energies as a function of chain length, (ii) calculation of relative energies for the $N \rightarrow V_1$ and $N \rightarrow V_2$ transitions, (iii) limiting condition for large molecules, (iv) calculation of intensities, and (v) some experiments on fluorescence. But the matter is not finally and completely settled.

§ 2. SYMMETRY PROPERTIES

In the notation of Mulliken (1933) all the molecules of this series are plane and have symmetry $V_h (= D_{2h})$. This means that there are only eight distinct types of m.o., shown in the character table below as $A_{1g}, \ldots . B_{3u}$. This table, devised in the manner of Mulliken, shows how each of the eight types behaves under the influence of the eight sets of covering operations of the symmetry group. It also shows the behaviour of the coordinates x, y, z. It is not difficult to show that provided we deal entirely with mobile electrons (that is, with electrons whose wave function is antisymmetrical with respect to reflection in the plane of the molecule, and may therefore be built up, approximately, from $2p_x$ atomic orbitals), then for the individual electrons, though not for the totality of mobile electrons, we need only consider four of the eight types given in the table. These are A_{1u}, B_{1g}, B_{2g}, B_{3u}. Now in a molecule such as pentacene there are 22 mobile electrons, occupying several orbits of each of the four types. Our notation will subsequently be much simplified if, instead of using the full names $A_{1u}, \ldots .$, we use other symbols P, Q, R, S for each separate electronic m.o., reserving the

* This convention for the x axis is by no means invariable. Sometimes the directions of the x and z axes are interchanged from figure 2 ; and then B_{1g}, B_{1u} etc. become B_{3g}, B_{3u} and *vice versa* ; but A_1 and B_2 are unchanged.

fuller description for the molecular states that result from the totality of the mobile electrons. The correlation between the two sets of names is shown below.

Table 1. Character table for $V_h \equiv D_{2h}$

	Coordinates	E	$C_2(z)$	$C_2(y)$	$C_2(x)$	i	$iC_2(z)$	$iC_2(y)$	$iC_2(x)$
A_{1g}		1	1	1	1	1	1	1	1
A_{1u}		1	1	1	1	−1	−1	−1	−1
B_{1g}		1	1	−1	−1	1	1	−1	−1
B_{1u}	z	1	1	−1	−1	−1	−1	1	1
B_{2g}		1	−1	1	−1	1	−1	1	−1
B_{2u}	y	1	−1	1	−1	−1	1	−1	1
B_{3g}		1	−1	−1	1	1	−1	−1	1
B_{3u}	x	1	−1	−1	1	−1	1	1	−1

Simplified notation	P	Q	R	S
Full group-theory notation ..	B_{3u}	B_{2g}	B_{1g}	A_{1u}

One advantage of the distinction that we are making is that it will always be obvious whether we are speaking of a single electron, or of the whole molecule. Another is that we can distinguish the m.o. of a given type (e.g. P) by a suffix, showing its order on an energy scale. Thus P_2 would denote the second m.o. of type P, and the long wavelength absorption in anthracene (see § 3) would be written

$$P_1^2 Q_1^2 R_1^2 P_2^2 Q_2^2 S_1^2 R_2^2 \quad {}^1A_{1g} \rightarrow P_1^2 Q_1^2 R_1^2 P_2^2 Q_2^2 S_1^2 R_2 P_3 \quad {}^1B_{2u}. \qquad \ldots\ldots(1)$$

In this description the electrons of greatest binding energy come first (though in this particular case R_1 and P_2 have equal energy, and so do Q_2 and S_1. This, as figure 3 shows, is unusual.) Equation (1) shows that absorption corresponds essentially to the excitation of an electron in orbit R_2 to a higher orbit P_3. A convenient abbreviation would be

$$R_2^2 \quad {}^1A_{1g} \rightarrow R_2 P_3 \quad {}^1B_{2u}. \qquad \ldots\ldots(2)$$

Since, as table 1 shows, two electrons in any orbit have combined symmetry A_{1g}, the selection rules and symmetry classes for the absorption jump are in fact entirely determined by the orbits shown in (2). Now, in what follows, we shall only be concerned with molecules in which, on excitation, there are two singly-occupied m.o. This means, in effect, that only one electron is excited from the ground state configuration. Table 2 shows the symmetry representation corresponding to any

Table 2. Symmetry class of product of two electrons

	P	Q	R	S
P	A_{1g}	B_{1u}	B_{2u}	B_{3g}
Q	B_{1u}	A_{1g}	B_{3g}	B_{2u}
R	B_{2u}	B_{3g}	A_{1g}	B_{1u}
S	B_{3g}	B_{2u}	B_{1u}	A_{1g}

two electrons in any pair of orbitals of the types P, Q, R or S. Thus the intersection of the row R and the column P gives the type (B_{2u}) associated with the

unpaired electron configuration RP, as in (2). There is, of course, usually both a singlet and a triplet level, e.g. $^1B_{2u}$ and $^3B_{2u}$; but we shall only be concerned with the singlet, since the ground state is always a singlet $^1A_{1g}$, and singlet-triplet transitions are not allowed. Now the ground state is A_{1g}, and allowed transitions must satisfy the $g \rightarrow u$ selection rule. Table 2 shows that this restricts excitation except to B_{1u} and B_{2u} configurations. The allowed upper states and the corresponding directions of polarization are shown in table 3.

Table 3. Allowed upper states and direction of polarization

Upper state	Absorption process	Polarization
PR, or QS	$A_{1g} \rightarrow B_{2u}$	y
PQ, or RS	$A_{1g} \rightarrow B_{1u}$	z

With this background, which is common to all the molecules of this series, we may now pass to a discussion first of the energy change in absorption, then of the direction and intensity of the transition. It will suffice to explain the analysis for one molecule, anthracene, in detail. The others are entirely similar.

§ 3. ANTHRACENE

Let us number the carbon atoms of anthracene as shown in figure 2. This is not the conventional chemical numbering, but it is the one best suited to this problem. Also, let ψ_j denote the $2p_x$ orbital of carbon atom j. Then we are to form the various allowed m.o. by linear combination of all the ψ_j and $\psi_{j'}$. Alternatively, as was shown by Hückel (1932), we may choose any suitable groupings of these. Now, by symmetry, ψ_1, $\psi_{1'}$, ψ_7, $\psi_{7'}$ must always occur with equal weight, and similarly for the others. This leads us to the following sub-groups, in which we have omitted the ψ and used simply j to stand for ψ_j. These are seen to conform to the symmetry classes discussed in § 2.

$$\left.\begin{array}{ll} \text{Group } P, & 1+1'+7+7',\ 2+2'+6+6',\ 3+3'+5+5',\ 4+4', \\ \text{Group } Q, & 1+1'-7-7',\ 2+2'-6-6',\ 3+3'-5-5', \\ \text{Group } R, & 1-1'+7-7',\ 2-2'+6-6',\ 3-3'+5-5',\ 4-4', \\ \text{Group } S, & 1-1'-7+7',\ 2-2'-6+6',\ 3-3'-5+5'. \end{array}\right\} \quad \ldots\ldots (3)$$

On account of their symmetry, the elements of different rows are non-combining, so that the allowed m.o. are formed solely out of members of any one row. Thus there are four m.o. found by suitable linear combination of the four members in the top row; all these are of P type and may be called P_1, P_2, P_3, P_4. The energies may be found by finding the roots of the appropriate secular determinants, as was done by Hückel (see also Wheland 1941). In the simplest approximation, where overlap between adjacent atomic orbitals is neglected, these energies are of the form

$$E = E_0 + k\beta, \qquad \ldots\ldots (4)$$

where E_0 is the energy of a $2p_x$ electron on any one nucleus, β is a resonance integral between adjacent nuclei, and k is a numerical coefficient different for each level and found from the secular determinant. As β is numerically negative, positive values of k correspond to bonding, negative values to anti-bonding, orbitals.

In the complete set of levels (3), positive and negative values of k occur equally often. If we do not neglect the overlap S between adjacent atomic orbitals, the energies are no longer given by (4), but, as Wheland showed, they are

$$E = E_0 + m\gamma, \qquad \text{where } m = k/(1+kS). \qquad \ldots\ldots (5)$$

Here γ is a new resonance integral which replaces β, and is equal to $E_0 - S\beta$. In calculations, S is given the value 0·25. Our procedure, therefore, is to solve the simpler equation to get the values of k in (4); then we use (5) to convert from k-values to m-values. In this way the energies shown in figure 3 are obtained.

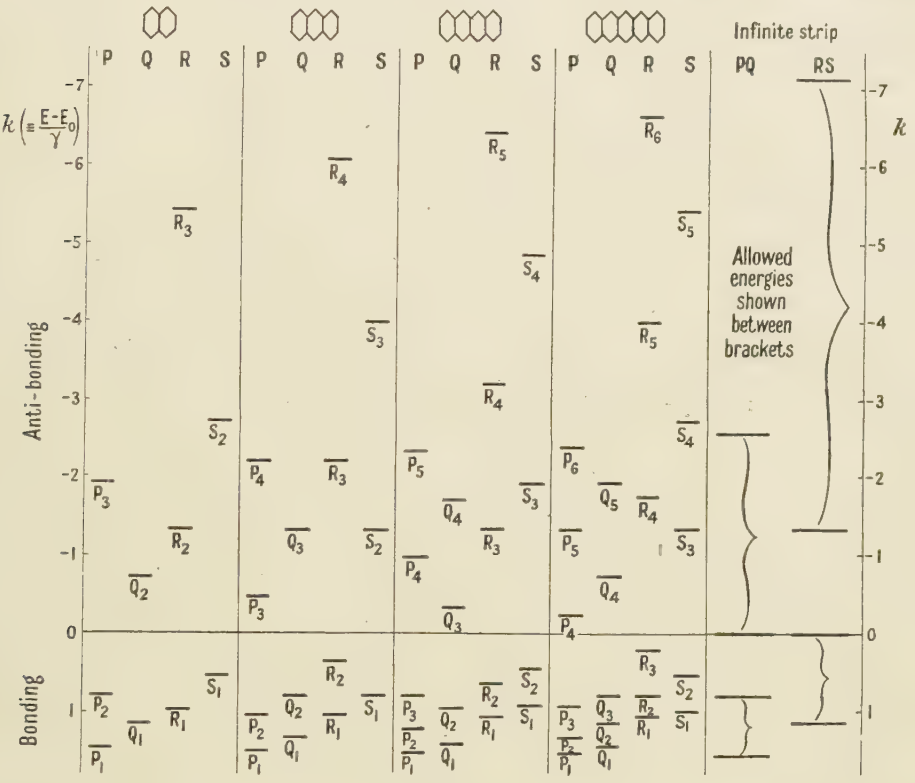

Figure 3.

This shows the allowed energies in each of the four groups P–S, plotted in terms of γ. The solid horizontal line corresponds to $E = E_0$, i.e. $m = 0$. Orbitals below the line are bonding, those above it are anti-bonding. Notice the very considerable asymmetry in the two halves—a situation already noted in the case of the continuous band distributions of infinite strips of carbon atoms by Coulson and Rushbrooke (1947). The simpler molecules of this series give secular equations which are fairly easily solved directly, but for the more complex members, and for the infinite polyacene chain (see later), the method explained in the appendix is useful.

In the ground state, all seven bonding orbitals are doubly occupied, leading to the assignment stated in (1).

Excited states are reached by taking one of the electrons from an orbital below the line and placing it in an orbital above the line. The excitation energy is

obviously least if the transition is $R_2 \rightarrow P_3$: or, more accurately, $R_2^2 \rightarrow R_2P_3$, as stated in (2). A glance at table 3 shows that this is an allowed transition with polarization along the y-direction. There are, of course, many other possible allowed transitions. Following M.R.'s notation we may call them $N \rightarrow V_1$, $N \rightarrow V_2$, ... The five lowest, including two forbidden ones, are shown below.

Table 4. $N \rightarrow V$ transitions in anthracene

Transition	Description	Excited configuration	Excitation energy	Polarization
$N \rightarrow V_1$	$R_2^2 \rightarrow R_2P_3$	B_{2u}	$0{\cdot}836\gamma$	y
$N \rightarrow V_2$	$Q_2^2 \rightarrow Q_2P_3$	B_{1u}	$1{\cdot}261\gamma$	z
$N \rightarrow V_3$	$S_1^2 \rightarrow S_1P_3$	B_{3g}	$1{\cdot}261\gamma$	forbidden
$N \rightarrow V_4$	$R_1^2 \rightarrow R_1P_3$	B_{2u}	$1{\cdot}506\gamma$	y
$N \rightarrow V_5$	$P_2^2 \rightarrow P_2P_3$	A_{1g}	$1{\cdot}506\gamma$	forbidden

Interaction between the lowest B_{2u} states V_1 and V_4 will slightly lower the $N \rightarrow V_1$ energy. So also will interaction between V_2 and V_6 and V_7 (all type B_{1u}) lower V_2. It is not the purpose of this paper to calculate these additional energy changes, which are zero in our approximation, and small in any case. Certainly they could not be responsible for driving the B_{1u} level below the B_{2u}. The position here is quite clear-cut: the y-polarization is of lowest energy.

§ 4. OTHER MOLECULES

Figure 3 shows the energy values for the other molecules of this series with $n = 2, 4, 5$. They are obtained in just the same way and are grouped into their P, Q, R, S types. In the molecules with odd values of n (such as anthracene) the lowest absorption is $R^2 \rightarrow RP$; in the even molecules it is $S^2 \rightarrow SQ$. Now both of these are allowed transitions, of the form $^1A_{1g} \rightarrow {}^1B_{2u}$, with polarization in the y-direction. As naphthalene is more important than the others, we give, below, the lowest five transitions for this molecule, similar to table 4 for anthracene.

Table 5. $N \rightarrow V$ transitions in naphthalene

Transition	Description	Excited configuration	Excitation energy	Polarization
$N \rightarrow V_1$	$S_1^2 \rightarrow S_1Q_2$	B_{2u}	$1{\cdot}267\gamma$	y
$N \rightarrow V_2$	$P_2^2 \rightarrow P_2Q_2$	B_{1u}	$1{\cdot}532\gamma$	z
$N \rightarrow V_3$	$R_1^2 \rightarrow R_1Q_2$	B_{3g}	$1{\cdot}715\gamma$	forbidden
$N \rightarrow V_4$	$S_1^2 \rightarrow S_1R_2$	B_{2u}	$1{\cdot}868\gamma$	z
$N \rightarrow V_5$	$Q_1^2 \rightarrow Q_1Q_2$	A_{1g}	$1{\cdot}884\gamma$	forbidden

Such tables as 4 and 5 are easily written down for other members of the series. They all show a y-polarization as having the lowest energy, the closest z-polarization being at an increasing distance above the y-polarization as n increases. Figure 4 shows how the excitation energies of the B_{2u} and B_{1u} transitions vary from molecule to molecule. In benzene, with its extremely high symmetry, the simple division valid for the other molecules no longer applies. But the

corresponding point at $2{\cdot}133\gamma$ may be said to belong to both groups, and we have drawn the two curves accordingly. At large values of n, it may be shown (see Appendix) that the lower (i.e. B_{2u}) curve tends to zero energy, whereas the upper (i.e. B_{1u}) curve tends to a finite value $0{\cdot}8\gamma$. We have, in fact, a case of partially overlapping bands, as found in the theory of metals (see also Coulson and Rushbrooke 1947). In the case of a large molecule we are effectively dealing with a crystal strip, and our method is synonymous with that known as the Bloch theory. This has given such good qualitative results in the theory of metals that it is almost inconceivable that its prediction for the large strip should be sufficiently inaccurate for the B_{1u} level to lie below the B_{2u} one. We may, indeed, regard this as substantial evidence in favour of the assignment of direction that we have made for the long wavelength transition.

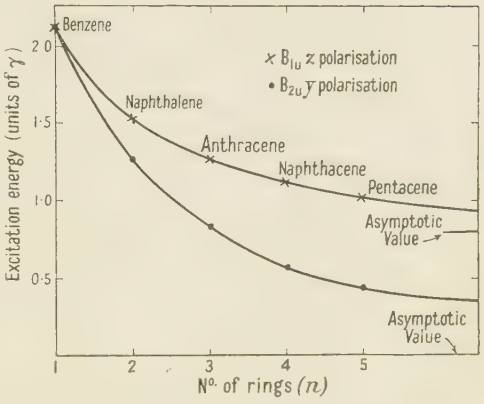

Figure 4.

This conclusion concerning the direction of polarization of absorbed light is unexpected. But it receives confirmation in some experimental work of Krishnan and Seshan (1936). These workers studied the fluorescence of small traces of naphthacene imbedded in solid solutions of anthracene or of chrysene. They found (i) that the absorption was much stronger when the direction of electric vibration was in the plane of the rings, (ii) that "whether the exciting light vibrations are along the b axis, or along a, the direction of polarization of fluorescent light remains the same, the component of the fluorescent light vibrating along the b axis being much more intense than the component along the a axis"; and (iii) "the b vibration is predominant in the fluorescent light not only when the exciting light vector is along the same direction—a result normally to be expected—but also when the light vector is along a, which is perpendicular to b—a very striking result". They called this phenomenon negative polarization. Now the molecules in the crystal (see e.g. Robertson 1933) are unfortunately not all parallel, but in naphthacene and anthracene the molecules are nearly normal to a, so that the b direction is quite close to the short direction in the plane—the direction which we have been calling y. This shows almost conclusively, first, that the upper state of the long wave absorption is a B_{2u} state; second, that absorption along the a axis, which may lead either to x or z polarization, requires greater energy; and third, that after excitation, some of this greater energy may be degraded with final emission of y-polarized light. All this is in complete agreement with our theoretical calculations.

But there is a further test that we may apply. We have seen that in every case the m.o. theory predicts that the V_1 state is B_{2u}, and (at least for the smaller molecules) the V_2 state is B_{1u}. It is possible (Jones 1945, Clar 1933) to observe the approximate positions of the first two u.v. bands and we may compare the ratio of the energies $(N \rightarrow V_2)/(N \rightarrow V_1)$ for the series of molecules naphthalene to pentacene. Table 6 shows both the observed and calculated values for this ratio. The agreement is good, judged on an absolute scale. But when it is recognized

that the variations of this ratio with the number of rings is not what would have been expected *a priori*, and yet theory and experiment are nowhere more than 15% apart, it must be admitted that there is very strong support for the interpretation of these transitions that we have given. In view of this it is hard to avoid the

Table 6. Variation of energy ratio $(N \rightarrow V_2)/(N \rightarrow V_1)$ with number of rings

Molecule	No. of rings	Experimental ratio	Calculated ratio
Naphthalene	2	1·14	1·21
Anthracene	3	1·48	1·51
Naphthacene	4	1·70	1·89
Pentacene	5	2·06	2·34

conclusion that the B_{2u} transition is the lowest, and that as n increases, λ increases without limit, giving what is known as a divergent sequence. But the energy of the B_{1u} transition tends to a finite non-zero value; in other words, this sequence is convergent. The question now arises—how accurate are the absolute values of the calculated absorption frequencies? There are several reasons why a great accuracy is not to be expected. First, the calculated frequency is directly proportional to the resonance integral γ, and the value of this quantity is not known with complete reliability. Second, the bond lengths, and hence the individual values of γ, have all been assumed equal, whereas Moffitt and Coulson in a paper in course of publication have shown that there are fairly large deviations from equality. Third, and most serious, we have completely neglected the singlet-triplet separation in the excited state. The writer will show in a later paper in this series that for polyene chains the excited singlet lies considerably above the triplet, the average of the two being given by the treatment we have here been using. It seems reasonable to suppose that the same relative separations are likely to occur for polyacenes as for polyenes. If this is so, corrections of up to 20%, or even 30%, have to be introduced. But if we are solely concerned with one set of levels, either the singlets or the triplets, but not both together, these corrections may be almost completely obviated by a simple change in the numerical value of the resonance integral γ; as a result we may, with some accuracy, calculate the transition energies by neglecting the spin interaction which leads to a distinction between singlet and triplet, by the simple expedient of using a different γ for the singlets and for the triplets. As we are here only interested in the singlets, this amounts to saying that the value of γ required for these u.v. transitions in our simple theory is of the order of 20 to 30% greater than the value of γ required to compare resonance energies and heats of formation. When this is admitted, we find a quite reasonable agreement. For example, the correct wavelength (2750 A.) for naphthalene requires γ to be about 3·5 ev. If we subtract 30% we get 2·3 ev., a value lying within the range 2 to 2·5 ev. commonly used for this integral in resonance calculations.

If the above argument is correct, we should be able to predict with considerably more reliability the characteristic red shift with increasing length of molecule, since we may express our results in a form independent of the precise numerical value of γ. This is indeed the case. Table 7 shows how the ratio of the wave-

lengths of the $N \rightarrow V_1$ transition in a given molecule (n) of this class and in naphthalene ($n = 2$) varies with n. The agreement between theory and experiment is as satisfactory as we should expect from this kind of treatment.

Table 7. Ratio of lowest absorption wavelength to that of naphthalene

n	2	3	4	5
Calculated ratio	1·00	1·51	2·11	2·86
Observed ratio	1·00	1·35	1·67	2·11

It may be mentioned that for large values of n, this theory predicts a variation of the absorption wavelength of the form

$$\lambda = \frac{h}{2\pi^2\gamma}(n+1)^2.$$

§ 5. INTENSITIES

A further test of the theory is found by calculating the intensities of the various transitions. This (see M.R. pp. 232–3) is achieved by means of either the dipole strength D, the transition moment Q or the oscillator strength f. Table 8 shows the values obtained in this way. The column headed f_{theor} represents the oscillator strengths deduced from the equation (M.R. equation (2))

$$f = 1{\cdot}085 \times 10^{11} \times \nu \times D,$$

and using the experimental values of ν shown in the previous column, which are quoted from Förster (1938). The column headed f_{exp} represents values deduced from experimental extinction curves. The writer gratefully acknowledges the provision of these, prior to publication, by Mr. D. Craig.

Table 8. Intensities of B_{2u} transition

Molecule	n	Q(A.)	D(A.^{2})	ν(cm.$^{-1}$)	f_{theor}	f_{exp}	$D(B_{1u})$
Naphthalene	2	1·706	2·910	36400	1·15	0·11	2·167
Anthracene	3	1·755	3·080	26600	0·89	0·09	3·316
Naphthacene	4	1·796	3·226	21700	0·76	0·08	4·331
Pentacene	5	1·829	3·345	17200	0·63	0·08	5·185

We may notice several features in table 8. First, the dipole strength is practically constant along the series. This is to be expected if the transition is along the short length of the molecule, but not if it is along the greater length. Verification of this is found in the last column, where we show the dipole strength calculated for the lowest $A_{1g} \rightarrow B_{1u}$ transition. Here D increases almost regularly with n, a situation found in almost identical terms by M.R. (table 5 on p. 258) for the diphenyl polyenes Ph–(CH = CH)$_n$–Ph, where the transition moment must necessarily lie along the length of the chain. This almost steady value of D in the B_{2u} transition leads to a slight decrease in the value of f as n increases. This decrease is just the same as that found experimentally and provides further justification for the B_{2u} interpretation. It is perhaps worth mentioning that a

consideration of the coefficients in the relevant m.o. shows that if all the C–C bonds are supposed to have the same length r_{CC} (in A.), then the $N \rightarrow V$ transition moments for all $A_{1g} \rightarrow B_{2u}$ transitions are such that Q lies between $\sqrt{2}r_{CC}$ and $2\sqrt{2}r_{CC}$. There is no such limitation in the $A_{1g} \rightarrow B_{1u}$ transitions, for which Q appears to increase almost linearly with $\sqrt{n}$.

The absolute value of f, as calculated, is much too high. This is a familiar situation. Thus M.R. (p. 263) introduce correction factors varying from 2/5 to 1/4, and for F_2 and Cl_2 (p. 251) a correction factor of 0·1 is required. This is of the same order as our ratio between f_{exp} and f_{theor}. It is a pity that such accuracy is about the best that can be expected if we are not prepared to consider more carefully the value of the overlap integrals, changes in bond length and effect of vibrations. The significant fact about the column f_{theor} is that the ratio f_{theor}/f_{exp} is substantially constant for the whole series of molecules.

A word may now be said about the relation of this work to the semi-classical theory of colour developed by Lewis and Calvin (1939). These authors speak of electron oscillations through the whole, or a part, of the system, and refer to absorption bands of complete or of partial oscillation. In the case of polyacenes, bands of complete oscillation would be those for which, in quantum language, the transition moment lay along the z-axis, and corresponded to a "charge transfer" across a fair proportion of the total length. The theory developed by Lewis and Calvin postulates that the restoring force on an electron moving along the greater length is less than along the shorter, so that the oscillations of least energy are in this direction; and therefore the long wavelength spectrum should be polarized this way. Our theory runs entirely counter to this view. For however long the molecule may be, the charge transfer is along the short direction in the molecular plane: and the observed red shifts with increasing size are accounted for quite adequately without recourse to the semi-quantum picture of Lewis and Calvin. Indeed, this latter theory cannot possibly explain what we believe to be the case, namely that the red shift is associated with oscillations *along* the chain length in polyenes and *across* the chain length in polyacenes (cf. particularly Lewis and Calvin, pp. 293–4, 314). It seems as if this theory must be abandoned. We can, in fact, see fairly easily where it goes wrong. Quantum-mechanically we know that there are various allowed energies for the molecular electrons; and the lowest energy is one in which (see e.g. Bowen 1946, pp. 106–113) there is no node in the wave function. Increasing energies are associated with increasing numbers of nodes. These nodes, like the nodes in a vibrating rectangular plate, are parallel to one or other of the axes of the molecule. In the ground state of the molecule all the lowest levels are filled, so that an electron making a transition of the kind we are discussing must already have a wave function with several nodes. Whether the extra node that it acquires on excitation is in the one direction or the other (i.e. whether the polarization is in the one direction or the other) cannot possibly be deduced from the kind of argument used by Lewis and Calvin, unless it be supposed, on some kind of parallel with a harmonic oscillator, that the energy difference between successive levels of the same kind (partial or complete) is effectively unchanged for the first seven or eight levels of each kind. Such a hypothesis is manifestly wrong, as the whole body of spectral evidence from atoms shows. All that these authors do is to determine whether it is easier, starting from a nodeless wave function, to create a node in the one direction or the other. They conclude that it is easiest to create a node which divides the long axis of the molecule in two.

This will be recognized, in figure 3, as a statement that when we start in the level P_1 (which has no nodes of the kind we are discussing) it requires less energy to go to Q_1 than to R_1; and, what is more, the energy separation P_1 to Q_1 decreases as $1/n$. Lewis and Calvin's error is that they have confused the level of the lowest possible molecular orbital with that of the highest occupied molecular orbital. For that reason their theory is quite invalid in this particular type of molecule.

§ 6. COMPARISON WITH VALENCE-BOND TREATMENT

We close with an account of the relation between our molecular orbital treatment and the corresponding valence-bond treatment, the only specific published calculations for which are due to Förster (1938). Let us consider as a particular example, the anthracene molecule. Förster regarded the ground state and the lowest excited state as combinations of the four unexcited (Kekulé) structures $A \ldots . D$. Their wave functions ψ_{I} and ψ_{II} were of the forms

$$\psi_{\mathrm{I}} = c_1(\psi_{\mathrm{A}} + \psi_{\mathrm{B}}) + c_2(\psi_{\mathrm{C}} + \psi_{\mathrm{D}}),$$
$$\psi_{\mathrm{II}} = c_3(\psi_{\mathrm{A}} - \psi_{\mathrm{B}}) + c_4(\psi_{\mathrm{C}} - \psi_{\mathrm{D}}),$$

with $c_1 \ldots . c_4$ as determined numerical constants. The transition $\psi_{\mathrm{I}} \rightarrow \psi_{\mathrm{II}}$

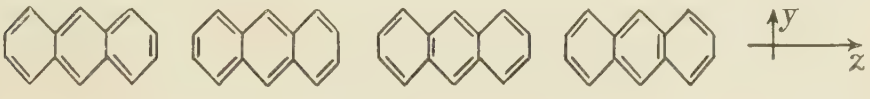

A *B* *C* *D*

Figure 5.

is clearly polarized in the z-direction, being $A_{1g} \rightarrow B_{1u}$. This is contrary to our own conclusions. But two comments must be made. First, all higher excited structures were omitted. Now both Jonsson (1942) and A. and B. Pullman (1946) have shown that these are very significant, even in the ground state, contributing at least 50% additional resonance energy, and having a total weight almost equal to that of the four Kekulé structures. Second, the very nature of the four wave functions $A \ldots . D$ precludes the possibility of any charge transfer in the y-direction. To get this we must include ionic structures, of which two types (cf. Jones 1945) are likely to be most important in determining intensities. We show (*E–F*, *G–H*) two examples of each, though there are many more from which we might have made our selection. *E* and *F* may be called y-ionic structures since they will

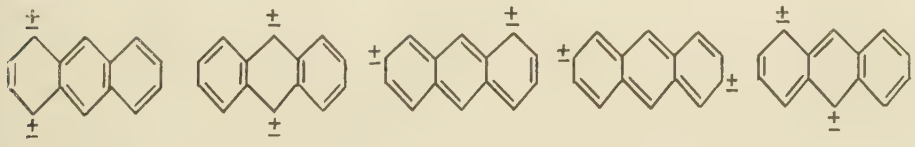

E *F* *G* *H* *I*

y-ionic structures z-ionic structures

Figure 6.

contribute to transitions polarized in that direction: *G* and *H* contribute mostly to z-polarization. There are, however, structures such as *I* which contribute to both polarizations, and which are not unfavourable energetically. Now a careful consideration of the ionic structures *E–H* shows that in the y-ionic type the resonance in at least one ring, and often in two rings, is unbroken, whereas in the z-ionic type, resonance is broken in every ring, the structures being essentially

quinonoid. This implies that the y-ionic structures will be far more effective than the z-ionic ones in reducing the total energy of the excited molecule. If, as is very possible, these structures contribute more to the excited state than to the ground state, it is at least plausible that the y-transition $A_{1g} \rightarrow B_{2u}$ is of lower energy than the z-transition $A_{1g} \rightarrow B_{1u}$, a conclusion obtained somewhat similarly in a qualitative way by Jones. However, only explicit calculations can show whether this is indeed the case, and such calculations by this method are wanting. The general conclusion seems to be that for molecules of this kind, the m.o. theory, by virtue of its automatic inclusion of ionic terms, has an advantage over the valence-bond theory.

In conclusion the writer would like to acknowledge gladly the benefit of helpful discussion and criticism from Dr. E. J. Bowen, F.R.S., and Mr. David Craig.

APPENDIX

The secular determinant for the general polyacene $C_{4n+2}H_{2n+4}$ may be evaluated by Rutherford's method (see Rutherford 1947, and Bradburn, Coulson and Rushbrooke 1947). But the following method seems rather simpler.

Number the atoms as shown. Then we may immediately separate the atomic orbitals into non-combining groups:

$$\begin{aligned}(+)\quad & 1+1',\ 2+2',\ 3+3',\ \ldots.\ 2n+2n',\ (2n+1)+(2n+1)',\\ (-)\quad & 1-1',\ 2-2',\ 3-3',\ \ldots.\ 2n-2n',\ (2n+1)-(2n+1)'.\end{aligned} \qquad \ldots\ldots(6)$$

Figure 7.

The group $(+)$ includes the previous P and Q groups. The group $(-)$ includes the R and S groups. Using the orbitals (6) as a base, writing $(E_0-E)/\beta=-k$, as in (4), and neglecting the overlap integral S, the secular determinant becomes

$$\Delta=\Delta_+\Delta_-$$

where

$$\Delta_\pm = \begin{vmatrix} -k\pm1 & 1 & & & & & & \\ 1 & -k & 1 & & & & & \\ & 1 & -k\pm1 & 1 & & & & \\ & & 1 & -k & 1 & & & \\ & & & & \cdots & & & \\ & & & & & 1 & -k & 1 \\ & & & & & & 1 & -k\pm1 \end{vmatrix} \qquad \ldots\ldots(7)$$

There are $2n+1$ rows and columns in each of the two factors. Consider the Δ_+ determinant first. If we multiply the 1st, 3rd, 5th.... rows by $\sqrt{k}$ and the 2nd, 4th, 6th.... rows by $\sqrt{(k-1)}$, and then divide the 1st, 3rd.... columns by $\sqrt{(k-1)}$ and the 2nd, 4th.... columns by $\sqrt{k}$, we find that

$$\Delta_+=\sqrt{\left(\frac{k-1}{k}\right)}\times \begin{vmatrix} x & 1 & & & & & \\ 1 & x & 1 & & & & \\ & 1 & x & 1 & & & \\ & & \cdots & & & & \\ & & & & 1 & x & 1 \\ & & & & & 1 & x \end{vmatrix} \qquad \ldots\ldots(8)$$

where

$$x^2=k(k-1). \qquad \ldots\ldots(9)$$

This last determinant is of familiar form. If (Coulson 1938) we put

$$x = -2\cos\theta,$$

it is $$\Delta_+ = \sin(2n+2)\theta/\sin\theta,$$

so that the roots are $x = -2\cos\{r\pi/(2n+2)\}$, $r = 1, 2, \ldots 2n+1$.

This means, from (9), that the allowed values of k are $k = +1$, together with all the roots of

$$k(k-1) = 4\cos^2\frac{r\pi}{2n+2}, \qquad r = 1, 2, \ldots n,$$

i.e. $$k = +1, \qquad k = \frac{1}{2}\left\{1 \pm \sqrt{\left(9 + 8\cos\frac{r\pi}{n+1}\right)}\right\}. \qquad \ldots\ldots(10)$$

Similarly the Δ_- determinant gives roots

$$k = -1, \qquad k = \frac{1}{2}\left\{-1 \pm \sqrt{\left(9 + 8\cos\frac{r\pi}{n+1}\right)}\right\}. \qquad \ldots\ldots(11)$$

It is easy to show that the roots of (10) correspond alternately to P and Q orbitals, with the P orbital lowest. Similarly the roots of (11) correspond alternately to R and S orbitals, with the R lowest. For $n = 1$ to $n = 5$, these conclusions are easily verified in figure 3.

When the k-values of the m.o. have been obtained, the m-values follow at once from (5).

An important application of (10) and (11) is to the case of a large molecule, or infinite strip. Then, as $n \to \infty$, the Δ_+ determinant gives a band, equally populated by P and Q type orbitals, stretching from $k = \frac{1}{2}(\sqrt{17}+1)$ to 1, and then from 0 to $-\frac{1}{2}(\sqrt{17}-1)$. Similarly Δ_- gives a band, equally populated by R and S type orbitals, stretching from $k = \frac{1}{2}(\sqrt{17}-1)$ to 0 and then from -1 to $-\frac{1}{2}(\sqrt{17}+1)$. These values, corrected to the m-notation, are shown at the extreme right of figure 3. This shows clearly that the lowest transition is of the type $R \to P$, or $S \to Q$, both being of y-polarization ($R \to Q$ and $S \to P$ are forbidden). On the other hand, the lowest transition with z-polarization is of the type $P \to Q$, or $Q \to P$. In the limit of an infinite molecule, the lowest y-transition involves zero energy, but the lowest z-transition requires $0{\cdot}8\gamma$, as stated in the text.

REFERENCES

Bowen, E. J., 1946, *Chemical Effects of Light* (Oxford : The Clarendon Press), Second Edition, p. 127.

Bradburn, M., Coulson, C. A., and Rushbrooke, G. S., 1947, *Proc. Roy. Soc., Edin.* (In the press.)

Clar, E., 1933, *Ber.*, **66,** 202.

Coulson, C. A., 1938, *Proc. Roy. Soc.*, A, **164,** 383.

Coulson, C. A., and Rushbrooke, G. S., 1947, *Proc. Roy. Soc., Edin.* (In the press.)

Forster, T., 1938, *Z. Phys. Chem.*, B, **41**, 287.

Hückel, E., 1932, *Z. Phys.*, **76,** 628.

Jones, R. N., 1945, *J. Amer. Chem. Soc.*, **67,** 2127.

Jonsson, V., 1942, *Arkiv Kemi. min. Geol.*, **15** A, No. 14.

Krishnan, K. S., and Seshan, P. K., 1936, *Acta Phys. Polonica*, **5,** 289.

Krishnan, K. S., and Seshan, P. K., 1938, *Proc. Ind. Acad. Sci.*, **8,** 487.

Lewis, G. N., and Calvin, M., 1939, *Chem. Rev.*, **25,** 273.

Mulliken, R. S., 1933, *Phys. Rev.*, **43,** 279.

Mulliken, R. S., and Rieke, C. A., 1941, *Rep. Progr. Phys.*, **8,** 231.

Pullman, A. and B., 1946, *Experientia*, **2,** 364.

Robertson, J. M., 1933, *Proc. Roy. Soc.*, A, **140,** 79.

Rutherford, D. E., 1947, *Proc. Roy. Soc., Edin.*, A, **62,** 229.

Scheibe, G., 1938, *Kolloidzschr.*, **82,** 1.

Scheibe, G, and Kandler, L., 1938, *Naturwissenschaften*, **26,** 412.

Wheland, G. W., 1941, *J. Amer. Chem. Soc.*, **63,** 2025.

Excited Electronic Levels in Conjugated Molecules: II. On the Symmetry and Multiplicity of Molecular States

By H. C. LONGUET-HIGGINS
Physical Chemistry Laboratory, Oxford

Communicated by C. A. Coulson; MS. received 28 *June* 1947

ABSTRACT. A comparison of the valence-bond method and the method of molecular orbitals shows that the valence-bond method, while often more reliable for the calculation of ground-state energies, leads to erroneous conclusions as to the number and nature of the excited states, whereas the method of molecular orbitals gives the right number of excited states of any specified symmetry and multiplicity, and leads to semi-quantitatively correct energies for the ground state and lowest excited states. The latter method therefore seems to be the more reliable for the interpretation of electronic absorption spectra in conjugated systems.

§ 1. INTRODUCTION

It is well known that there are many molecules for which the two standard approximate methods of solving the wave equation, namely the valence-bond method and the method of molecular orbitals, lead to different results for the multiplicities and symmetries of the ground state and of the first, second, and subsequent excited states, and even lead to different results for the number of molecular states of given multiplicity and symmetry.

In this paper we shall enquire into the origin of these discrepancies, and shall attempt to assess the relative merits and defects of the two approaches in the interpretation of molecular spectra.

§ 2. THE HYDROGEN MOLECULE*

We shall first deal briefly with the hydrogen molecule, as it illustrates simply certain general points that we shall make later on. We assume the wave function of any molecular state to be expressible as a sum of products of 1*s* atomic wave functions for the atoms composing the molecule (*AO* approximation). Let us denote the 1*s* atomic wave function for an electron of spin $\frac{1}{2}$ on nucleus A by a, and the 1*s* wave function for an electron of spin $-\frac{1}{2}$ on the same nucleus by $\bar{a}$. b, $\bar{b}$ will denote atomic wave functions for electrons of spin $\frac{1}{2}$, $-\frac{1}{2}$ on nucleus B. Further, we shall adopt the convention that the first factor in a product of atomic wave functions is a function of the coordinates of electron 1, and the second factor a function of the coordinates of electron 2. Thus, $b\bar{a}$ denotes the wave function for a hypothetical state in which electron 1 is on nucleus B with spin $\frac{1}{2}$, and electron 2 on nucleus A with spin $-\frac{1}{2}$.

Now, by Pauli's exclusion principle, the total molecular wave function must change sign when we interchange the two electrons. Therefore in the *AO* approximation the wave function for any molecular state must be some linear combination of the terms

$$ab-ba,\ a\bar{b}-\bar{b}a,\ b\bar{a}-\bar{a}b,\ \bar{a}\bar{b}-\bar{b}\bar{a},\ a\bar{a}-\bar{a}a \text{ and } b\bar{b}-\bar{b}\bar{b}.$$

* The argument of this section follows closely the lines of a discussion given by Hund (1932), and quoted by Van Vleck and Sherman (1935).

Of these the first four are called *covalent terms*, and the other two *ionic terms*. Further, any wave function for the molecule must have the symmetry of some irreducible representation of the molecular group; for H_2 this means that the wave function must be either symmetric or antisymmetric with respect to exchange of the nuclei.

It follows from this that the possible molecular wave functions are, apart from normalization factors:—

I $\lambda_1\{(a\bar{b}-\bar{b}a)+(b\bar{a}-\bar{a}b)\}+\mu_1\{(a\bar{a}-\bar{a}a)+(b\bar{b}-\bar{b}b)\}$ S_N

II $\lambda_2\{(a\bar{b}-ba)+(b\bar{a}-\bar{a}b)\}+\mu_2\{(a\bar{a}-\bar{a}a)+(b\bar{b}-\bar{b}b)\}$ S_N

where $\lambda_1:\mu_1$ and $\lambda_2:\mu_2$ may be determined by a variation method

III $(a\bar{a}-\bar{a}a)-(b\bar{b}-\bar{b}b)$ A_N

IV (i) $(ab-ba)$ A_N

(ii) $(a\bar{b}-\bar{b}a)-(b\bar{a}-\bar{a}b)$ A_N

(iii) $(\bar{a}\bar{b}-\bar{b}\bar{a})$ A_N

The symbols S_N, A_N denote whether the wave function is symmetric or antisymmetric with respect to interchange of the nuclei.

The above wave functions may all be factorized into an orbital part and a spin part. When this is done it turns out that I, II and III all contain the spin function $\alpha(1)\beta(2)-\beta(1)\alpha(2)$, and have different orbital functions, whereas the wave functions IV contain the same orbital function multiplying three different spin functions, namely $\alpha(1)\alpha(2)$, $\beta(1)\beta(2)$ and $\alpha(1)\beta(2)+\beta(1)\alpha(2)$. I, II and III are therefore singlet levels, and IV is a triplet level.*

In the simple valence-bond picture the terms $a\bar{a}$, $b\bar{b}$ are ignored, so that we are left with the molecular wave functions:

V $(a\bar{b}-\bar{b}a)+(b\bar{a}-\bar{a}b)$ S_N

VI (i) $(ab-ba)$ A_N

(ii) $(a\bar{b}-\bar{b}a)-(b\bar{a}-\bar{a}b)$ A_N

(iii) $(\bar{a}\bar{b}-\bar{b}\bar{a})$ A_N

Of these the first is obtained by putting $\mu_1=0$ in I, or $\mu_2=0$ in II; and the others are the same as IV. We have thus discarded the A_N singlet state and one of the S_N singlet states.

In the molecular-orbital treatment we construct the molecular wave functions out of wave functions u and v, each of which represents a possible wave function for a single electron in the field of both nuclei. It is clear that u and v must each be symmetric or antisymmetric with respect to exchange of the nuclei, so that $u=a+b$, $v=a-b$.

* The conventional notation for classifying molecular wave functions compounded of atomic orbitals of the s type is as follows:—

Multiplicity	Behaviour with respect to interchange of the nuclei	Symbol
Singlet	Symmetric	$^1\Sigma_g$
Singlet	Antisymmetric	$^1\Sigma_u$
Triplet	Symmetric	$^3\Sigma_g$
Triplet	Antisymmetric	$^3\Sigma_u$

The possible molecular wave functions are then:

VII	$(u\bar{u}-\bar{u}u)$	S_N
VIII	$(v\bar{v}-\bar{v}v)$	S_N
IX	$(u\bar{v}-\bar{v}u)+(v\bar{u}-\bar{u}v)$	A_N
X (i)	$(uv-vu)$	A_N
(ii)	$(u\bar{v}-\bar{v}u)-(v\bar{u}-\bar{u}v)$	A_N
(iii)	$(\bar{u}\bar{v}-\bar{v}\bar{u})$.	

Substitution of $a+b$ for u, and $a-b$ for v, gives:

VII	$(a\bar{a}-\bar{a}a)+(b\bar{b}-\bar{b}b)+(\bar{a}b-\bar{b}a)+(b\bar{a}-\bar{a}b)$	S_N
VIII	$(a\bar{a}-\bar{a}a)+(b\bar{b}-\bar{b}b)-(a\bar{b}-\bar{b}a)-(b\bar{a}-\bar{a}b)$	S_N
IX	$2(a\bar{a}-\bar{a}a)-2(b\bar{b}-\bar{b}b)$	A_N
X (i)	$-2(ab-ba)$	A_N
(ii)	$-2(a\bar{b}-\bar{b}a)+2(b\bar{a}-\bar{a}b)$	A_N
(iii)	$-2(\bar{a}\bar{b}-\bar{b}\bar{a})$	A_N

We see at once that, when account has been taken of normalization, the functions X are identical with IV, and that IX is identical with III. VII and VIII are simply linear combinations of I and II, and vice versa. The molecular-orbital method therefore gives us the right number of molecular states, with the right symmetry and multiplicity. On the other hand, if we take I as representing the ground state, calculation shows that $\lambda_1 \gg \mu_1$, so that V gives a better representation of the ground state than VII.

It is well known that if we take into account the ionic terms in the valence-bond method, the wave functions I and II that we shall get by a variational treatment will be as good as can be obtained on the *AO* approximation. What is not so commonly realized is that by taking into account interactions between the wave functions VII and VIII we can obtain the same best-possible wave functions I and II; that is to say, at the next degree of approximation the two methods converge.

We have considered the familiar case of H_2 in some detail because it exemplifies the results that will be established later: namely that in the valence-bond method a quite simplified treatment will give perhaps a better value for the energy in the ground state, but leads to errors of omission in the excited states; whereas the method of antisymmetrized molecular orbitals, though it may not give such an accurate wave function for the ground state, always leads to qualitatively correct conclusions about the number, symmetry and multiplicity of the excited states. In principle, of course, this defect in the valence-bond method could be eliminated by the inclusion of all possible ionic terms, but this is not feasible in complex molecules.

§ 3. MORE COMPLEX MOLECULES

We shall now consider the relation between the valence-bond and molecular-orbital methods in more complex molecules. In particular we shall study conjugated systems, that is, sets of more than two overlapping atomic orbitals.

These are well exemplified, of course, by the poly-unsaturated hydrocarbons and their derivatives, where the π-electrons move in overlapping sets of dumb-bell-shaped atomic orbitals.

Let us denote by $a, b, c, \ldots$ the atomic wave functions for a single electron of spin $\frac{1}{2}$ on atoms A, B, C, ... of a conjugated system, and by $\bar{a}, \bar{b}, \bar{c}, \ldots$ the corresponding wave functions when the electron has spin $-\frac{1}{2}$. Let us again adopt the convention that the first term in a product of these atomic orbitals is a function of the coordinates of electron 1, the second term a function of the coordinates of electron 2, and so on. Then in the *AO* approximation, using the exclusion principle, we write the molecular wave function as a sum of terms of the type

$$\Sigma P \,.\, ab\bar{c}d\bar{d},$$

where ΣP denotes the sum of the even permutations of $ab\bar{c}d\bar{d}$ minus the sum of the odd permutations. We shall call such an expression an *atomic term.* For example, the atomic term $\Sigma P \,.\, ab\bar{c}$, when written out in full, becomes

$$a(1)b(2)\bar{c}(3)+b(1)\bar{c}(2)a(3)+\bar{c}(1)a(2)b(3)-a(1)\bar{c}(2)b(3)-\bar{c}(1)b(2)a(3)-b(1)a(2)\bar{c}(3).$$

It is clear that such a sum will vanish if the same atomic orbital (a.o.) occurs twice in the sum and with the same spin, which means physically that two electrons cannot occupy the same orbital with the same spin. We may therefore classify our atomic terms according to the number of atomic orbitals that are doubly occupied in the corresponding configuration. For instance, in a system of 4 electrons and 4 atomic orbitals we have:

(i) covalent terms, e. g. $\Sigma P \,.\, ab\bar{c}d$,

(ii) singly ionic terms, e. g. $\Sigma P \,.\, a\bar{a}bc$,

(iii) doubly ionic terms, e. g. $\Sigma P \,.\, a\bar{a}c\bar{c}$.

In general, if there are $2n$ electrons and $2n-p$ atomic orbitals, we shall have

$$\frac{(2n-p)!\,2^{2n-2r}}{r!\,(r-p)!\,(2n-2r)!} \quad r\text{-ply ionic terms, } (r \geqslant p),$$

because there are

$$\frac{(2n-p)!}{r!\,(r-p)!\,(2n-2r)!}$$

ways of choosing r doubly occupied a.o. and $r-p$ unoccupied ones, and we may then assign spins to the remaining singly occupied a.o. in 2^{2n-2r} different ways. The total number of terms to be considered is therefore

$$\sum_{r=p}^{n} \frac{(2n-p)!\,2^{2n-2r}}{r!\,(r-p)!\,(2n-2r)!}.$$

We could determine the wave functions and energies of the various molecular states by setting up the secular equation in terms of all the atomic terms, and solving it by straightforward methods. However, before doing this it is best to group the atomic terms corresponding to any given distribution of electrons among the a.o. into certain combinations such that the secular equation automatically factorizes into smaller equations when set up in terms of these combinations, each of the smaller equations giving the energies and wave functions of the molecular states of one particular multiplicity. We shall call these special combinations of

atomic terms *spin-grouped atomic terms*. Any one spin-grouped atomic term will only contribute to the molecular states of one particular multiplicity, and may therefore be designated as a singlet, triplet etc., atomic term. For instance, in a molecule with 4 electrons and 4 a.o., the following will be typical spin-grouped atomic terms:

$$\Sigma P\,.\,(a\bar{b}c\bar{d}-\bar{a}\bar{b}cd),\quad \Sigma P\,.\,(\bar{a}bc\bar{d}-\bar{a}\bar{b}cd),\quad \Sigma P\,.\,(a\bar{b}\bar{c}d-\bar{a}bcd),$$

which contribute to the triplet states, and

$$\Sigma P\,.\,(a\bar{b}c\bar{d}-a\bar{b}\bar{c}d-\bar{a}bc\bar{d}+\bar{a}b\bar{c}d),\quad \Sigma P\,.\,(a\bar{b}c\bar{d}-a\bar{b}\bar{c}d-\bar{a}\bar{b}cd+\bar{a}\bar{b}\bar{c}d),$$

which contribute to the singlet levels.

Now the molecular wave functions belonging to a degenerate molecular state will differ in total electronic spin; and it can be shown that every degenerate molecular state has just one wave function of zero spin belonging to it. For instance, for the triplet level of H_2 the wave function of zero spin is

$$(a\bar{b}-\bar{b}a)-(b\bar{a}-\bar{a}b).$$

Therefore the total number of molecular states of multiplicity $2q-1$ is equal to the total number of spin-grouped atomic terms of the same multiplicity and zero total spin. Now, corresponding to a given r-ply ionic distribution of electrons among the atoms of our system, there are $\binom{2n-2r}{n-r}$ different r-ply ionic terms with zero total spin. From these we can construct

$$\binom{2n-2r}{n-r}-\binom{2n-2r}{n-r-1} \text{ singlet spin-grouped atomic terms,}$$

$$\binom{2n-2r}{n-r-1}-\binom{2n-2r}{n-r-2} \text{ triplet terms,}$$

etc., and one $(2n-2r+1)$-plet term. (Eckart 1930)

Therefore the total number of spin-grouped terms of multiplicity $2q-1$ which can be constructed out of r-ply ionic terms is

$$\frac{(2n-p)!}{r!\,(r-p)!\,(2n-2r)!}\left\{\binom{2n-2r}{n-r-q+1}-\binom{2n-2r}{n-r-q}\right\}$$

$$=\frac{(2n-p)!\,(2q-1)}{r!\,(r-p)!\,(n-r-q+1)!\,(n-r+q)!} \text{ when } p\leqslant r\leqslant n-q,$$

or

$$\frac{(2n-p)!}{r!\,(r-p)!\,(2n-2r)!}=\frac{(2n-p)!}{(n-q+1)!\,(n-q-p+1)!\,(2q-2)!},$$

when $r=n-q+1$, or 0 when $r>n-q+1$.

The total number of molecular wave functions of multiplicity $2q-1$ is therefore

$$\sum_{r=p}^{n-q}\frac{(2n-p)!\,(2q-1)}{r!\,(r-p)!\,(n-r-q+1)!\,(n-r+q)!}+\frac{(2n-p)!}{(n-q+1)!\,(n-q-p+1)!\,(2q-2)!}$$

when $q\leqslant n-p$, and 0 otherwise.

This is the number we should obtain by the valence-bond method taking into account up to s-fold ionic terms, provided $s\geqslant n-q+1$. If s were less than

$n-q+1$, we should get only some of the molecular states of multiplicity $2q-1$; and in particular we shall only get the correct number of singlet states by taking account of all possible ionic terms ($s=n$).

In the molecular orbital approximation we express the molecular wave function in terms of single-electron wave functions, each of which is a linear combination of the atomic orbitals in the system. These single-electron wave functions are called molecular orbitals (m.o.), and are equal in number to the component atomic orbitals.

Let us denote the molecular orbitals for an electron of spin $\frac{1}{2}$ by $u, v, w, \ldots$ and those for an electron of spin $-\frac{1}{2}$ by $\bar{u}, \bar{v}, \bar{w}, \ldots$. We shall continue in the convention that the first factor in a product of single-electron functions is a function of the coordinates of the first electron, the second a function of the coordinates of the second electron, and so on.

Then using the exclusion principle we write the molecular wave function as a sum of terms of the type $\Sigma P \,.\, uv\bar{w}x\bar{x}$, where the operator ΣP has the same significance as before. We call such an expression a *molecular term*. A molecular term will vanish if the same m.o. occurs in it twice with the same spin, so two electrons with the same spin cannot occupy the same m.o. Just as for atomic terms we may classify our molecular terms according to their numbers of doubly filled m.o. Thus if we have a system of 4 electrons and 4 atomic orbitals, and hence 4 molecular orbitals, then there will be three kinds of molecular term, viz:

(i) uncoupled terms, e.g. $\Sigma P \,.\, uv\bar{w}x$,

(ii) singly coupled terms, e.g. $\Sigma P \,.\, u\bar{u}v\bar{x}$,

(iii) doubly coupled terms, e.g. $\Sigma P \,.\, u\bar{u}v\bar{v}$.

There is a complete analogy between r-ply coupled molecular terms and r-ply ionic atomic terms, as we shall see at once. If our system has $2n$ electrons and $2n-p$ m.o. (compounded of the same number of a.o.), then there will be

$$\frac{(2n-p)!\,2^{2n-2r}}{r!\,(r-p)!\,(2n-2r)!}\ r\text{-ply coupled molecular terms } (r \geqslant p),$$

since there are

$$\frac{(2n-p)!}{r!\,(r-p)!\,(2n-2r)!}$$

ways of choosing r m.o. to be doubly filled and $r-p$ to be unfilled, and we may then assign spins to the remaining m.o. in 2^{2n-2r} different ways. The total number of molecular terms to be considered is therefore

$$\sum_{r=p}^{n} \frac{(2n-p)!\,2^{2n-2r}}{r!\,(r-p)!\,(2n-2r)!}.$$

From these molecular terms one can construct certain linear combinations—"spin-grouped molecular terms"—analogous to spin-grouped atomic terms, such that the secular equation would factorize into smaller equations if set up in terms of them, each smaller equation giving the energies and wave functions of the molecular states of one particular multiplicity. Any one spin-grouped term will only contribute to the molecular states of one particular multiplicity, and may therefore be designated as a singlet, triplet, $(2q-1)$-plet molecular term. The construction of

spin-grouped molecular terms is precisely analogous to the construction of spin-grouped atomic terms. For example, to get a set of linearly independent singlet molecular terms we may write down the m.o. in a circle and apply Rumer's theorem. Thus if we have 4 electrons and 4 m.o. u, v, w and x, the non-crossing diagrams

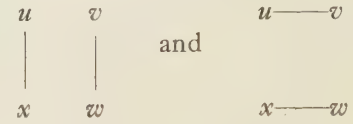

will represent the singlet terms

$$\Sigma P\,.\,(u\bar{x}-\bar{u}x)(v\bar{w}-\bar{v}w) \qquad \text{and} \qquad \Sigma P\,.\,(u\bar{v}-\bar{u}v)(w\bar{x}-\bar{w}x).$$

The total number of spin-grouped molecular terms of multiplicity $2q-1$ and zero spin which can be constructed out of r-ply coupled molecular terms is

$$\frac{(2n-p)!}{r!\,(r-p)!\,(2n-2r)!}\left\{\binom{2n-2r}{n-r-q+1}-\binom{2n-2r}{n-r-q}\right\}$$
$$=\frac{(2n-p)!\,(2q-1)}{r!\,(r-p)!\,(n-r-q+1)!\,(n-r+q)!} \quad \text{when } p\leqslant r\leqslant n-q,$$

or

$$\frac{(2n-p)!}{r!\,(r-p)!\,(2n-2r)!}=\frac{(2n-p)!}{(n-q+1)!\,(n-q-p+1)!\,(2q-2)!},$$

when $r=n-q+1$, and zero otherwise. But the total number of $(2q-1)$-plet molecular states must be equal to the total number of $(2q-1)$-plet molecular terms of zero spin, and this number is

$$\sum_{r=p}^{n-q}\frac{(2n-p)!\,(2q-1)}{r!\,(r-p)!\,(n-r-q+1)!\,(n-r+q)!}+\frac{(2n-p)!}{(n-q+1)!\,(n-q-p+1)!\,(2q-2)!}$$

when $q\leqslant n-p$, and 0 otherwise. Therefore whether we express our molecular wave functions as combinations of molecular or atomic terms, we get the same number of $(2q-1)$-plet molecular states. This must necessarily be so, since the $(2q-1)$-plet molecular terms are linear combinations of $(2q-1)$-plet atomic terms, and so whichever we use as basis for solving the secular equation we shall get the same final molecular wave functions.

Having obtained our spin-grouped molecular terms we might then solve the secular equations in terms of them. However, this would give us the same results as a valence-bond treatment taking account of all ionic terms, and with even greater labour. So in the method of m.o. as ordinarily applied we observe that the wave functions for the $(2q-1)$-plet molecular states are equal in number to the $(2q-1)$-plet molecular terms, and we identify the latter with the former. This short cut is valid so long as the energies of the various spin-grouped molecular terms differ considerably, since then the interactions between them will be small; but if the molecule has symmetry, some additional considerations are necessary.

§ 4. SYMMETRY OF MOLECULAR STATES

If the molecule has spatial symmetry, any actual wave function for the molecule must have the symmetry of some irreducible representation of the molecular group. It follows that the linear combinations of atomic or molecular terms by which we represent the wave function must also have such symmetry. Now an atomic term does not in general have irreducible symmetry, being a product of arbitrarily

selected atomic wave functions; but a molecular term, being a product of molecular orbitals each of which has irreducible symmetry, usually does have irreducible symmetry. In molecules whose symmetry groups contain degenerate representations, the molecular terms will not all have irreducible symmetry, but very simple combinations of them can be found which do; we shall ignore this case for the moment. Now a molecular wave function of given multiplicity and irreducible symmetry must be compounded of spin-grouped molecular terms of the same symmetry and multiplicity. Hence the number of spin-grouped molecular terms of given symmetry and multiplicity and zero total spin is equal to the number of molecular states of the same symmetry and multiplicity.

In the method of antisymmetrized m.o., as mentioned in the last paragraph, it is customary to identify the spin-grouped molecular terms with the actual molecular wave functions (in molecules whose symmetry groups contain no degenerate representations). We found that this leads to the correct number of singlet, triplet, etc., molecular states, and we now see that it gives us the correct number of singlet, triplet, etc., molecular states of given irreducible symmetry. We also saw in the last paragraph that this short cut is equivalent to neglecting the interactions between different spin-grouped molecular terms. When the molecule is symmetrical there can be no interactions between terms of different symmetry, and so we only have to consider whether terms of the same symmetry and multiplicity are going to interact appreciably. If their energies are close together there will be considerable interaction, but it often happens that this is not so; for instance in H_2 the energies of the molecular terms VII and VIII differ considerably, since the former corresponds to a situation in which both electrons are in the bonding m.o. $a+b$, and the latter to both electrons being in the antibonding m.o. $a-b$.

In the valence-bond method, the spin-grouped ionic terms are frequently referred to as "excited states". This nomenclature is misleading, as it implies that they approximate to the wave functions for actual molecular states, which is not generally the case, for two reasons. First, if the molecule is symmetrical, any arbitrarily selected atomic term will in general be asymmetric; it is only selected combinations of similar terms that will have irreducible symmetry in the molecular group. Secondly, the energies of these selected combinations will be roughly equal for terms with the same ionicity, so that the interactions between combinations with the same symmetry and multiplicity are by no means negligible. It is perhaps too much to hope that the use of the term "excited states" in this connection will disappear altogether; but it would be a step forward if its use could be confined at least to irreducibly symmetric *and* spin-grouped combinations of atomic terms.

There is one point which has been passed over in the above treatment. If we are treating a molecule by the method of antisymmetrized m.o., then, as mentioned above, we identify the actual molecular states with spin-grouped molecular terms; this is equivalent to saying that in a given molecular state such and such m.o. are singly or doubly occupied, and the multiplicity is $2q-1$, say. This procedure gives an unambiguous wave function for the given state provided that not more than two m.o. are singly occupied; for instance, the wave function for the singlet state u^2v^2 is $\Sigma P\,.\,u\bar{u}v\bar{v}$, and those for the triplet state u^2vw are $\Sigma P\,.\,u\bar{u}(v\bar{w}+\bar{v}w)$, $\Sigma P\,.\,u\bar{u}vw$ and $\Sigma P\,.\,u\bar{u}\bar{v}\bar{w}$. On the other hand, all we know about the wave functions for the singlet states $uvwx$ is that they are two orthogonal linear combinations of $\Sigma P\,.\,(u\bar{v}-\bar{u}v)(w\bar{x}-\bar{w}x)$ and $\Sigma P\,.\,(u\bar{x}-\bar{u}x)(v\bar{w}-\bar{v}w)$. To find the

correct combinations we should have to solve the secular equation, which necessitates knowing the interactions between the m.o. Fortunately, however, the important excited states of a molecule are generally the lowest ones, in which not more than two electrons are simultaneously unpaired, so that there is no ambiguity about the form of the wave function.

§ 5. AN EXAMPLE: 4 ELECTRONS IN 4 ATOMIC ORBITALS

It will probably clarify the above argument if we consider in detail a hypothetical molecule consisting of 4 atoms arranged at the corners of a rectangle. Such a molecule is the prototype of naphthalene and anthracene, which belong to the same symmetry group D_{2h}, and so our general conclusions will apply to these molecules also. Let us assume that the atomic orbitals in our rectangular molecule are antisymmetric with respect to the plane of the molecule, like the $2p_z$ orbitals in which π-electrons move. Then it will be impossible to construct molecular wave functions that are anything but antisymmetric with respect to the molecular plane, and so we shall lose nothing by taking the symmetry group of the molecule to be the simpler group C_{2v}. The character table of the group C_{2v} is as follows:—

	E	C_2	σ_x	σ_y
A_1	+1	+1	+1	+1
A_2	+1	+1	−1	−1
B_1	+1	−1	+1	−1
B_2	+1	−1	−1	+1

We will represent the molecule diagrammatically thus:

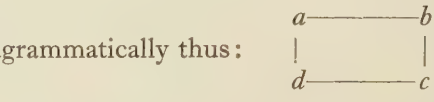

where the bonds lengths are not all equal, but $x_{ab} = x_{cd}$ and $x_{bc} = x_{da}$.

Let us first take the valence-bond approach. Then there are three kinds of atomic term—covalent, singly ionic and doubly ionic. These may be combined into singlet, triplet and quintuplet spin-grouped atomic terms. The singlet terms may be represented by structures of the conventional type; for instance (1) represents $\Sigma P \,.\, (a\bar{b} - \bar{a}b)(c\bar{d} - \bar{c}d)$, (3.1) represents $\Sigma P \,.\, b\bar{b}(c\bar{d} - \bar{c}d)$ and (8.1) represents $\Sigma P \,.\, c\bar{c}d\bar{d}$. The following diagram gives all such structures which are possible. Of these singlet atomic terms only the first two have irreducible symmetry. As for the others, we can group congruent structures into combinations having irreducible symmetry: for example, the combination (7.1) + (7.2) belongs to the irreducible representation A_1, and (7.1) − (7.2) belongs to A_2. There will be as many of these irreducibly symmetric combinations of a set of congruent atomic terms as there are atomic terms in the set.

We may draw up a table giving the number of irreducibly symmetric combinations of atomic terms in each irreducible representation. The following is such a table:—

	A_1	A_2	B_1	B_2
(1)	1			
(2)	1			
(3.1) to (3.4)	1	1	1	1
(4.1) to (4.4)	1	1	1	1
(5.1) to (5.4)	1	1	1	1
(6.1) and (6.2)	1	1		
(7.1) and (7.2)	1		1	
(8.1) and (8.2)	1			1
Total	8	4	4	4 = 20

Since the molecular wave functions are built up of these symmetric combinations, there must be eight singlet molecular wave functions of symmetry A_1, and four in each of the representations A_2, B_1 and B_2. If we had ignored the doubly ionic terms (6.1) to (8.2), we should only have found five singlet states of symmetry A_1, three of symmetry A_2, three of symmetry B_1, and three of symmetry B_2. That is, we should have missed six possible singlet molecular states.

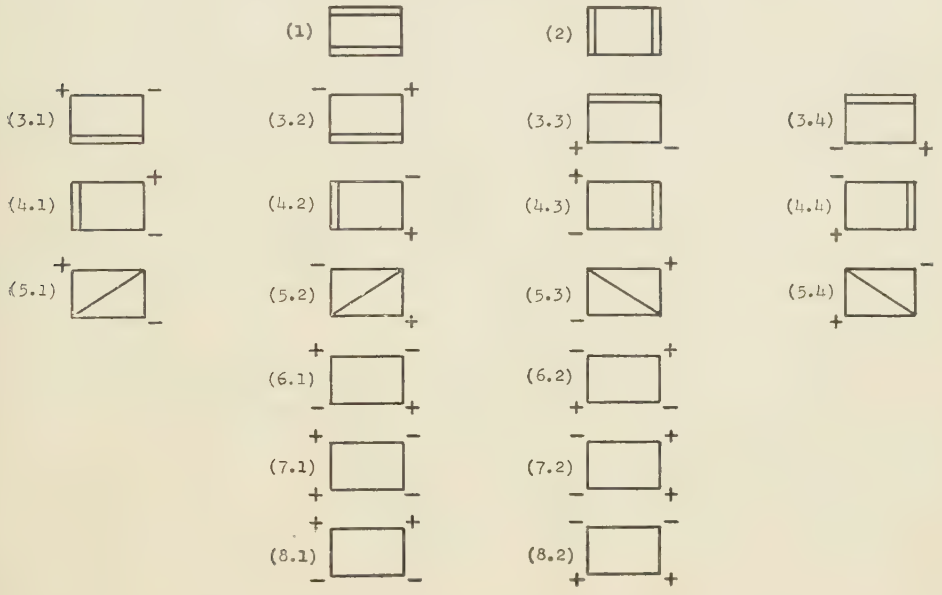

List of singlet structures in rectangular molecule.

The triplet states may be discussed in a similar way. There are altogether fifteen triplet atomic terms of zero spin, namely the following:—

$\Sigma P\,.\,(ab\bar{c}\bar{d}-\bar{a}\bar{b}cd)$, (9.1) $\Sigma P\,.\,(a\bar{b}c\bar{d}-\bar{a}b\bar{c}d)$, (9.2) $\Sigma P\,.\,(a\bar{b}\bar{c}d-\bar{a}bc\bar{d})$, (9.3)

$\Sigma P\,.\,b\bar{b}(c\bar{d}+\bar{c}d)$, (10.1) $\Sigma P\,.\,a\bar{a}(c\bar{d}+\bar{c}d)$, (10.2) $\Sigma P\,.\,c\bar{c}(a\bar{b}+\bar{a}b)$, (10.3) $\Sigma P\,.\,d\bar{d}(a\bar{b}+\bar{a}b)$, (10.4)

$\Sigma P\,.\,c\bar{c}(d\bar{a}+\bar{d}a)$, (11.1) $\Sigma P\,.\,b\bar{b}(d\bar{a}+\bar{d}a)$, (11.2) $\Sigma P\,.\,d\bar{d}(b\bar{c}+\bar{b}c)$, (11.3) $\Sigma P\,.\,a\bar{a}(b\bar{c}+\bar{b}c)$, (11.4)

$\Sigma P\,.\,a\bar{a}(b\bar{d}+\bar{b}d)$, (12.1) $\Sigma P\,.\,c\bar{c}(d\bar{b}+\bar{d}b)$, (12.2) $\Sigma P\,.\,b\bar{b}(c\bar{a}+\bar{c}a)$, (12.3) $\Sigma P\,.\,d\bar{d}(a\bar{c}+\bar{a}c)$. (12.4)

It is probably misleading to represent these by bond diagrams, as the symmetry is obscured. As before, we may group these triplet terms into irreducibly symmetrical combinations. For instance, (9.2) belongs to A_2, (9.1)+(9.3) to B_1, and (9.1)−(9.3) to B_2. The following gives the number of combinations in each representation:—

	A_1	A_2	B_1	B_2
(9.2)		1		
(9.1) and (9.3)			1	1
(10.1) to (10.4)	1	1	1	1
(11.1) to (11.4)	1	1	1	1
(12.1) to (12.4)	1	1	1	1
Total	3 +	4 +	4 +	4=15

There are therefore three triplet molecular states of irreducible symmetry A_1 and four in each of the symmetry classes A_2, B_1 and B_2. Since the doubly ionic terms contribute nothing to the triplet levels, we should not miss any triplet states by neglecting them; but we should miss all except three of the triplet states if we neglected singly ionic terms as well.

There is only one quintuplet spin-corrected atomic term of zero spin, namely

$$\Sigma P\,.\,(ab\bar{c}\bar{d}+a\bar{b}c\bar{d}+a\bar{b}\bar{c}d+\bar{a}bc\bar{d}+\bar{a}b\bar{c}d+\bar{a}\bar{b}cd).$$

This has symmetry A_1, and as there is no other quintuplet with which it can interact, it must be the molecular wave function for the quintuplet level of zero spin.

Now let us attack the problem by the method of molecular orbitals. There will be one m.o. in each symmetry class, namely

$$(a+b+c+d)=a_1, \text{ say, in class } A_1,$$
$$(a-b+c-d)=a_2, \text{ say, in class } A_2,$$
$$(a+b-c-d)=b_1, \text{ say, in class } B_1,$$
$$(a+b-c-d)=b_2, \text{ say, in class } B_2.$$

The possible molecular terms are of three types: doubly coupled, e.g. $\Sigma P\,.\,a_1\bar{a}_1b_1\bar{b}_1$, singly coupled, e.g. $\Sigma P\,.\,a_1\bar{a}_1a_2\bar{b}_1$, and uncoupled, e.g. $\Sigma P\,.\,a_1\bar{a}_2\bar{b}_1b_2$. Each of these has irreducible symmetry, as the group C_{2v} has no degenerate representations. Proceeding as usual, we group the molecular terms of zero total spin into spin-grouped terms. For example,

$\Sigma P\,.\,(a_1\bar{a}_2-\bar{a}_1a_2)(b_1\bar{b}_2-b_1\bar{b}_2)$ is a singlet molecular term,

$\Sigma P\,.\,a_1\bar{a}_1(b_1\bar{b}_2+\bar{b}_1b_2)$ is a triplet molecular term, and

$\Sigma P\,.\,(a_1a_2\bar{b}_1\bar{b}_2+a_1\bar{a}_2b_1\bar{b}_2+a_1\bar{a}_2\bar{b}_1b_2+\bar{a}_1a_2b_1\bar{b}_2+\bar{a}_1a_2\bar{b}_1b_2+\bar{a}_1\bar{a}_2b_1b_2)$ is the only quintuplet term.

We may draw up a table of possible distributions of electrons among the m.o., giving the class of the distribution and the number of levels of given multiplicity belonging to it. A doubly coupled distribution gives rise to one singlet term, a singly coupled distribution to one singlet and one triplet, and the uncoupled distribution $a_1a_2b_1b_2$ gives rise to 2 singlets, three triplets and one quintuplet term. We identify these spin-corrected terms with the actual molecular wave functions.

Distribution of electrons among m.o.				Symmetry class	Number of levels		
					Singlet	Triplet	Quintuplet
a_1	a_2	b_1	b_2				
2	2			A_1	1		
2	1	1		B_2	1	1	
2	1		1	B_1	1	1	
2		1	1	A_2	1	1	
2		2		A_1	1		
2			2	A_1	1		
1	2	1		B_1	1	1	
1	2		1	B_2	1	1	
1	1	2		A_2	1	1	
1	1	1	1	A_1	2	3	1
1		2	1	B_2	1	1	
1		1	2	B_1	1	1	
	2	2		A_1	1		
	2	1	1	A_2	1	1	
	2		2	A_1	1		
	1	2	1	B_1	1	1	
	1	1	2	B_2	1	1	
		2	2	A_1	1		
1	1		2	A_2	1	1	

It will be observed that the number of levels of given symmetry and multiplicity is exactly the same as is obtained by the complete valence-bond treatment. In particular it can be verified by expansion that, apart from a normalization factor, the quintuplet level obtained by the m.o. method is identical with that obtained by the valence-bond method, and contains no ionic terms although it can be expressed entirely in terms of molecular orbitals. Hence the method of m.o. does not always exaggerate the importance of ionic terms.

One further point should be noted. If the energies of the m.o., a_1, a_2, b_1, b_2 are nearly in arithmetic progression, the excited states (singlet or triplet) $a_1^2 a_2 b_2$ and $a_1 a_2^2 b_1$, being of the same symmetry and multiplicity, and about the same energy, will interact; and the states represented by the descriptions $a_1^2 b_2^2$, $a_1 a_2 b_1 b_2$ and $a_2^2 b_1^2$ will also interact, so that the molecular orbital method will give inaccurate energies for the resulting molecular states. However, in the ground state and first excited state this difficulty does not arise; and in the absorption of light by unsaturated molecules it is the ground state and usually the first excited state between which the visible transition occurs.

§6. CONCLUSION

We may summarize the situation as follows:—

(1) Although neither the valence-bond method nor molecular orbital method as usually applied gives an unequivocal answer to the question of the symmetry and multiplicity of states of progressively increasing energy (see Wheland 1938), the latter method will always give the correct *number* of molecular states of given symmetry and multiplicity, whereas the former method will only do so if all possible ionic terms are taken into account.

(2) As to the quantitative merits of the two theories, it seems fair to say that the valence-bond method neglecting some or all ionic states will probably give a more accurate value for the energy of the ground state when this is a singlet, but that it will be unreliable for estimating the energies of specified excited states, partly owing to the difficulty of deciding which actual molecular state is being discussed. On the other hand, the method of m.o. will lead to fairly reliable values of the energies of ground state and first one or two excited states (so long as there are no other states of the same symmetry and multiplicity and nearly the same energy as the state under consideration). If interaction between m.o. molecular wave functions of the same symmetry and multiplicity is considered, the resulting molecular wave functions and energies will be identical with those obtained by a valence-bond treatment with all ionic terms taken into account. In practice either of these last procedures is excessively laborious.

(3) The method of molecular orbitals therefore seems to be the more reliable for the interpretation of what Mulliken calls $N \rightarrow V$ type molecular spectra, where the most important lines are due to transitions between the ground state and lower excited states. For Rydberg type transitions in electronic spectra, the *AO* approximation breaks down, and so either method is inappropriate.

REFERENCES

ECKART, C., 1930, *Rev. Mod. Phys.*, **2**, 366–370.
HUND, F., 1932, *Z. Phys.*, **73**, 1.
VAN VLECK, J. H., and SHERMAN, A., *Rev., Mod. Phys.*, **7**, 183.
WHELAND, G. W., 1938, *Proc. Roy. Soc.* A, **164**, 397.

The Measurement of the Permeability of Low-conductivity Ferromagnetic Materials at Centimetre Wavelengths

By J. B. BIRKS
I.C.I. Research Fellow, University of Glasgow

MS. received 21 *April* 1947

ABSTRACT. A waveguide impedance method for the measurement of the permeability of low-conductivity ferromagnetic materials at centimetre wavelengths is described. The method avoids the difficulties and anomalies present in earlier measurements. The complex magnetic and dielectric properties of a specimen filling a section of waveguide are derived from standing-wave measurements of the short-circuit and open-circuit impedances of the section. The experimental apparatus and techniques which have been employed at wavelengths of 60–20 cm., 15–6 cm., 3 cm. and $1\frac{1}{4}$ cm. are described, and some typical results of measurements on γ-ferric oxide are given. It is shown that the observed magnetic dispersion is an inherent property of the material, and is not attributable to skin-effect.

§ 1. INTRODUCTION

Almost all the previous experimental work on high-frequency permeability, reviewed by Allanson (1945), has been concerned with ferromagnetic metals. These materials, because of their high conductivity, may be studied as conducting elements in a high-frequency transmission line, or in a cavity resonator (Griffiths 1946). The experimental values of permeability thus obtained fall into two distinct groups, dependent on the method of measurement employed. The permeability μ_R (or μ_k), derived from measurements of the resistive losses of the high-frequency circuit, differs from the value μ_L (or μ_n), obtained from measurements of the circuit reactance. This anomaly has been shown by Kittel (1946) to arise from the implicit assumption that μ is a real (rather than a complex) quantity at high frequencies. By confining the measurements to either the real or imaginary component of the circuit impedance, different values of the *apparent* real permeability, μ_R and μ_L, are obtained, neither of which is equal to, or simply related to, the true permeability μ. The measurement of both impedance components of the same circuit element, and the consequent determination of μ, is made difficult by the presence of a high conductivity, equivalent to an imaginary permittivity of large magnitude intimately associated with the permeability. These difficulties may be readily overcome, however, when the material has a low conductivity.

A waveguide impedance method for the measurement of the high-frequency permeability and permittivity of ferromagnetic materials of low conductivity has been developed, and used at wavelengths from 60 cm. to 1·25 cm. The method was primarily developed for the investigation of ferromagnetic compounds, such as magnetite, γ-ferric oxide and the ferrites. It may also be used, however, for the study of ferromagnetic metals, in the form of finely divided powders dispersed in a non-conducting medium. The ferromagnetic compounds are of

particular interest because, due to their low conductivity, the high-frequency magnetic field can penetrate much more deeply than in a metal. It may be possible, therefore, to detect magnetic dispersion and absorption effects due to internal phenomena, which are completely obscured in a metal by the skin-effect. For example, Becker (1938) has given a theory of magnetic dispersion, due to internal eddy-current fields produced by the oscillatory displacements of the domain walls, while Landau and Lifshitz (1935) have predicted resonance phenomena, occurring at the Larmor frequency of the electron spins in the crystalline anisotropy field. Both of these theoretical effects have yet to be verified experimentally.

The permeability μ and permittivity ϵ of a medium, relative to their free-space values, are determined at high frequencies from the electromagnetic wave properties of the medium. These properties may be defined in terms of two parameters, the intrinsic impedance z, relative to free space, and the propagation coefficient γ. The relative intrinsic impedance

$$z=(\mu/\epsilon)^{\frac{1}{2}}, \qquad \ldots\ldots(1)$$

in conjunction with Fresnel's equations, determines the reflection and transmission coefficients of the wave at a boundary of the medium. The propagation coefficient

$$\gamma=i\frac{2\pi}{\lambda}(\mu\epsilon)^{\frac{1}{2}}, \qquad \ldots\ldots(2)$$

where λ is the free-space wavelength, determines the phase velocity (imaginary component of γ) and the attenuation coefficient (real component of γ) of the wave propagated through the medium.

For non-magnetic media $\mu=1$, and for perfect dielectrics, ϵ is real. For lossy dielectrics ϵ is complex, and may be written

where
$$\left.\begin{aligned}\epsilon&=\epsilon'-i\epsilon''=|\epsilon|e^{-i\delta_\epsilon}\\ \tan\delta_\epsilon&=\epsilon''/\epsilon'\end{aligned}\right\}\ldots\ldots(3)$$

is known as the dielectric loss tangent. For ferromagnetic materials at high frequencies it had been found experimentally by the author (1946) that, in accordance with the theory of Arkadiew (1913), μ is also complex, and hence may be written

where
$$\left.\begin{aligned}\mu&=\mu'-i\mu''=|\mu|e^{-i\delta_\mu}\\ \tan\delta_\mu&=\mu''/\mu'\end{aligned}\right\}\ldots\ldots(4)$$

may be called the magnetic loss tangent.

It will be seen from equations (1) and (2) that, while a measurement of either of the complex quantities z or γ is adequate to derive ϵ for non-magnetic materials, a measurement of both z and γ is necessary and sufficient for the determination of ϵ and μ for ferromagnetic materials.

§ 2. THEORY OF THE METHOD

Measurements are made on a sample of the ferromagnetic material, filling a section of length d of an empty waveguide. Coaxial waveguides are used at wavelengths of 60–20 cm. and 15–6 cm., and H_{10} rectangular waveguides at 3 cm. and 1·25 cm. The input impedances of the filled section, relative to the characteristic impedance of the empty guide, are measured when the section is terminated in

a short-circuit, and when it is terminated in a closed quarter-wavelength line, which is equivalent to an open-circuit. The relative short-circuit and open-circuit input impedances are given by

$$\left.\begin{aligned} z_{sc} &= z_0 \tanh \gamma_0 d, \\ z_{oc} &= z_0 \coth \gamma_0 d, \end{aligned}\right\} \quad \ldots\ldots (5)$$

where γ_0 is the propagation coefficient and z_0 is the characteristic impedance of the section relative to that of the empty guide. Hence

$$\left.\begin{aligned} z_0 &= (z_{sc} z_{oc})^{\frac{1}{2}}, \\ \tanh \gamma_0 d &= (z_{sc}/z_{oc})^{\frac{1}{2}}. \end{aligned}\right\} \quad \ldots\ldots (6)$$

For a coaxial waveguide, operating in its principal mode,

$$\left.\begin{aligned} z_0 &= z = (\mu/\epsilon)^{\frac{1}{2}}, \\ \gamma_0 &= \gamma = i(2\pi/\lambda)(\mu\epsilon)^{\frac{1}{2}}. \end{aligned}\right\} \quad \ldots\ldots (7)$$

For an H_{10} rectangular waveguide, z_0 and γ_0 are dependent on the cut-off wavelength of the empty guide, λ_c ($=2a$, where a is the guide width), and they are given by

$$\left.\begin{aligned} z_0 &= \mu \left[\frac{1-(\lambda/\lambda_c)^2}{\mu\epsilon-(\lambda/\lambda_c)^2}\right]^{\frac{1}{2}}, \\ \gamma_0 &= i(2\pi/\lambda)[\mu\epsilon-(\lambda/\lambda_c)^2]^{\frac{1}{2}}. \end{aligned}\right\} \quad \ldots\ldots (8)$$

Equation (8) reduces to (7) for λ_c infinite, as in the coaxial case.

Determination of input impedances, z_{sc} and z_{oc}. The relative input impedance is obtained from the measurement of the voltage standing-wave pattern in the empty waveguide, which has negligible attenuation. It is given by

$$z_{input} = \frac{1/n - i\tan\beta l}{1 - i(\tan\beta l)/n}, \quad \ldots\ldots (9)$$

where n is the voltage standing-wave ratio (ratio of voltage maximum to minimum), l is the distance of the voltage minimum from the input face of the sample, β ($=2\pi/\lambda_g$) is the phase velocity and λ_g is the measured wavelength, in the empty guide ($=\lambda$, for the coaxial case).

Determination of n. For experimental reasons to be discussed later, n is not measured directly, but is obtained from the width of the voltage curve near the minimum. The voltage distribution on a lossless line may be written

$$V^2 = V_{min}^2(\cos^2\beta x + n^2 \sin^2 \beta x), \quad \ldots\ldots (10)$$

where V_{min} is the minimum voltage, and V the voltage at a distance x from the minimum. Rewriting (10) as

$$n^2 = 1 + (V^2/V_{min}^2 - 1)\,\mathrm{cosec}^2\,\beta x, \quad \ldots\ldots (11)$$

it is seen that n may be determined from a measurement of x, for a given value of V^2/V_{min}^2. In practice V^2/V_{min}^2 is normally taken as 2, so that (11) simplifies to

$$n^2 = 1 + \mathrm{cosec}^2\,\beta x_0, \quad \ldots\ldots (12)$$

where $2x_0$ is the measured distance between points on each side of the minimum, at which the voltage is $\sqrt{2}$ of its value at the minimum.

Determination of l and λ_g. The distance l from the voltage minimum to the input face of the sample is also measured indirectly. The dial gauge or scale used for recording the position of the high-frequency voltage detector has an arbitrary zero, which must be calibrated. This is done by the measurement of the position b of a voltage minimum, with the guide empty and terminated in a short-circuit (figure 1 (*a*)). This minimum is known theoretically to be $m\lambda_g/2$ from the end of the guide (where m is a positive integer). If, then, c is the position of the voltage minimum when the sample, length d, is introduced into the guide (figure 1 (*b*)),

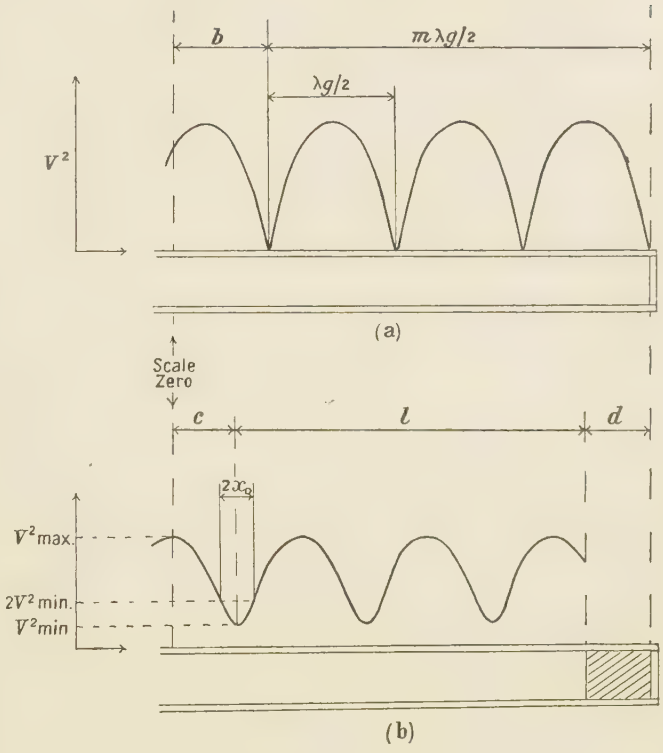

Figure 1. Determination of input impedance.

$$\left.\begin{aligned} b+m\lambda_g/2 &= c+l+d, \\ \text{i.e.} \qquad \tan\beta l &= \tan\beta(b-c-d). \end{aligned}\right\} \quad \ldots\ldots(13)$$

The value of $\lambda_g/2$, and hence β, is obtained from the difference between two consecutive values of b.

Computation. The sequence of measurements and computation may be best illustrated by a typical set of results.

Table 1

	d	b	λ_g	c	$b-c-d$	$\tan\beta l$	x_0
Source	Expt.	Expt.	b	Expt.		Eqn. (13)	Expt.
	1·940	8·059	23·422	s.c. 4·279	1·840	0·5362	2·123
		−3·652		o.c. 6·252	−0·133	−0·0356	0·597

	$\sin\beta x_0$	$1/n$	z_{sc}	z_{oc}	z_0	$\tanh\gamma_0 d$
Source		Eqn. (12)	Eqn. (9)	Eqn. (9)	Eqn. (6)	Eqn. (6)
s.c.	0·5388	0·4745	0·6933	0·1610	0·3341	2·075
o.c.	0·1590	0·1570	exp (−*i*34·25°)	exp (*i*12·45°)	exp (−*i*10·9°)	exp (−*i*23·35°)

	$\gamma_0 d$	γ_0	$\lvert\mu\rvert$	δ_μ	$\lvert\epsilon\rvert$	δ_ϵ
Source	Chart		Eqn. (7), (4)	Eqn. (7), (4)	Eqn. (7), (3)	Eqn. (7), (3)
	1·86 exp (*i*75·95°)	0·959 exp (*i*75·95°)	1·20	24·95°	10·7	3·15°

s.c. = short circuit; o.c. = open circuit. All lengths are in tenths of an inch.

$\gamma_0 d$ is obtained from the complex hyperbolic tangent, using the *Chart Atlas* compiled by Kennelly (1914). Any ambiguity in the value of $\gamma_0 d$ is removed by the measurement of a second sample of different thickness.

§ 3. DESCRIPTION OF APPARATUS

Waveguide and detector system. The voltage standing-wave is measured by means of a tuned crystal detector, mounted in a sliding carriage, which is moved manually along the length of the waveguide. A short, thin probe from the detector projects into the waveguide through a narrow longitudinal slot, milled parallel to the axis of the guide, and, in the case of the rectangular waveguide, along the centre of its broad side. The high-frequency voltage induced in the probe is rectified by the crystal, and the crystal current is measured by a sensitive galvanometer. Particular care has been taken in the mechanical construction to ensure that the probe moves centrally along the guide, and that its depth of penetration remains constant as the position of the carriage is varied. The tuning of the detector by means of a variable reactance increases its sensitivity and discriminates against the detection of harmonics.

The general arrangement of the complete apparatus used on each of the four wavelength ranges is similar, and it differs only in detail from the schematic diagram of figure 2.

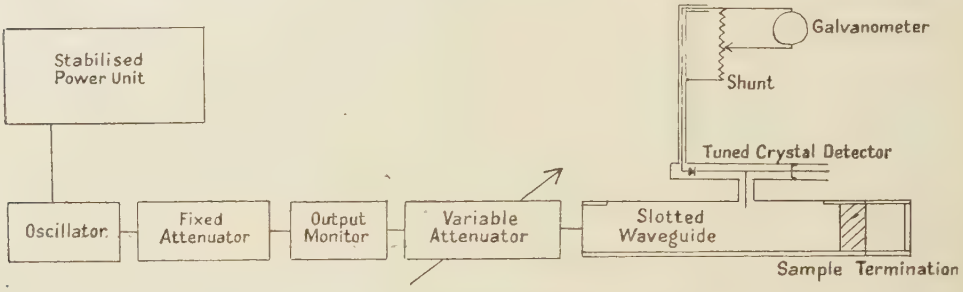

Figure 2. General schematic diagram of apparatus.

60–20 cm. apparatus. A variable-frequency triode oscillator (446 tube with concentric-line tuning) is loosely coupled through a lossy cable to the coaxial waveguide. The oscillator output is monitored at the source by a bolometer bridge circuit. The coaxial waveguide has an outer conductor diameter of 4·45 cm., an inner conductor diameter of 1·35 cm., and a slot length of 110 cm. The inner conductor, which is constructed of light thin-walled tube, is supported at 40 cm. intervals by sets of three thin polystyrene rods, screwed through the outer conductor, at 120° to each other. These spacing rods have been found to have a negligible effect on the wave in the guide. The position of the detector carriage is read on a 0·1 mm. vernier scale. The crystal sensitivity is varied by slightly detuning the detector instead of using a variable attenuator.

15–6 cm. apparatus. At wavelengths near 9 cm. a standard reflex klystron oscillator is used. For other wavelengths in this range a modified oscillator of this type is used (figure 3). The central cylindrical cavity of the oscillator is extended on each side by rectangular waveguide sections, whose length may be varied by short-circuiting pistons, geared to move in synchronism. It is found that

by variation of the transit-time of the electron beam, by adjustment of the electrode voltages, high-order modes of resonance of various wavelengths from 15 cm. to 6 cm. can be induced in this composite cavity. Care must be exercised in the choice of suitable modes, to ensure that the oscillations are stable and monochromatic.

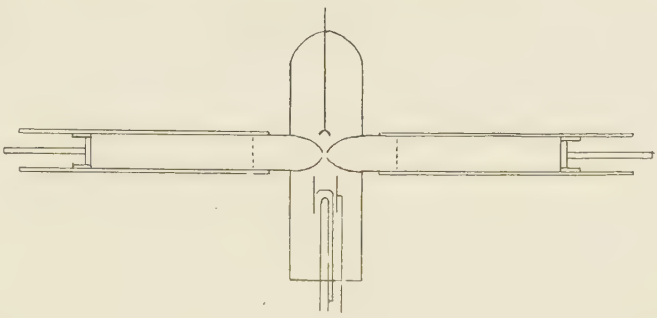

Figure 3. Broad-band reflex klystron.

The klystron oscillator is loosely coupled to a long length of cable feeding the coaxial waveguide, which has an outer conductor diameter of 2·225 cm., inner conductor diameter of 0·775 cm., and a slot length of 16 cm. The inner conductor is supported at the input end by a polythene insulator, and at the load end by the sample and termination. The position of the detector carriage is measured by two 1″ micrometer dial gauges mounted on opposite sides of the carriage and recording consecutive 1″ traverses. For the longer wavelengths, a single dial gauge and calibrated 1″ and 2″ sliding steel blocks are used. The oscillator power is monitored by a crystal at the waveguide input, and the sensitivity is varied by slight detuning of the crystal detector.

3 cm. apparatus. A reflex klystron oscillator feeds a $1'' \times \frac{1}{2}''$ H_{10} rectangular waveguide system through a short coaxial cable. The sequence of units in the waveguide system is as shown in figure 2. The fixed attenuator, which consists of a flat prism of lossy dielectric material, attached to the broad inner face of the waveguide, has an attenuation of about 6 decibels. The oscillator output is monitored by a fixed crystal detector, or alternatively a resonant cavity wavemeter may be substituted, when required. The variable attenuator consists of a thin circular segment of resistive material, which may be lowered through a longitudinal central slot in the broad face of the guide. The slotted waveguide section is machined from brass plate to obtain the required constructional accuracy. The position of the crystal detector is measured by a micrometer dial gauge attached to the detector carriage, and bearing against a fixed block on the side of the waveguide.

1¼ cm. apparatus. This is similar to the 3 cm. apparatus, except in minor details, with the oscillator feeding directly into a $0{\cdot}42'' \times 0{\cdot}17''$ H_{10} rectangular waveguide system.

§ 4. EXPERIMENTAL TECHNIQUE

Crystal characteristics. A knowledge of the rectifying characteristics of the crystal detector is essential, particularly in view of the opinion expressed by Collie *et al.* (1946) that "no reliance should be placed on the crystal rectifier obeying an exact law; at best, crystals are unstable, and hard to calibrate". An investigation has therefore been made of the properties of a number of crystals of standard Service type. The bulk of the measurements were made at a wavelength of 9 cm., with the slotted waveguide empty and terminated in a short-circuit.

The crystals were inserted in turn into the detector, and readings of the crystal current I against detector position were taken over a complete quarter-wavelength from minimum to maximum. The voltage distribution on a lossless short-circuited line is from (10), putting $V_{\min}=0$, $n=\infty$, $nV_{\min}=V_{\max}$,

$$V^2=V_{\max}\sin^2\beta x. \qquad \ldots\ldots(14)$$

The crystal current I was, therefore, plotted against $\sin^2\beta x$. Typical results for a single crystal are shown in figure 4.

The results of the measurements may be summarized as follows. All the crystals investigated have a square-law characteristic (I proportional to V^2) for crystal currents up to a few micro-amperes. At higher currents they deviate in different degrees, often considerably, from the square-law. Mechanical shock and ageing may affect the characteristic, but they do not appear to alter the square law property for low currents. The characteristic is markedly dependent on the galvanometer circuit resistance. The optimum resistance for I to be nearly proportional to V^2 for crystal currents up to 20 μa. varies from crystal to crystal, but, is on the average, about 400 ohms.

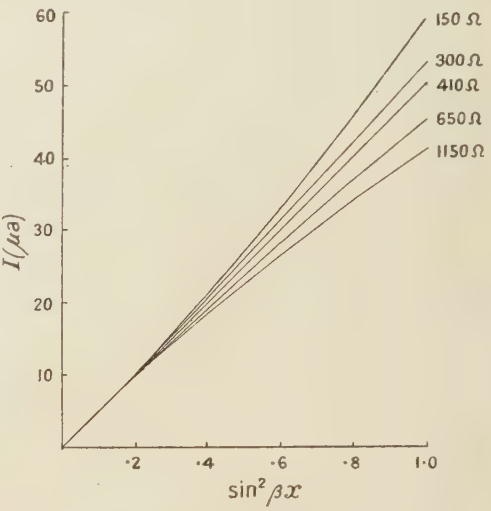

Figure 4. Dependence of crystal law on external resistance.

Impedance measurement. It was, therefore, decided to make all impedance measurements at low crystal currents, using a spot galvanometer with a sensitivity of 1 μa. for full-scale deflection, and an internal resistance of 400 ohms. For voltage standing-wave ratios greater than 3, it is not possible to measure the ratio of maximum to minimum current directly with sufficient accuracy, and the indirect method of measuring the width of the voltage curve near the minimum is therefore used (equation (12)).

At the shorter wavelengths with large values of n, the value of $2x_0$ (the width at $2I_{\min}$) is also too small to be measured accurately. It is then necessary to take values of $V^2/V^2_{\min}$ greater than 2, using (11) to evaluate n. A simple procedure has been employed which avoids the measurement of very low currents. $I_{\min}$ is measured, the current sensitivity of the galvanometer is then reduced by Y ($=V^2/V_{\min}$), and the distance $2x$ is measured between points at which the galvanometer current is equal to $I_{\min}$. A shunt of the type shown in figure 5 is used to avoid changing the resistance of the galvanometer circuit and affecting the crystal characteristic.

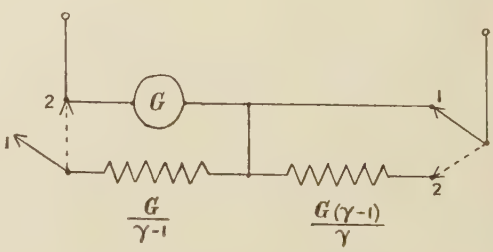

Figure 5. Constant resistance shunt.

Experimental accuracy. A check on the accuracy of each of the waveguide systems has been made, measuring I vs $\sin^2 \beta x$ in an empty short-circuited guide as described above, with a maximum crystal current of 1 μa. The constancy of the ratio $I/\sin^2 \beta x$ depends not only on the validity of the crystal square law, but also on the overall accuracy of construction and measurement.

Deviations in this ratio might arise from:

(*a*) variations in the depth of penetration of the detector probe,

(*b*) irregularities in the movement of the carriage,

(*c*) rectification of any harmonics present,

(*d*) interaction of the detector probe on the waveform, or

(*e*) errors in the measurement of current or position.

The results indicate that none of these effects are pronounced, since over the range of currents used in impedance measurements (0·05 to 1 μa.) the variations of $I/\sin^2 \beta x$ are random, for each of the four waveguide systems, and have the maximum values given in table 2.

Table 2

Wavelength ..	60 cm.	25 cm.	9 cm.	6 cm.	3 cm.	$1\frac{1}{4}$cm.
Variation ..	$\pm\frac{1}{2}\%$	$\pm\frac{3}{4}\%$	$\pm\frac{3}{4}\%$	$\pm 1\%$	$\pm 1\frac{1}{2}\%$	$\pm 3\%$

No general estimate of error in the determination of ϵ and μ can be given, since it depends on their magnitude and also on the electrical thickness of the sample. Ideally, d should be chosen to give reasonably large values of l and $2x_0$ in both the short-circuit and open-circuit cases. This choice is complicated by the various measured quantities varying in different directions with d, but a suitable compromise can be arrived at by a few preliminary measurements on samples of different thicknesses.

§ 5. PREPARATION AND PROPERTIES OF MIXTURES

Preparation of samples. In studying finely-divided ferromagnetic compounds it is convenient to mix the compound with a lossless, non-magnetic base material to form solid samples for measurement. Paraffin wax has been found very suitable for this purpose. Homogeneous mixtures can be formed by vigorously stirring the compound into molten paraffin wax as it is cooling. The solid mixture is moulded into the required sample shape at room temperature, using a hand-vice for applying pressure. The sample is made slightly oversize, as the material is sufficiently soft to be force-fitted into the waveguide, thereby eliminating experimental errors due to gaps between the sample and the waveguide conductors.

Measurements on paraffin wax. The permittivity of a non-magnetic dielectric can be derived from a measurement of either z_0 or γ_0, or alternatively from a single measurement of z_{sc}. For a low-loss dielectric, terminated in a short-circuit, equations (9), (5) and (8) simplify and combine to give

$$\left.\begin{aligned} \frac{\tan\phi}{\phi} &= -\frac{\lambda_g \tan 2\pi l/\lambda_g}{2\pi d}, \\ \text{where} \qquad \phi &= \frac{2\pi d[\epsilon - (\lambda/\lambda_c)^2]^{\frac{1}{2}}}{\lambda}, \end{aligned}\right\} \quad \ldots\ldots(15)$$

for the H_{10} rectangular waveguide, and also, putting $\lambda_g = \lambda$, $\lambda_c = \infty$, for the coaxial

waveguide. Equation (15) may be solved using the tables of Jahnke and Emde (1933). Measurements have been made on paraffin wax: ϵ and μ have been calculated from z_{sc} and z_{oc} using the general method; and ϵ has also been calculated from z_{sc}, assuming $\mu = 1$, using (15). Comparative results are given in table 3.

Table 3

	λ in cm.	8·93	3·09	1·236
From z_{sc} and z_{oc}	ϵ	2·27	2·30	2·28
	μ	0·99	0·98	1·00
From (15)	ϵ	2·28	2·29	2·28

Properties of mixtures. Measurements are still in progress on various mixtures of paraffin wax with γ-ferric oxide, magnetic and other ferromagnetic materials, though preliminary reports of some of the results have been published (Birks 1946, 1947). Since it is hoped to give a detailed account of these measurements at a later date, the present discussion will be limited to some typical results obtained with γ-ferric oxide mixtures. These illustrate the applications of the experimental method, and certain other points of general interest.

The relationship between the properties μ, ϵ of the mixtures, and v, the proportion by volume of γ-Fe_2O_3, has been investigated. It is found that, within the limits of experimental error, $|\mu|$ and $|\epsilon|$ vary according to the logarithmic law originally proposed by Lichtenecker (1918) for dielectric mixtures:

$$\log|\mu| = v \log|\mu|, \qquad \ldots\ldots(16)$$

$$\log|\epsilon| = v \log|\epsilon_a| + (1-v)\log|\epsilon_0|, \qquad \ldots\ldots(17)$$

where suffix 'a' refers to the (extrapolated) properties of the ferromagnetic powder, and suffix '0' to the properties of the wax ($\mu_0 = 1$). The experimental values of $|\mu|$, obtained for various γ-Fe_2O_3-wax mixtures, at wavelengths from 58·5 cm. to 3·09 cm., are plotted against v in figure 6. The present measurements have been limited to values of v up to 0·41, but Legg and Given (1940), using compressed powdered molybdenum Permalloy, found (16) to be valid for v up to 1·0, and Büchner (1939) and Wul (1946) using rutile mixtures, found (17) to be also tenable up to 100% concentration.

The magnetic and dielectric loss tangents of the mixtures vary linearly with v within the range of the measurements, and may be represented by relations of the form

$$\tan\delta_\mu = v \tan\delta_{\mu_a}, \qquad \ldots\ldots(18)$$

$$\tan\delta_\epsilon = v \tan\delta_{\epsilon_a}. \qquad \ldots\ldots(19)$$

The experimental values of $\tan\delta_\mu$ vs v for different wavelengths are plotted in figure 6. Figure 7 shows the variation with wavelength of the real and imaginary components of μ_a for γ-ferric oxide, derived from these measurements.

Skin-effect. Leigh Page (1941) has shown that, at sufficiently high frequencies, magnetic dispersion and absorption will be exhibited by a medium loaded with

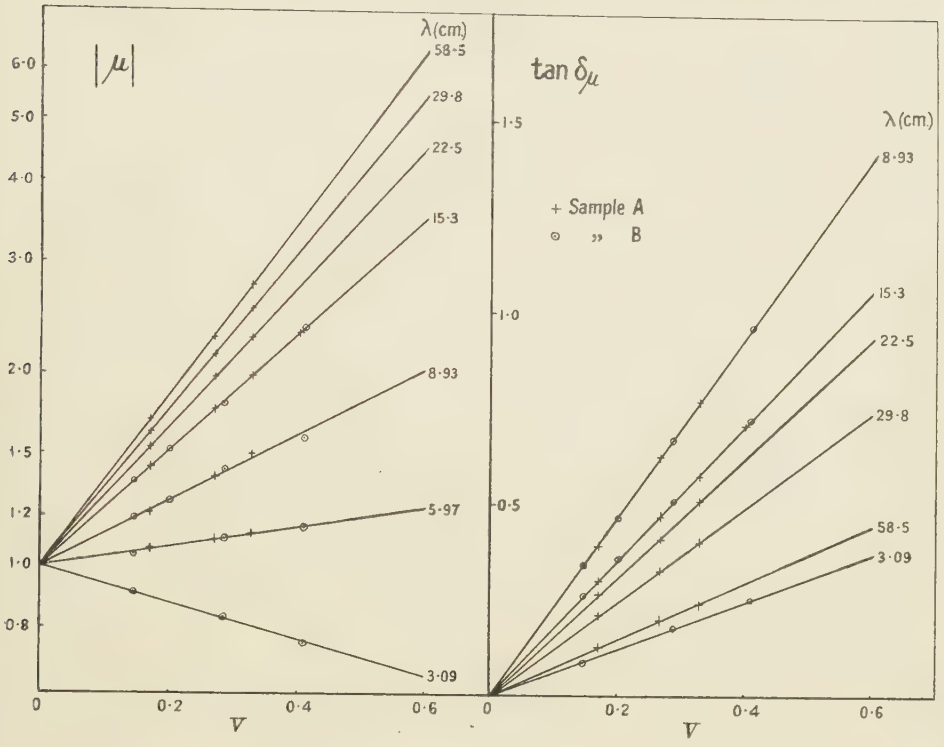

Figure 6. Magnetic properties of γ-Fe_2O_3-wax mixtures.

conducting ferromagnetic particles, due to skin-effect, even though the ferromagnetic material retains its static permeability. It is, therefore, relevant to enquire whether the results observed with dispersions of ferromagnetic semiconductors at centimetre wavelengths are due wholly or partially to skin-effect.

It may be shown from an analysis, similar to that used by Leigh Page, that the ratios of the magnetic and electric moments, p_H and p_E, of a spherical particle, radius r, in a high-frequency electromagnetic field, to the magnetic and electric moments, p_{H_0} and p_{E_0}, in static fields, are given by

$$\frac{p_H}{p_{H_0}} = \frac{\mu+2}{\mu-1+\kappa(\alpha)}, \quad \ldots\ldots(20)$$

$$\frac{p_E}{p_{E_0}} = \frac{\epsilon+2}{\epsilon-1+\kappa(\alpha)}, \quad \ldots\ldots(21)$$

where

$$\alpha = \frac{2\pi r}{\lambda}(\epsilon\mu)^{\frac{1}{2}}, \quad \ldots\ldots(22)$$

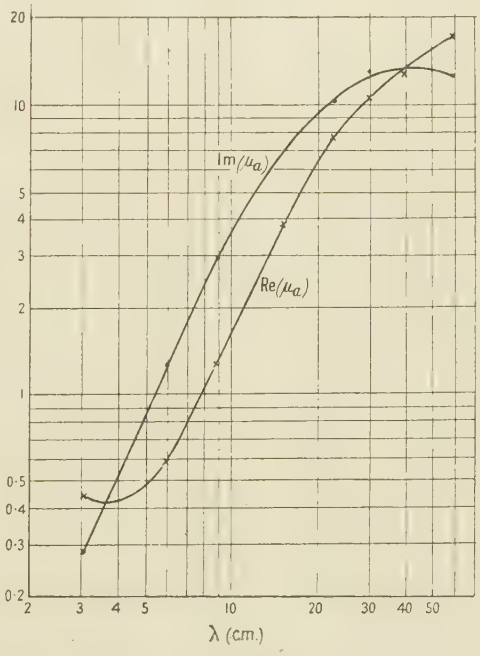

Figure 7. Magnetic spectrum of γ-Fe_2O_3

and $$\kappa(\alpha)=\frac{\alpha^2\sin\alpha}{\sin\alpha-\alpha\cos\alpha}, \qquad \ldots\ldots(23)$$

which, for small α, approximates to

$$\kappa(\alpha)=3-\alpha^2/5. \qquad \ldots\ldots(23\,a)$$

For the purpose of the skin-effect analysis only, the properties μ, ϵ, of the ferromagnetic are assumed to retain their static values, thus giving a maximum estimate of any possible skin-effect dispersion, since both μ and ϵ are found experimentally to decrease with increasing frequency. Taking upper limit values for γ-Fe_2O_3 of $\epsilon=\mu=30$, $r=0{\cdot}01$ cm., we obtain from the above equations, at $\lambda=10$ cm.

$$p_H/p_{H_0}=p_E/p_{E_0}=1{\cdot}0002,$$

thus demonstrating that the skin-effect in such a particle is negligible.

An experimental verification of this has been obtained from measurements at three wavelengths on two samples of γ-Fe_2O_3, differing considerably in particle size. If the complex permeabilities observed were due to any significant extent to skin-effect, then they would be critically dependent on the particle radius, r. The measurements on the two samples gave values of μ_a and ϵ_a which are identical within the limits of experimental error, although their radii differed by a factor of about 10. The magnetic properties of the two specimens, referred to as A and B, are distinguished in figure 6.

It may therefore be concluded that the complex permeability observed for γ-ferric oxide and for similar ferromagnetic semiconductors is a property of the material itself, and its further study should therefore provide data on the internal structure of ferromagnetics. It is hoped to discuss the experimental results, in the light of the various theories of ferromagnetic dispersion that have been proposed, in a subsequent paper.

ACKNOWLEDGMENTS

The author wishes to thank Professor P. I. Dee, F.R.S., for the use of the facilities of his laboratory, Professor E. C. Stoner, F.R.S., for his helpful criticism of the preliminary draft of this paper, and the Chief Superintendent, T.R.E., Malvern, for the loan of centimetre-wave valves and other apparatus.

REFERENCES

Allanson, J. T., 1945, *J. Instn. Elect. Engrs.*, **92**, III, 247.
Arkadiew, W., 1913, *Phys. Z.*, **14**, 928.
Becker, R., 1938, *Phys. Z.*, **39**, 856.
Birks, J. B., 1946, *Nature, Lond.*, **158**, 671.
Birks, J. B., 1947, *Nature, Lond.*, **159**, 775.
Büchner, A., 1939, *Wiss. Veröff. a.d. Siemens-Werken*, **18**, 84.
Collie, C. H., Ritson, D. M., and Hasted, J. B., 1946, *Trans. Faraday Soc.*, Discussion on Dielectrics.
Griffiths, J. H. E., 1946, *Nature, Lond.*, **158**, 670.
Jahnke, E., and Emde, F., 1933, *Funktionentafeln.* (Leipzig : B. G. Teuchner.)
Kennelly, A. E., 1914, *Chart Atlas of Complex Hyperbolic and Circular Functions.* (Cambridge, Mass. : Harvard University Press.)
Kittel, C., 1946, *Phys. Rev.*, **70**, 281.
Landau, L., and Lifshitz, E., 1935, *Phys. Z. Sowjet*, **8**, 153.
Legg, V. E., and Given, F. J., 1940, *Bell Syst. Tech. J.*, **19**, 385.
Lichtenecker, K., 1918, *Phys. Z.*, **19**, 374.
Page, Leigh, 1941, *Phys. Rev.*, **60**, 675.
Wul, B., 1946, *J. Phys. U.S.S.R.*, **10**, 95.

On Perfect Optical Instruments

By T. SMITH
National Physical Laboratory, Teddington

MS. received 15 *May* 1947

ABSTRACT. The angular characteristic function T is used to investigate optical systems of finite focal length in which one extended surface is imaged on another without aberration. The forms of T found earlier to correspond to perfect imagery are shown to be exhaustive.

When perfect imagery is achieved the image surface is similar to the object surface, with the exception that it may be stretched uniformly by arbitrary amounts in each of three mutually perpendicular directions. The length of the optical path between conjugate points of these surfaces is proportional to the distance of either from a fixed plane. In general only one object surface can be imaged without aberration.

In an exceptional group two pairs of conjugate surfaces—parts of centred second-order surfaces—can be perfectly imaged. The two surfaces of the same space have coincident principal axes, and in each of these directions the product of the two magnifications is equal to the square of the ratio of the refractive indices of the external media. In general the centre of the object is not perfectly imaged. The length of the path from any point of either object surface to its image is invariable. The only elementary example of this group is a single spherical refracting surface.

Another exceptional case is when the conjugate surfaces are plane. It is shown that in addition to being free from all aberrations for a single magnification, a system such as a photographic lens can produce images free from curvature, astigmatism and distortion for all magnifications.

The properties found for both these groups contradict some general conclusions reached by Clerk Maxwell.

Though the existence of perfect instruments is not inconsistent with optical laws, material systems of reflecting or refracting surfaces, whatever their shapes, do not enable this ultimate standard to be fully realized. This shortcoming bears significantly on the methods used in designing optical instruments.

§1. INTRODUCTION: MEANING OF "PERFECT"

The designer of optical instruments seeks to evolve systems which are free from aberrations. In geometrical terms this means that all rays originating at the same object point meet again in a point of the image space. It has been customary to regard as perfect only an instrument in which this condition is satisfied for all points of the object space. Examples of such instruments are a plane mirror and Maxwell's fish's eye (Maxwell 1854). In the latter the refractive index varies from point to point of the object and image spaces, and we shall not consider systems of this kind here. When the external media are homogeneous and isotropic, perfection in the sense just mentioned is only attainable when every image is geometrically similar to the object, and the linear magnification is the inverse ratio of the refractive indices of the two external spaces. The system is therefore afocal (Maxwell 1858, Whittaker 1907). This conclusion follows from the equality of anharmonic ratios for the two spaces, and the equality of all optical paths between given conjugate points. Perfection

in this comprehensive sense is obviously of little interest—it means in practice that the only perfect instruments we can achieve are constructed solely with plane mirrors. Instead we require a definition which can be applied to instruments of finite focal length. The primary aim of the designer of these systems is to image one particular surface on another with the least residual aberrations. This suggests that a perfect optical instrument may be defined as one which deflects all rays emanating from any point of a definite object surface so that they meet again in a single point of an image surface. This is the only kind of perfection of optical significance when the wavelength of the light is considered infinitely small.

The properties of perfect instruments are naturally of special interest, and to investigate them comprehensively it is convenient to use Characteristic Function theory. In this inquiry the function T, the so-called angular characteristic function, will be employed. The variables are the modified direction cosines ξ, η, ζ and ξ', η', ζ' of a ray in the external spaces, and T represents the length of the optical path between the feet of perpendiculars to the ray from the origins of coordinates in these spaces. The adoption of this function implies that afocal systems are not included in the investigation, but this limitation is not important. The choice is advantageous in that the location of the origins is not restricted; for instance, a pair of conjugate points may be chosen. We have first to consider what forms of T are consistent with perfect imagery.

§ 2. DEGREES OF FREEDOM

In the first place we make no assumptions about symmetry. Clearly any function of the modified direction cosines can be expressed as a function of variables u_1, u_2, u_3, ... where

$$u_p = a_p + b_{p1}\xi + b_{p2}\eta + b_{p3}\zeta - c_{p1}\xi' - c_{p2}\eta' - c_{p3}\zeta',$$

the a's, b's, c's being constants. There cannot be more than six linearly independent variables of this kind, and we first show that if T represents a perfect instrument there cannot be more than three when the origins are suitably chosen. Changes of origin are represented by the addition to T of any u, and as such a term is without effect on the theory which follows it will not be considered.

For brevity denote the differential coefficient of T with respect to u_p by T_p, and the matrices

$$\begin{pmatrix} b_{11} & b_{12} & b_{13} \\ b_{21} & b_{22} & b_{23} \\ \dots & \dots & \dots \\ \dots & \dots & \dots \end{pmatrix} \quad \text{and} \quad \begin{pmatrix} c_{11} & c_{12} & c_{13} \\ c_{21} & c_{22} & c_{23} \\ \dots & \dots & \dots \\ \dots & \dots & \dots \end{pmatrix}$$

by b and c respectively. By a fundamental property of the function T the points whose coordinates are given by the equations

$$\left.\begin{aligned} (x\ y\ z) &= (T_1\ T_2\ \dots)b \\ (x'\ y'\ z') &= (T_1\ T_2\ \dots)c \end{aligned}\right\} \qquad \dots\dots(1)$$

lie on the incident and emergent rays respectively. It is readily seen that if a unique connection exists between a pair of points on this ray it will relate to these particular points. There will be such a connection if T_1, T_2 ... can be

expressed in terms of x, y, z or of x', y', z' by solving one of equations (1), for this solution can then be substituted in the other. This requires b and c to be non-singular matrices of the third order, and the number of functions u is therefore limited to three. In general each u includes at least one variable appertaining to each space. From the relations

$$(x' \ y' \ z') = (x \ y \ z)b^{-1}c$$

or

$$(x \ y \ z) = (x' \ y' \ z')c^{-1}b$$

it appears that the conjugate surfaces are similar to one another, though the magnification may vary with direction. In any one direction the magnification is constant, and in this sense there is no distortion. In the absence of the arbitrarily additive u the two origins are conjugate to one another, if either lies on a perfectly imaged surface.

§ 3. T A HOMOGENEOUS FUNCTION

We have not yet taken into account that in a perfect instrument the length of the optical path between an object point and its image is independent of the ray along which it is measured. Denote this path length by P. Then from the meaning of T

$$\begin{aligned} P &= T - (x\xi + y\eta + z\zeta) + (x'\xi' + y'\eta' + z'\zeta') \\ &= T - (u_1 - a_1)T_1 - (u_2 - a_2)T_2 - (u_3 - a_3)T_3. \end{aligned} \qquad \ldots\ldots (2)$$

This length must depend on the coordinates x, y, z (or alternatively on x', y', z') only, whatever the values of u_1, u_2, u_3 may be. This condition must be satisfied either automatically because the right side of (2) is in fact independent of u_1, u_2, u_3 or because u_1, u_2, u_3 can be determined as functions of T_1, T_2, T_3, and so by (1) P can be expressed as a function of the coordinates of the object or image point.

We shall see later that the second of these alternatives must be rejected. The first implies that T is a homogeneous function of the first order in u_1, u_2, u_3 (Smith 1928). The path length is then

$$P = P_0 + a_1T_1 + a_2T_2 + a_3T_3 \qquad \ldots\ldots (3)$$

or by (1)

$$P - P_0 = (x \ y \ z)b^{-1}\begin{pmatrix} a_1 \\ a_2 \\ a_3 \end{pmatrix} = (x' \ y' \ z')c^{-1}\begin{pmatrix} a_1 \\ a_2 \\ a_3 \end{pmatrix}, \qquad \ldots\ldots (4)$$

where P_0 is the length of the path between the two origins when these lie on the conjugate surfaces. The path length for any point of the perfectly imaged surfaces is proportional to the distance of the point from a fixed plane.

The form of the conjugate surfaces depends on the way in which u_1, u_2, u_3 are combined in T. Since T is homogeneous of the first order, T_1, T_2 and T_3 are homogeneous of order zero, and the elimination of the ratios $u_1 : u_2 : u_3$ gives an equation

$$\theta(T_1, T_2, T_3) = 0. \qquad \ldots\ldots (5)$$

The equations of the conjugate surfaces are found by substituting in (5) for T_1, T_2, T_3 from the solutions of equations (1).

For example, if

$$T=u_1u_2/u_3,$$

then
$$T_1=\frac{u_2}{u_3},\quad T_2=\frac{u_1}{u_3},\quad T_3=-\frac{u_1u_2}{u_3^2},$$

and therefore
$$T_1T_2+T_3=0,$$

so that the conjugate surfaces are of the second order and pass through the origins of coordinates.

Another example leading to conjugate surfaces of the second order is

$$T=(au_1^2+bu_2^2+cu_3^2+2fu_2u_3+2gu_3u_1+2hu_1u_2)^{1/2},$$

which gives

$$T(T_1\ T_2\ T_3)=(u_1\ u_2\ u_3)m,$$

where
$$m=\begin{pmatrix} a & h & g \\ h & b & f \\ g & f & c \end{pmatrix}.$$

Since
$$T^2=(u_1\ u_2\ u_3)m\begin{pmatrix} u_1 \\ u_2 \\ u_3 \end{pmatrix},$$

the equation connecting T_1, T_2, T_3 is

$$(T_1\ T_2\ T_3)m^{-1}\begin{pmatrix} T_1 \\ T_2 \\ T_3 \end{pmatrix}=1,$$

and those of the object and image surfaces are of the form

$$(x\ y\ z)M\begin{pmatrix} x \\ y \\ z \end{pmatrix}=1.$$

The surfaces are therefore of the second order and the origins are at their centres.

§ 4. AXIALLY SYMMETRICAL INSTRUMENTS

Most optical instruments in which fine correction is sought have an axis of rotational symmetry, which will be assumed to coincide with the axes of z and z'. In consequence of this symmetry ξ, η, ξ', η' can only enter T in the combinations $\xi^2+\eta^2$, $\xi\xi'+\eta\eta'$, $\xi'^2+\eta'^2$, and the variables can always be chosen so that

$$T=uf(w), \qquad \ldots\ldots(6)$$

where
$$u=\beta+\gamma\zeta-\gamma'\zeta',\quad w=\frac{(\alpha\xi-\alpha'\xi')^2+(\alpha\eta-\alpha'\eta')^2}{u^2}. \qquad \ldots\ldots(7)$$

The length of the optical path is P where

$$P=\beta(f-2wf'), \qquad \ldots\ldots(8)$$

f' being the differential coefficient of the function f.

In terms of cylindrical coordinates r, z, the conjugate surfaces are obtained by eliminating w between the equations

$$\frac{r^2}{\alpha^2}=\frac{r'^2}{\alpha'^2}=4wf'^2,\quad \frac{z}{\gamma}=\frac{z'}{\gamma'}=f-2wf'. \qquad \ldots\ldots(9)$$

The path length and the surface coordinates therefore depend on the single variable w, though this is not true of T. The equations of the surfaces are most simply obtained by expanding z/γ in a series of ascending powers of r^2 $4x^2$, and when the equation of the surface is given in this form an exactly similar process yields f as a power series in w. This is a simple generalization of the normal procedure for constructing T for a single refracting surface (Smith 1927); in that case the conjugate surfaces coincide with the refracting surface, and without loss of generality we can put $\alpha=\alpha'=\gamma=\gamma'=1$, $\beta=0$. Systems in which β is zero are of limited interest, since by (8) the path length between conjugate surfaces is zero or at least is invariable over the whole of these surfaces, and this condition is inconsistent with properties desired in many instruments. The group $\beta=0$ is chiefly important because instrumental design must be based on the properties of single surfaces which are necessarily members of the group.

§ 5. SPHERICAL SURFACES: SYSTEMS WITH TWO PAIRS OF PERFECTLY DEFINED SURFACES

Much interest has been taken in recent years in instruments designed to give good definition over an image surface which is spherical rather than plane. Instruments perfectly corrected for spherical conjugate surfaces are represented by

$$T=kv^{\frac{1}{2}}, \qquad \ldots\ldots(10)$$

where $$v=(\alpha\xi-\alpha'\xi')^2+(\alpha\eta-\alpha'\eta')^2+(\beta+\alpha\zeta-\alpha'\zeta')^2.$$

The conjugate surfaces have radii $k\alpha$ and $k\alpha'$ respectively and are centred at the origins. The path length is given by

$$P-P_0=z\beta/\alpha=z'\beta/\alpha',$$

in agreement with equations (8) and (9).

Systems with spherical surfaces fall into two groups—in one β vanishes and in the other it does not—with an interesting difference in their properties. This may be illustrated by the simplest possible case, a single refracting surface, in which $\alpha=\alpha'=1$, $\beta=0$. As is well known, in addition to the self-conjugate refracting surface, there exists a pair of conjugate spheres on which the imagery is perfect, the magnification being the square of the ratio of the two refractive indices (Huygens 1653). The condition for the existence of these additional surfaces is $\beta=0$, so that they are necessarily associated with constancy of optical path over the whole of the conjugate surfaces. This peculiarity of having two pairs of aplanatic conjugate surfaces is not limited to a single refracting surface, nor even to systems with spherical conjugate surfaces. For in equation (10) consider the variable

$$\begin{aligned} v=&\{(\alpha+\phi\omega^2)^{\frac{1}{2}}\xi-(\alpha'+\phi\omega'^2)^{\frac{1}{2}}\xi'\}^2+\{(\alpha+\psi\omega^2)^{\frac{1}{2}}\eta-(\alpha'+\psi\omega'^2)^{\frac{1}{2}}\eta'\}^2\\ &+\{(\alpha+\theta\omega^2)^{\frac{1}{2}}\zeta-(\alpha'+\theta\omega'^2)^{\frac{1}{2}}\zeta'\}^2, \qquad \ldots\ldots(11)\end{aligned}$$

where ω and ω' are the reciprocals of the refractive indices μ and μ'. In virtue of the identities

$$\xi^2+\eta^2+\zeta^2=\mu^2, \quad \xi'^2+\eta'^2+\zeta'^2=\mu'^2,$$

it may be seen that v is also given identically by the equation

$$\begin{aligned} v=&\{\omega(\alpha'\mu'^2+\phi)^{\frac{1}{2}}\xi-\omega'(\alpha\mu^2+\phi)^{\frac{1}{2}}\xi'\}^2+\{\omega(\alpha'\mu'^2+\psi)^{\frac{1}{2}}\eta-\omega'(\alpha\mu^2+\psi)^{\frac{1}{2}}\eta'\}^2\\ &+\{\omega(\alpha'\mu'^2+\theta)^{\frac{1}{2}}\zeta-\omega'(\alpha\mu^2+\theta)^{\frac{1}{2}}\zeta'\}^2. \qquad \ldots\ldots(12)\end{aligned}$$

We conclude that in general a system of the $\beta=0$ group which produces perfect imagery over any centred surface of the second order will yield perfect imagery over another concentric second order surface, and that the product of the two magnifications in the direction of any principal axis is equal to μ^2/μ'^2. But this generalization fails when the system consists of a single refracting surface; for the condition that in one solution the coefficients of ξ and ξ' should be equal, and similarly for the other coordinates, gives

$$\frac{\alpha'-\alpha}{\omega^2-\omega'^2}=\phi=\psi=\theta,$$

so that the refracting surface is spherical.

It would be easy at this stage to draw conclusions which are not warranted. We have shown that one centred conicoid can be perfectly imaged on another without distortion. This apparently means that if P and Q are the extremities of any diameter of the object surface they will have as images points P′ and Q′ which are the extremities of a diameter of the image surface. If this were correct all rays through the centre C of the one surface would necessarily pass through the centre C′ of the other surface, so that these centres would be perfectly imaged conjugate points. The existence of three equally-spaced collinear points P, C, Q which have equally-spaced collinear images P′, C′, Q′ implies that the points at infinity on the incident and emergent rays are conjugate to one another, for these sets of four points form harmonic ranges, and this in turn suggests that the system may be afocal, in which case analysis with the aid of the T function is not valid. But a decisive consideration is that we apparently have two separate object points P and Q and two separate image points P′ and Q′ for which the magnification has the same value. This is possible in an afocal system, but otherwise we must understand that only one of these pairs of points exists. This is not at all surprising. When light is refracted at a single surface we tacitly suppose that we are only dealing with light which has passed through one part of the surface, and, whether or no the surface represented by the algebraic equation is closed, only one refraction occurs. Similarly, when rays are refracted at a spherical surface, the aplanatic surfaces for the magnification μ^2/μ'^2 are not closed; their properties only hold for those parts of the aplanatic spheres, more remote from the point of refraction, determined by the tangent cone from this point to the smaller of the surfaces. It is clear that a similar limitation must hold in the more general cases we have been considering.

The question whether the centres of the perfectly defined surfaces are imaged without aberration has therefore to be considered independently. The conclusion reached is that this perfect imagery is only attained when the surfaces are spherical. In other cases only an incident ray which coincides with one of the principal axes of the object surface will, on emergence, coincide with the corresponding axis of the image surface and so pass through the centre of this surface. When the surfaces are surfaces of revolution a more important union of rays at the centre follows from the indeterminacy of two of the axes.

To show this suppose that

$$v=(\alpha_1\xi-\alpha_1'\xi')^2+(\alpha_2\eta-\alpha_2'\eta')^2+(\alpha_3\zeta-\alpha_3'\zeta')^2,$$

so that a point on the object surface is x, y, z where

$$\frac{x}{\alpha_1(\alpha_1\xi-\alpha_1'\xi')}=\frac{y}{\alpha_2(\alpha_2\eta-\alpha_2'\eta')}=\frac{z}{\alpha_3(\alpha_3\zeta-\alpha_3'\zeta')}=\frac{k}{v^{\frac{1}{2}}}. \quad \ldots\ldots(13)$$

This ray passes through the centre of the surface if

$$\frac{x}{\xi}=\frac{y}{\eta}=\frac{z}{\zeta}=\frac{k}{\left\{\left(\frac{\xi}{\alpha_1}\right)^2+\left(\frac{\eta}{\alpha_2}\right)^2+\left(\frac{\zeta}{\alpha_3}\right)^2\right\}^{\frac{1}{2}}}=\frac{k}{s}\text{ say.}$$

Similar equations hold for the image space. Equating the values of x/k etc. given by these equations we have, if the same ray passes through both origins,

$$\frac{\alpha_1\xi-\alpha_1'\xi'}{v^{\frac{1}{2}}}=\frac{\xi}{\alpha_1 s}=\frac{\xi'}{\alpha_1' s'},$$

or

$$v^{\frac{1}{2}}=\alpha_1^2 s-\alpha_1'^2 s',$$

with corresponding equations when α_1, α_1' are replaced by α_2, α_2' and α_3, α_3'. These three simultaneous equations require $\alpha_1=\alpha_2=\alpha_3$ and $\alpha_1'=\alpha_2'=\alpha_3'$ if the condition is to be satisfied for rays in all directions. For a ray coincident with a principal axis, say that of x, we have $y=z=\eta=\zeta=0$, so that η' and ζ' are zero, and hence also y' and z', i.e. the emergent ray coincides with the axis of x'.

§ 6. SYSTEMS WITH PLANE CONJUGATE SURFACES

This investigation started with the consideration of degrees of freedom, and subsequent developments have depended on the existence of non-singular matrices b and c of the third order. For axially symmetrical systems this has led to the general equations (6) to (9), and we note that these equations are still valid if $\gamma=\gamma'=0$, when the object and image surfaces become plane. The variables ζ and ζ' have now disappeared from T, and it is clear that in a number of important respects the case is abnormal. The first thing to be noted is that the conjugate surfaces are plane whatever the form of f may be—this is the only case in which the shape of the conjugate surfaces does not determine the characteristic function. Regarded as a function of the single variable w, T is no longer tied to the requirement of being a homogeneous function of the first order.

The normal condition that the path length is proportional to the distance of an object point from a fixed transverse plane obviously does not hold in this case.

Corresponding to different forms of f there will be differences in the aberrations for objects outside the corrected planes. For photographic lenses and other instruments used to image objects at different distances the form of this function is not unimportant. With many of these instruments it is convenient to fit an aperture stop (often an iris diaphragm) effectively in a plane through a principal point, and it is advantageous to choose f so that this point is imaged without aberrations. This condition is satisfied if

$$T=c\{(\alpha-\alpha')^2-(\alpha\xi-\alpha'\xi')^2-(\alpha\eta-\alpha'\eta')^2\}^{\frac{1}{2}}. \quad \ldots\ldots(14)$$

To consider the use of the instrument for magnification m, take new variables

$$h=\frac{(\xi-m\xi')^2+(\eta-m\eta')^2}{(1-m)^2}, \quad j=\frac{(\xi-m\xi')(\xi-\xi')+(\eta-m\eta')(\eta-\eta')}{(1-m)^2},$$

$$k=\frac{(\xi-\xi')^2+(\eta-\eta')^2}{(1-m)^2},$$

so that h measures the area of the field of view, k the area of the aperture stop, and j is the intermediate variable which occurs in the measure of all unsymmetrical aberrations. Referred to the new axial object and image points the characteristic function is

$$c\{(\alpha-\alpha')(1-h+2Mj-M^2k)^{\frac{1}{2}}-M\frac{\alpha}{m}(1-h+2mj-m^2k)^{\frac{1}{2}}+M\alpha'(1-h+2j-k)^{\frac{1}{2}}\}$$

where $$M=\frac{m\alpha-\alpha'}{\alpha-\alpha'}.$$

By inspection this function vanishes when $\alpha=0$, $\alpha'=0$, or $m=1$, and when $M=0$ or $q\equiv(1-h)k+j^2=0$ it reduces to $c\alpha\alpha'(1-m)^2(1-h)^{\frac{1}{2}}/m(\alpha-\alpha')$. If it is expanded in a series of ascending powers of q the value is found to be

$$\frac{c\alpha\alpha'(1-m)^2(1-h)^{\frac{1}{2}}}{\alpha-\alpha'}\{m^{-1}+\tfrac{1}{2}Mqpj+\tfrac{1}{8}Mq^2p^3\times(\text{quintic in } 1-h, j)+\ldots\},$$

where $$p^{-1}=(1-h+Mj)(1-h+mj)(1-h+j).$$

The absence of a term in j when $q=0$ shows that there is no distortion, and the absence of a term in q without j as a factor indicates freedom from curvature and astigmatism with the stop in this special position. Of Seidel aberrations only coma and spherical aberration are present. It follows that, no matter how large the field of view may be, an instrument described by equation (14) is suitable for use over an extended range of magnifications provided the numerical aperture is properly restricted. It will be observed that since k enters only through q, i.e. since k is always associated with $hk-j^2$, all aberrations found when the object surface is changed involve differences between skew and meridional rays.

§ 7. FAILURE OF OTHER FORMS OF T FOR PERFECT IMAGERY

We have hitherto considered forms of T homogeneous of the first order in the three linear variables u_1, u_2, u_3, but have found that when T is a function of only two linear variables it need not be homogeneous. The necessity for homogeneity in the general solution of equation (2) is tied up with the number of variables.

To show this it will be sufficient to take simple forms of u_1, u_2, u_3, each involving one variable from each external space. When T is not homogeneous of the first order the constant path condition shows that rays through a given object point are determined by conditions reducible to the form

$$\alpha_1\xi-\alpha_1'\xi'=\text{constant},\quad \alpha_2\eta-\alpha_2'\eta'=\text{constant},\quad \alpha_3\zeta-\alpha_3'\zeta'=\text{constant}.$$

In addition, the two identities

$$\xi^2+\eta^2+\zeta^2=\mu^2,\quad \xi'^2+\eta'^2+\zeta'^2=\mu'^2$$

must be satisfied. These five relations between the six ray variables leave only one degree of freedom, so that absence of aberrations can be secured for a one-dimensional fan of rays, but not for a solid-angular bundle. The only escape from homogeneity therefore occurs when T does not involve all six direction cosines. If only one is missing, say ζ', the image surface is plane, but the rays from any given object point must make ζ constant, i.e. the object is at infinity;

this case may therefore be treated as a member of the second group, with the two variables ζ and ζ' absent, already considered. We need not consider any other cases for their properties are not of interest. For example, all rotationally symmetrical instruments of finite focal length must have a non-vanishing term in $\xi\xi'+\eta\eta'$.

§ 8. A THEOREM OF CLERK MAXWELL

An elegant proof of the impossibility of a perfect instrument in the wider sense mentioned at the beginning of this paper was given by F. Klein, and has been included in the tract on *The Theory of Optical Instruments* by E. T. Whittaker. The result seems to have been reached first by Clerk Maxwell in a well-known paper (Maxwell 1854), but the fact that his argument is erroneous has apparently escaped notice.* The most important result given by Maxwell is Proposition IX which states:

"It is impossible, by means of any combination of reflections and refractions, to produce a *perfect* image of an object at two different distances, unless the instrument be a telescope and $l=n=\mu_1/\mu_2$, $m=1$". (l and n are the transverse and longitudinal magnifications, and m the angular magnification.)

This proposition is false; it is clearly inconsistent with the result given above that two aberrationless pairs of conjugate surfaces which are in the form of centred conicoids are possible. Maxwell's inference was drawn from an argument intended to show that equality of path cannot be attained for two positions of an object along a ray. It may therefore not be superfluous to note that if x_1, y_1, z_1 and x_1', y_1', z_1' are the coordinates of object and image points when v is defined by (11), and x_2, y_2, z_2 and x_2', y_2', z_2' those when v is put in the form (12), differentiation of T gives

$$\begin{aligned}(x_2-x_1)v^{\frac{1}{2}} &= k\omega(\alpha'\mu'^2+\phi)^{\frac{1}{2}}\{\omega(\alpha'\mu'^2+\phi)^{\frac{1}{2}}\xi-\omega'(\alpha\mu^2+\phi)^{\frac{1}{2}}\xi'\}\\ &\quad -k(\alpha+\phi\omega^2)^{\frac{1}{2}}\{(\alpha+\phi\omega^2)^{\frac{1}{2}}\xi-(\alpha'+\phi\omega'^2)^{\frac{1}{2}}\xi'\}\\ &= \xi k\omega^2(\alpha'\mu'^2-\alpha\mu^2),\end{aligned}$$

and

$$\begin{aligned}(x_2'-x_1')v^{\frac{1}{2}} &= k\omega'(\alpha\mu^2+\phi)^{\frac{1}{2}}\{\omega(\alpha'\mu'^2+\phi)^{\frac{1}{2}}\xi-\omega'(\alpha\mu^2+\phi)^{\frac{1}{2}}\xi'\}\\ &\quad -k(\alpha'+\phi\omega'^2)^{\frac{1}{2}}\{(\alpha+\phi\omega^2)^{\frac{1}{2}}\xi-(\alpha'+\phi\omega'^2)^{\frac{1}{2}}\xi'\}\\ &= \xi' k\omega'^2(\alpha'\mu'^2-\alpha\mu^2),\end{aligned}$$

with similar equations for the other coordinates. Thus

$$\frac{k(\alpha'\mu'^2-\alpha\mu^2)}{v^{\frac{1}{2}}} = \frac{\mu(x_2-x_1)}{\omega\xi} = \frac{\mu(y_2-y_1)}{\omega\eta} = \frac{\mu(z_2-z_1)}{\omega\zeta}$$

$$= \text{reduction of path in object space,}$$

and

$$\frac{k(\alpha'\mu'^2-\alpha\mu^2)}{v^{\frac{1}{2}}} = \frac{\mu'(x_2'-x_1')}{\omega'\xi'} = \frac{\mu'(y_2'-y_1')}{\omega'\eta'} = \frac{\mu'(z_2'-z_1')}{\omega'\zeta'}$$

$$= \text{increase of path in image space,}$$

so that the path length from object to image is unaltered by moving the object from position 1 to position 2.

* Since this was written I have been reminded that M. Herzberger has pointed out that Maxwell's conclusion is erroneous. Herzberger's paper should be consulted in connection with the general problem considered here.

Maxwell went on to say: "In this way we might show that we cannot in general have an astigmatic, plane, undistorted image of a plane object. But we can prove that we cannot get perfectly focused images of an object in two positions even at the expense of curvature and distortion", and these conclusions also are wrong. Simultaneous correction of all aberrations over plane conjugate surfaces is consistent with constancy of optical path, and, as we have shown, freedom from curvature, astigmatism, and distortion can be achieved for all positions of the object.

§ 9. THE POWER AND THE UNIT SURFACES

The elementary theory of optical instruments is often based on the existence of unit planes and the focal lengths of a typical system. The focal lengths are immediately derivable from a more fundamental quantity, the power. When we leave the paraxial region the power is associated with particular rays rather than with the system itself, and it is known that the unit surfaces are not in fact plane even where they meet the axis. But both the power and the unit surfaces are valuable concepts whether we are dealing with rays within or without the paraxial region, and a word should be said about them in the case of axially-symmetrical perfect instruments.

In the notation introduced in equations (6) and (7) the power for a typical ray is $u/2\alpha\alpha' f'$, and since the magnification for which the system is corrected is α'/α it follows from the usual equations that the distance from the object surface to the object-space unit surface measured along the ray is $2\mu\alpha(\alpha'-\alpha)f'/u$, and similarly that from the image-space unit surface to the image surface is $2\mu'\alpha'(\alpha-\alpha')f'/u$. If $\alpha=\alpha'$ the unit surfaces are those for which the system is corrected, and so are known. In general the shapes of the unit surfaces will vary with the shapes of the perfectly defined surfaces. When these surfaces are plane u is a constant and f a function of w only. The focal lengths therefore depend only on w, and are fixed when the point of intersection with the object plane is known. The unit surfaces are accordingly spherical. In all other cases the unit surfaces depart from the sphere. For instance, if

$$T=k\{(\alpha\xi-\alpha'\xi')^2+(\alpha\eta-\alpha'\eta')^2+(\beta+\gamma\zeta-\gamma'\zeta')^2\}^{\frac{1}{2}},$$

the corrected surfaces are of the second order, and the power is given by

$$\text{power}=\frac{T}{\alpha\alpha' k^2}=\frac{\alpha\xi-\alpha'\xi'}{\alpha' x}=\frac{\alpha\eta-\alpha'\eta'}{\alpha' y}=\frac{\gamma(\beta+\gamma\zeta-\gamma'\zeta')}{\alpha\alpha' z}.$$

The argument already used to prove that T must be a homogeneous function then shows that the number of degrees of freedom when the power is constant is less than two unless γ is zero.

§ 10. THE REALIZATION OF PERFECT INSTRUMENTS

We have so far been considering imagery in which freedom from aberrations is consistent with the laws of light propagation, and have reached the conclusion that optical systems with very desirable properties are theoretically possible. The question how these desirable properties are to be achieved in practice immediately arises. Apart from cases which, from our present point of view, are trivial, we know that a plane reflector and a spherical refractor are the only elements which yield aberrationless images, and in all the known systems the path

from object to image is zero, so that the practical need for a real image of a real object is not achieved. Can perfect systems with these practically essential properties be constructed from such unpromising materials, which are all we can use ? For systems with a limited number of reflecting or refracting surfaces the answer appears to be definitely no. The best we can expect to do is to approach the theoretically possible standard by balancing aberrations arising at the various refracting surfaces so that the residual errors are, for a given aperture and field of view, small enough to be unimportant in comparison with the size of the images of point sources inseparable from the appreciable magnitude of the wavelength of light. When the numerical aperture or the field of view or both are enlarged this aim will probably necessitate a corresponding elaboration of the lens system. The task facing the lens designer is thus not likely to become easier. If this view of the situation is correct the most promising field for work is the study of aberrations of higher orders than those hitherto fully examined, and particularly, by algebraic analysis, the examination of means by which they can be controlled separately or in combination. Research of this kind, if successful, would at least reduce the waste of energy on schemes that are incapable of yielding a satisfactory outcome, and the advances now being made in the construction of computing machines should make possible the tabulation of any functions which proved to be important for the numerical utilization of the knowledge gained. But whatever may be the stage to which such algebraic work is carried there will always be omitted from the analysis aberrations of still higher orders, and before a design is finished it will be necessary to make sure that they are taken into account. Checks of this kind, if made on paper, will take the form, as now, of tracing selected rays through the proposed system. This, of course, is quite a different matter from using ray-tracing as the normal tool for lens designing, and the methods of ray-tracing adopted may bear little resemblance to those now in common use. It is known that laborious tasks of this kind can be carried out by a suitable fully-automatic machine far more rapidly and with greater accuracy than is ever achieved by the methods employed today; and there is every reason to believe that by the use of such machines notable advances in the performance of optical instruments will be achieved.

§ 11. THE COMBINATION OF OPTICAL SYSTEMS

The view that a scheme for the construction of perfect instruments with useful characteristics cannot be devised may be thought unduly pessimistic, though it will probably not be seriously questioned by experienced designers. The reason for this belief is that there appears to be no means of building up a characteristic function of the type given by equations (6) and (7), with β not zero, by combining elementary systems in which β vanishes. If, with the notation of these equations, we combine two perfect instruments, distinguished by the suffixes 1 and 2 respectively, to form another perfect instrument distinguished by the omission of a suffix, it is readily shown that in general the variables w_1, w_2, w are equal, that the functions f_1, f_2, f are in constant ratios to one another, and that

$$\alpha f-\alpha_1 f_1=\alpha_1' f_1-\alpha_2 f_2=\alpha_2' f_2-\alpha' f=0,$$
$$\gamma f-\gamma_1 f_1=\gamma_1' f_1-\gamma_2 f_2=\gamma_2' f_2-\gamma' f=0,$$
$$\beta f=\beta_1 f_1+\beta_2 f_2.$$

When T is constructed from the sum of the characteristic functions T_1 and T_2 of the two parts by applying the stationary path conditions, these relations cause the third intermediate direction cosine to disappear from T when two are eliminated and, as the last equation shows, when this elimination is automatic the values $\beta_1=\beta_2=0$ involve $\beta=0$. But in the typical case encountered in the construction of real instruments the stationary conditions take the form of equations expressing the intermediate ξ and η in terms of the six external direction cosines and also of the third intermediate variable ζ. This variable has to be found from the equation $\xi^2+\eta^2+\zeta^2=\mu^2$ before it can be eliminated from the combined characteristic function. The result is an expression for T which involves all the external direction cosines and is in general less simple than those for the component systems. No plan has been devised which ensures that the T obtained in this way will take the form (6) characteristic of a perfect instrument.

It may be observed that the theory just given must be supplemented where systems with plane conjugate surfaces are combined.

The work described above has been carried out as part of the research programme of the National Physical Laboratory, and this paper is published by permission of the Director of the Laboratory.

REFERENCES

Herzberger, M., 1946, *Ann. N.Y. Acad. Sci.*, **48** (no. 1).
Huygens, Chr., 1653, *Dioptrica*, Prop. XII. (The discovery is often attributed to Th. Young.)
Maxwell, J. Clerk, 1854, *Camb. and Dubl. Math. Jour.*
Maxwell, J. Clerk, 1858, *Quart. J. Pure and Applied Math.*, II, and *Scientific Papers*, I, 271.
Smith, T., 1927, *Trans. Opt. Soc.*, **28**, 225.
Smith, T., 1928, *Trans. Opt. Soc.*, **29**, 179.
Whittaker, E. T., 1907, in *Cambridge Tracts in Mathematics and Mathematical Physics*, no. 7.

A New Device for Maintaining Constant Stress in a Rod Undergoing Plastic Extension

By E. N. da C. Andrade
University College, London

MS. received 11 *October* 1947

ABSTRACT. A simple mechanical device is described by which constant stress may be maintained during the plastic extension of a wire. The mid-point of the wire maintains its position during extension, so that it may be observed by a fixed microscope.

§ 1. INTRODUCTION

Two devices have been described in the past which maintain constant stress in a wire extending vertically under a load, the hyperbolic weight (Andrade 1910) and the constant stress bar (Andrade and Chalmers 1932). For work now in progress in our laboratory it is desired to observe microscopically the behaviour of the crystallites in a specimen of polycrystalline metal during extension

under constant stress, with the object of interpreting the β flow and the k flow (Andrade 1910)—which may alternatively be called the transient flow and the permanent flow—in terms of physical processes. For this purpose a device is required which will extend a horizontal specimen by a pull from each end, in such a way that the centre of the specimen maintains its position, while further, as the specimen extends, the pull is automatically diminished in such a way that the force per unit cross-sectional area of the specimen remains constant.

§ 2. GENERAL THEORY

AB and CD are rigid rods, pivoted at B and D so as to be free to turn in the plane of the paper (figure 1). GL and HL are rigid rods pivoted at G and H to AB and CD, and at L to a rod LL′, running through a guide M, to which a weight W is attached. PS and QS′ are members attached to the cylindrical specimen S′S, so that when, owing to the applied weight W, A and C tend to approach, the specimen is put into tension. It can be seen at once that as the distance AC diminishes and the specimen extends, the force acting longitudinally on the specimen diminishes. It remains to find the conditions that make the stress approximately constant.

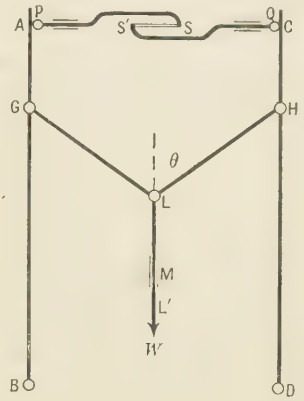

Figure 1.

Let the length of the specimen be l_0, $AG=c$, $GB=f$, so that

$$AB/GB=CD/HD=r=1+c/f$$

and let $GL=HL=p$ and angle $GLH=2\theta$.

The horizontal force at G and H is $F=\frac{1}{2}W\tan\theta$ and the axial force on the specimen is $(1/2r)W\tan\theta$.

The length of the specimen is*

$$l=l_0+2pr(\sin\theta-\sin\theta_0),$$

where θ_0 is the value of θ when $l=l_0$.

$$l=l_0\{1+c(\sin\theta_0-\sin\theta)\},$$

when $$c=2pr/l_0.$$

Putting $\theta=\theta_0-\alpha$ we have

$$l=l_0\{1+c\sin\theta_0(1-\cos\alpha)+c\cos\theta_0\sin\alpha\},$$

which, expanding in terms of α and retaining terms up to α^5, becomes

$$l=l_0\{1+\alpha\,.\,c\cos\theta_0+\tfrac{1}{2}\alpha^2\,.\,c\sin\theta_0-\tfrac{1}{6}\alpha^3\,.\,c\cos\theta_0-\tfrac{1}{24}\alpha^4\,.\,c\cos\theta_0+\tfrac{1}{120}\alpha^5\,.\,c\cos\theta_0\}.$$

The tension in the specimen $=T=(1/2r)W\tan(\theta_0-\alpha)$.

Expanding in terms of α, we have

$$\tan(\theta_0-\alpha)=\frac{\tan\theta_0-\tan\alpha}{1+\tan\theta_0\tan\alpha}$$

$$=\tan\theta_0+\sec^2\theta_0\{-\alpha+\alpha^2\tan\theta_0-\alpha^3(\tfrac{1}{3}+\tan^2\theta_0)+\alpha^4\tan\theta_0(\tfrac{2}{3}+\tan^2\theta_0)$$
$$-\alpha^5(\tfrac{2}{15}+\tan^2\theta_0+\tan^4\theta_0)\}.$$

* The motion of A and C is not strictly horizontal, but along the arc of a circle. However, in the actual apparatus the range of angular displacement of A and C will be less than 2°, and throughout the calculation all corrections for the difference between the arc and a horizontal line are negligible.

The required condition for constancy of stress is $Tl\rho = \text{constant}$, where ρ is the density, or, assuming the density constant during extension, which is true to a high degree of approximation, $Tl = \text{constant}$. This means, calling the product p,

$$p = l/l_0 \tan(\theta_0 - \alpha) = \text{constant},$$

$$\begin{aligned} l/l_0 \tan(\theta_0 - \alpha) = {} & \tan\theta_0 + \alpha(c\sin\theta_0 - \sec^2\theta_0) \\ & + \alpha^2\{\sec^2\theta_0 \tan\theta_0 - c\sec\theta_0(1 - \tfrac{1}{2}\sin^2\theta_0)\} \\ & + \alpha^3\{c\sin\theta_0(\tfrac{1}{2}\sec^2\theta_0 - \tfrac{1}{6}) - \tfrac{1}{3}\sec^2\theta_0 - \tan^2\theta_0\sec^2\theta_0\} \\ & + \alpha^4\sec\theta_0\{\tan\theta_0\sec\theta_0(\tfrac{2}{3} + \tan^2\theta_0) \\ & \qquad - \tfrac{1}{2}c(\tfrac{1}{3} + \tan^2\theta_0 + \tfrac{1}{12}\sin^2\theta_0)\} \\ & + \alpha^5\{c(\tfrac{1}{120}\sin\theta_0 + \tfrac{9}{24}\sec\theta_0\tan\theta_0 + \tfrac{1}{2}\sec\theta_0\tan^3\theta_0) \\ & \qquad - \sec^2\theta_0(\tfrac{2}{15} + \tan^2\theta_0\sec^2\theta_0)\} \end{aligned}$$

The conditions for the terms in α and α^2 to vanish are

$$c\sin\theta_0 = \sec^2\theta_0$$

$$c\sec\theta_0(1 - \tfrac{1}{2}\sin^2\theta_0) = \sec^2\theta_0\tan\theta_0,$$

which gives

$$\sin\theta_0 = \sqrt{(2/3)},$$

$$c = 3\sqrt{(3/2)}.$$

This makes the coefficients of α^3, α^4 and α^5 to be -3, 3·71 and -6 respectively, which, for $\alpha = 10° = 0{\cdot}17453$ radians, gives for the sum of the three terms $-0{\cdot}0135$ in comparison with $\tan\theta_0 = 1{\cdot}414$, a comparatively small deviation for a range of angles which can be readily made to correspond to a high percentage—say 40%—elongation of the specimen.

§ 3. POINTS AFFECTING DESIGN

The variation of $l/l_0 \tan(\theta_0 - \alpha)$ with α for the case of $c = 3\sqrt{(3/2)}$ is shown in the lowest curve in figure 2. The two broken horizontal lines represent a variation of 0·1% from the value of $\tan\theta = \sqrt{2}$. The curve representing the product p starts as a horizontal line and then falls at an increasingly rapid rate as α

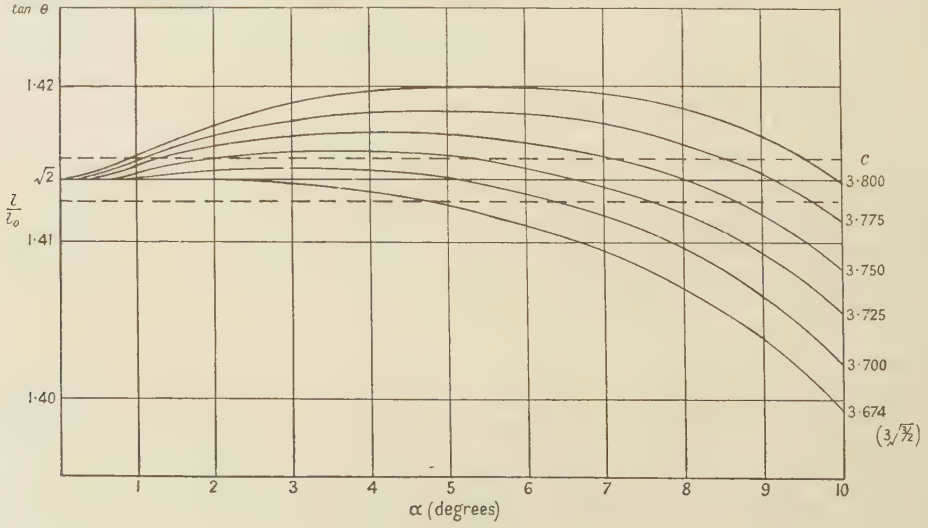

Figure 2.

increases, but up to $\alpha = 4{\cdot}5°$ it has not changed by 0·1%. Up to $\alpha = 10°$ the variation is 1·0%.

By increasing c slightly the curve is raised in the initial part, as shown, with the result that, if desired, the total variation for a given range of α can be slightly decreased. Curves are shown for values of c up to 3·8. It is evident that for $c = 3{\cdot}725$ the variation of the product ranges from about $+0{\cdot}12$ to $-0{\cdot}12\%$ up to $\alpha = 7{\cdot}75°$, that is, there is a total variation of 0·24%, while for the same range the $c = 3{\cdot}674$ curve shows a total variation of about 0·43%. It is clear that the method gives an easy way of maintaining stress constant to a high degree for α up to 8° or so, with a limited range of possibilities of adjusting the slight variations that exist.

It remains to consider what percentage extension of the specimen will correspond to this range of α. The expression

$$(l - l_0)/l = c\{\sin\theta_0(1 - \cos\alpha) + \cos\theta_0 \sin\alpha)\}$$

gives the following values:

α	2°	4°	6°	8°	10°
$(l-l_0)/l \times 100$	7·6	15·5	23·8	32·4	41·2

Therefore an extension of about 30%, which is all that is likely to be required, can be obtained with a stress constant to within 0·2%. An extension of 41% involves an overall departure of about 0·44% from constancy of stress.

We are proceeding to the construction of an apparatus along these lines.

I am indebted to Mr. A. J. Kennedy for the preparation of figure 2.

REFERENCES

ANDRADE, E. N. DA C., 1910, *Proc. Roy. Soc.* A, **84**, 1.
ANDRADE, E. N. DA C., and CHALMERS, B., 1932, *Proc. Roy. Soc.* A, **138**, 348.

LETTERS TO THE EDITOR

The Effect of Temperature on the Heat Changes accompanying Magnetization of the Nickel-Silicon Alloy W.5

In a communication to the Society at its meeting in Nottingham on 8 November 1947, E. G. Harrison mentioned the interesting behaviour of the nickel-silicon alloy W.5 (Ni 94·84, Cu 0·1, Fe 0·4, C 0·05, Si 4·0, Mn 0·6), and stated that preliminary experiments had shown that the thermal effects associated with magnetization were very greatly reduced by a rise of temperature of some 25° c. above that of the room.

We have made experiments using the same apparatus modified in such a way that a reasonably steady temperature of 30° c. could be maintained over the specimen. We find that the heat of magnetization given by $\oint H\,dI$ for a maximum field of 183 oersteds falls from 316 ergs/cm³ per cycle at 20° c. to 212 ergs/cm³ per cycle at 30° c., while I_{max} falls from 18·3 to 6·1 gauss ; obviously, we are dealing with an alloy whose Curie point is near room temperature. At the same time the individual values of the directly measured heat changes were reduced, the maximum cooling observed in any half-cycle falling from 98,460 to 23,300 ergs/cm³.

University College,
Nottingham,
21 January 1948.

L. F. BATES.
J. H. DAVIS.

CORRIGENDA

"The Adiabatic Temperature Changes Accompanying the Magnetization of Cobalt in Low and Moderate Fields", by L. F. BATES and A. S. EDMONDSON (*Proc. Phys. Soc.*, 1947, **59**, 329).

It is regretted that, by an oversight, the values of $\int I\,dH$ instead of $\int H\,dI$ were given in table 8, column 4; columns 4 and 6 and figures 7 and 11*b* should be corrected accordingly. The quantity -3960 should be added to each line, except the first, in column 4 of table 2; the figures in column 5 reduced in the ratio 19/21 and column 6 recalculated; figures 4 and 11*a* are only slightly affected. The first line in column 3 of table 7 should read -1200.

"Distribution Coefficients for the Calculation of Colours on the C.I.E. Trichromatic System for Total Radiators at 1500–250–3500° K., and 2360° K. ($C_2 = 14350$)", by H. G. W. HARDING and R. B. SISSON (*Proc. Phys. Soc.*, 1947, **59,** 814).

Page 824. "$E_{2750}\bar{y}$ (0·45μ), 0·1703" should read "0·1073".
"$E_{3000}\bar{z}$ (0·42μ), 1·5102" should read "1·5012".
"$E_{3000}\bar{z}$ (0·48μ), 3·9238" should read "3·9328".

REVIEWS OF BOOKS

Methods of Measuring Temperature, by EZER GRIFFITHS. Third Edition. Pp. x+223. (London: Charles Griffin and Co., Ltd., 1947.) 20*s*.

Many of the subjects which receive a chapter in ordinary general text-books are also worthy of whole treatises to themselves, and in some cases they do, in fact, form the subjects of separate treatises. In other cases, however, the recognition of their importance is confined to a relatively small number, and so the demand for full-length treatment is small. Such a subject is that of temperature measurement. Nearly all thermal measurements depend at some point on the measurement of a temperature or temperature difference, and perhaps more measurements have been marred by failure to take adequate precautions here than in any other way, yet the student, hard-pressed for time, generally feels that there is no time for detailed study of it, because it does not loom large in the examination papers.

This book certainly gives the best general survey of the subject at present available, both for measurements at normal temperature and for those at high temperature. It comes from a man of experimental outlook, and consequently contains just those hints that can come only from practice. When it first appeared, it dealt with a subject which was only then emerging into the stage of real accuracy, and now, having been for some time out of print, it has been revised so as to represent the art at its present, much more advanced, stage. In preparing the new edition, the whole text has been re-set, and the book is now much more pleasant to handle than in its old form. J. H. A.

Measurement by Mullard

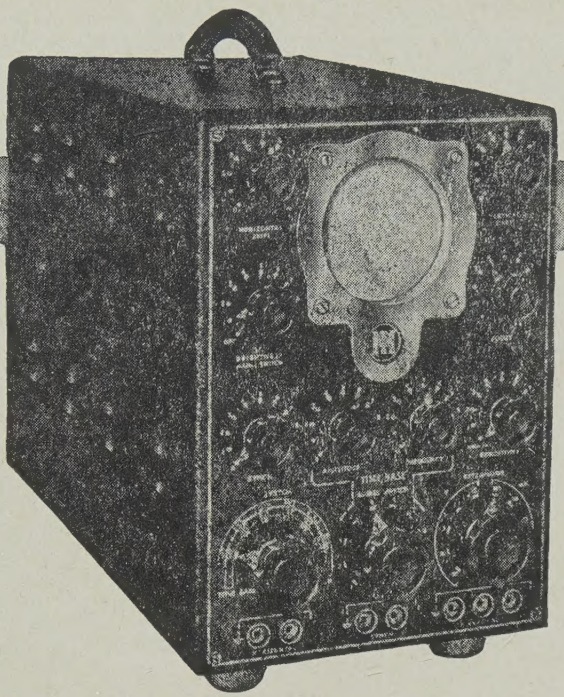

Cathode Ray Oscillograph Type E.800

THIS OSCILLOGRAPH is particularly well suited to investigations of a low frequency character, its time base circuit covering a range of from 0.25 c/s. to 16 kc/s. (also single-stroke firing). The vertical axis amplifier is flat within 2 dB at frequencies between 0.1 c/s. and 40 kc/s. and at maximum gain a sensitivity of 1 mV. (r.m.s.) per cm. is achieved.

These characteristics, together with other important factors, make this equipment an ideal one for the study of stress and vibration problems and transient or recurrent electrical phenomena in the low frequency spectrum.

Mullard

Leaflet MP.438 available upon request

THE MULLARD WIRELESS SERVICE COMPANY LTD.
(Measuring Apparatus Section)
CENTURY HOUSE, SHAFTESBURY AVENUE, LONDON, W.C.2.

(M.I.200B)

ELECTRICAL MEASURING INSTRUMENTS OF THE HIGHER GRADES

ERNEST TURNER ELECTRICAL INSTRUMENTS LIMITED

CHILTERN WORKS
HIGH WYCOMBE
BUCKS

Telephone :
High Wycombe 1301/2

Telegrams
Gorgeous, High Wycombe